ADSORPTIVE REMOVAL OF INDIGO CARMINE DYE FROM AQUEOUS SOLUTION USING LOW-COST ADSORBENTS

A DISSERTATION

Submitted in partial fulfillment of the requirements for the award of the degree of

MASTER OF TECHNOLOGY

in

CHEMICAL ENGINEERING

(With Specialization in Industrial Pollution Abatement)

By

UMA RAJYA LAKSHMI.T

DEPARTMENT OF CHEMICAL ENGINEERING
INDIAN INSTITUTE OF TECHNOLOGY ROORKEE
ROORKEE - 247 667 (INDIA)
JUNE, 2006

CANDIDATE'S DECLARATION

I hereby declare that the work, which is being presented in the dissertation entitled **"ADSORPTIVE REMOVAL OF INDIGO CARMINE DYE FROM AQUEOUS SOLUTION USING LOW-COST ADSORBENTS"** in the partial fulfillment of the requirements of the award of the degree of Master of Technology in Chemical Engineering with specialization in Industrial Pollution Abatement, submitted in the Department of Chemical Engineering, Indian Institute of Technology Roorkee, Roorkee, is an authentic record of my own work carried out during the period from June 2005 to June 2006 under supervision of Dr. I. D. Mall, Professor, Department of Chemical Engineering, Indian Institute of Technology Roorkee, Roorkee.

The matter embodied in this dissertation has not been submitted by me for the award of any other degree.

Date: June 30, 2006.

Place: Roorkee.

(UMA RAJYA LAKSHMI .T)

CERTIFICATE

This is to certify that the above statement made by the candidate is correct to the best of my knowledge and belief.

(Dr. I. D. MALL)
Professor,
Department of Chemical Engineering,
Indian Institute of Technology Roorkee,
Roorkee – 247 667 (India).

ACKNOWLEDGEMENT

I express my deep sense of gratitude to my guide **Dr. I. D. Mall,** Professor, Department of Chemical Engineering, Indian Institute of Technology Roorkee, Roorkee, for his keen interest, constant guidance and encouragement throughout the course of this work, his experience, assiduity and deep insight of the subject held this work always on a smooth and steady course. Useful criticism and constant help extended in the hours of need had been immensely useful.

Thanks are due to Dr. Shri Chand, Professor and Head, Department of Chemical Engineering, Indian Institute of Technology Roorkee, Roorkee, for providing various facilities during this dissertation.

I would like to thank Dr. Vimal Chandra Srivastava, Lecturer, Department of Chemical Engg. and Technology, Banaras Hindu University, Varanasi, for his support, advice and interest shown in my work. I am also thankful to Mr. Dilip Lataye and Mr. S. Mahesh, Reaserch Scholars, Pollution Abatement Research Lab, IIT Roorkee, Roorkee, for their constant help and advice throughout my work.

I am thankful to Shri B. K. Arora (Senior Technical Assistant) and Shri Ayodhya Prasad (Senior Lab. Attendant), Pollution Abatement Research Lab., Dept.of Chemical Engineering., IIT Roorkee, Roorkee for their continuous help during the experimental work. I am greatly indebted to all my friends whose enthusiastic support, encouragement and help, made me come up with this report. Though it is not possible to mention everyone, none can be forgotten for their direct/indirect help.

It is very hard to express my feeling in proper words for my family members who, apart from providing me the best available education, have encouraged me in all my endeavors. I owe much of my academic success to them.

Uma Rajya Lakshmi .T

ABSTRACT

Dyes and Dye Intermediates industry is an important sector of the Indian Chemical Industry. The Indian companies together account for around 6.6 % of the world production. Dyes and pigments are widely used in textile, leather, paper, plastic, food and other industries. India produces 64,000 tonnes of dyes, 2 percent of which - 7,040 tonnes are directly discharged into the environment.

Discharging large amount of dyes into water resources, accompanied by organics, bleaches, and salts, can affect the physical and chemical properties of fresh water. The colour of the effluent discharged into receiving waters affects the aquatic flora and fauna, and causes many water borne diseases. Many dyes and pigments have toxic as well as carcinogenic, mutagenic and teratogenic effects on aquatic life and also on humans. The dyes are, generally, stable to light, oxidizing agents and heat, and their presence in wastewaters offers considerable resistance to their biodegradation, and thus upsetting aquatic life. Ludhiana, Panipat, Pali, Bichchri, Patancheru, Jetpur, Ahmedabad, Surat and Tirupur are some of the country's most polluted zones.

Various treatment processes used for the removal of dyes from the waste water include adsorption, coagulation and sedimentation, chemical oxidation, photochemical, electrochemical technique, chlorination, ozonation, irradiation, ion exchange, reverse osmosis, membrane separation, biological treatment, etc. Adsorption is the best available techniques for the removal of dyes from the waste water which is economically feasible. Variety of adsorbents are available which can be utilized for treatment of dye bearing wastewater. Usually activated carbon is used for adsorption. But due to its high cost there is need of low cost adsorbent. During recent years large numbers of low cost adsorbents have been investigated.

In the present study Bagasse fly ash (BFA) and Rice husk ash (RHA) are used for the removal of Indigo Carmine (IC) from the aqueous solution and adsorption studies have been carried out for evaluating their suitability as low cost adsorbents. Batch studies were conducted to see the effects of various parameters like pH, adsorbent dose, initial

concentration of IC dye, contact time and temperature on the removal of Indigo Carmine dye using bagasse fly ash (BFA) and rice husk ash (RHA).

Kinetic study shows that adsorption of Indigo Carmine on rice husk ash and bagasse fly ash follows the second order kinetics. Percent removal of Indigo Carmine dye increases with the increase in adsorbent amount for both RHA and BFA. But the percent removal of Indigo Carmine decreases with increase in Indigo Carmine concentration for both RHA and BFA. The kinetic study shows that the adsorption of IC follows Pseudo-second order kinetic model for both RHA and BFA. Freundlich isotherm best-fitted the isotherm data for IC adsorption on RHA and BFA at almost all temperatures. However, the error analysis values and the non-linear correlation coefficients, R^2, are comparable for Freundlich and Langmuir isotherms. Hence any one of the isotherms could be used for IC adsorption on RHA and BFA. Adsorption increases with increase in temperature for both the adsorbents, showing the endothermic nature of adsorption.

CONTENTS

NOMENCLATURE

C_o	Initial concentration of effluent
C_e	Concentration of adsorbate solution at equilibrium (mg/l)
K	Adsorption rate constant (1/min)
K_L	Langmuir isotherm constant, (l/mg)
K_T	Temkin isotherm constant, (l/mg)
K_F	Freundlich isotherm constant, $((mg/g)/(mg/l)^{1/n}$
$1/n$	Heterogeneity factor, dimensionless
Q_t	Amount of adsorbate adsorbed per unit amount of adsorbent at time t, (mg/g)
Q_e	Amount of adsorbate adsorbed per unit amount of adsorbent at equilibrium, (mg/g)
R_L	Separation Factor
k_f	First order rate constant, (1/min)
k_s	Second order rate constant, (g/mg min)
h	Initial sorption rate, mg/g min
$\Delta G°$	Gibbs free energy, (KJ/mol)
$\Delta H°$	Enthalpy, (KJ/mol)
$\Delta S°$	Entropy, (J/ mol K)
R	Universal gas constant, 8.314 J/K mol
SSE	Sum of the Squares of the Errors
SAE	Sum of the Absolute Errors
ARE	Average Relative Error
HYBRID	Hybrid Fractional Error Function
MPSD	Marquardt's Percent Standard Deviation
n	Number of data points
p	Number of parameters
α	Bangham constant (<1)

LIST OF FIGURES

LIST OF TABLES

CHAPTER-1

INTRODUCTION

Over the last decade, India has successfully emerged as one of the fastest developing countries around the globe and chemical industry is one of its fastest growing sectors. It ranks 12th by volume in the world production of chemicals with dyes and pigment industry being one of the major segments. The Indian dye industry is valued at approximately $3 billion with an estimated export of about 1 billion. India is now the second largest producer of dyes and intermediaries in Asia. The Central Pollution Control Board (CPCB), government of India, puts their number at 900 units. The production is estimated to be around 60,000 tonnes or about 6.6 per cent of the world production. There are around 700 varieties of dyes and dye intermediaries produced in India (http://www.centralchronicle.com/20050228/2802303.htm). In spite of large production of dyes and their intermediates, the per capita consumption of India is very low (50 g) as compared to world average (400 g). The dye industry in India has about 90% of concentration on the West Coast of India i.e., Maharashtra and Gujarat due to availability of raw materials and pre-dominance of textile industry in these states. The main domestic markets are Rajasthan, Gujarat, Maharashtra, Tamilnadu, Haryana and Uttar Pradesh (http://www.agriculture-industry-india.com/agricultural-commodities/dye.html). Within India, the major players in the pigments industry are Colour Chem and Sudarshan Chemicals while in the dyestuff industry companies such as are Atul, Clariant India, Dystar, Ciba Specialities and IDI are important players (http://myiris.com/shares/sectors/sectorReport.php?secode+DYESTUFF&peercode=AII &fname=./data/dyestuff/dyestuff.htm).

Most of the dyes being used in different industries have not been evaluated for their impact on health and the environment. Yet, they are widely used by textiles, leather, paper, paints, plastics, printing, pharmaceutical, lubricant, cosmetic industries and food industry. Faced with spiraling labour and environment costs, developed countries are slowly disengaging themselves from the manufacture of dyestuffs. Lack of enforcement

and monitoring of regulations related to environment also made the industrializing countries like India, a lucrative place to set up polluting industries. Now in India, the detrimental nature of the synthetic dye industry has been recognized. The CPCB has included it in its "hyper-red" category reserved for the seventeen most polluting industries in the country.

Dyes and pigments are an environment and health problem as cellulose dyeing uses massive amounts of salt, whose presence in effluent leads to very high quanta of total dissolved solids in the surface water to which the effluent is discharged. Dyes and colour pigments also contain metals such as copper, nickel, chromium, mercury and cobalt. Metals are difficult to remove from wastewater and may escape the capacities of the effluent treatment system. Moreover, the unused dyes and colour released in effluent from dyeing vats, interferes with the transmission of light in the water bodies that receive the effluent, which in turn inhibits the photosynthesis activity of aquatic biota besides direct toxic effects on biota. Several textile and food dyes, and dye intermediates like benzidines, have been linked to carcinogenicity, such as dye intermediaries like benzidines. The large number of dyes and high potential for toxicity of dyes and its component has made this class of compounds the most extensively reviewed and regulated under various pollution acts around the world.

1.1 CLASSIFICATION AND CONSUMPTION PATTERN OF DYES

Dyestuff is a broad term which includes dyes and pigments. A dye is a coloured substance or an organic compound, which when applied in a solution to a fabric, imparts a colour resistant to washing. They are largely used by the textiles, paper and leather industry, with textiles accounting for over 80% in India. This links the dyestuff industry's fortunes to that of the textile industry. Dyes are classified according to various systems. The detailed description of dyes is given in chapter 2. The most commonly used one is the one used by the US International Trade Commission. According to this system, there are different types of dyes and their applications, as given in Table 1.1. The different types of dyes used in paper industry are given in Table 1.2.

Table 1.1. Classification of dyes and their applications

Group	Application
Acid	Wool, silk, paper, synthetic fibers, leather
Azoic	Printing Inks and Pigments
Basic	Silk, wool, cotton
Direct	Cotton, cellulosic and blended fibers
Disperse dyes	Synthetic fibers
Reactive	Cellulosic fiber and fabric
Mineral and pigments dyes	Cotton, cellulosic, blended fabric, paper
Sulphur	Cotton, cellulosic fiber
Vat dyes	Cotton, cellulosic and blended fiber

Source: *Best Management Practices for Pollution Prevention in the Textile Industry,* EPA, Office of Research and Development, 1995; Snowden- Swan, L.J. "Pollution Prevention in the Textile Industries," in *Industrial Pollution Prevention Handbook,* Freeman, H.M. (Ed.), McGraw-Hill, Inc., New York, 1995.

Table 1.2. Dyes used in paper industry

Sl No.	Dyes	Quality of Paper	Consumption in Coloured Paper Board, kg per tonne of paper
1.	Methylene Blue	File board, maplitho	2.5 - 3.5
2.	Brilliant Green	Cover paper	0.8 - 1.0
3.	Methyl Violet	Violet poster, maplitho paper, cream wove, coloured wove	8.0 - 9.0
4.	Scarlet Red	File board	0.6 - 1.0
5.	Acid Orange	Buff board, buff manila board	5.0 - 6.0
6.	Malachite Green	File board, coloured	1.0 - 2.0
7.	Metanil Yellow	File board, coloured poster	2.5 - 4.5

1.2 DISCHARGE STANDARDS FOR INDUSTRIAL WASTEWATERS

Standards for the discharge of wastewaters from various industries are directly linked to the wastewater regulations and the water pollution control policies in force in the country/state concerned. After reviewing the technological capability and the limitations of the wastewater treatment systems as existing in the industries; CPCB has set Minimal National Standards (MINAS), for the discharge of pollutants from various industries. MINAS for a particular industry is the effluent standard achievable by the industry by installing pollution control measures which are within the techno-economic capability of the industry and MINAS should not be violated under no circumstances. MINAS for some dye utilizing industries are tabulated below.

Table 1.3. MINAS for Cotton textile industries (composite and processing)

	Parameter	Concentration not to exceed, milligram per liter (except for pH and bioassay)
Common :	pH	5.5. to 9.0
	Suspended solids	100
	Bio-chemical oxygen demand, 3 days at 27 °C	150
	Oil and grease	10
	Bio-assay test	90% survival of fish of after 96 hours in 100% effluent
Special :	Total chromium (as Cr)	2
	Phenolic compounds (as C_6H_5OH)	5

Source: http://www.cpcb.nic.in/standard41.htm

Table 1.4. MINAS for Dye and Dye Intermediate Industry

Parameter	Concentration not to exceed milligrams per liter (except for pH, temperature and bio-assay)
pH	6.0 – 9.0
Colour Hazen Unit	400.0
Suspended Solids	100.0
BOD (3 days at 27 °C)	100.0
Oil and Grease	10.0
Phenolics as C_6H_5OH	1.0
Cadmium as Cd	0.2
Copper as Cu	2.0
Manganese as Mn	2.0
Lead as Pb	0.1
Mercury as Hg	0.01
Nickel as Ni	2.0
Zinc as Zn	5.0
Chromium as Cr^{6+}	0.1
Total Chromium	2.0
Bio-assay test	90% survival in 96 hours.

Source: http://www.cpcb.nic.in/standard24.htm, EPA Notification GSR 742(E) dt.,30th Aug., 1990

1.3 TOXICITY OF COLOUR AND DYES

The dye effluents are considered to be highly toxic and affect the symbiotic process by disturbing the natural equilibrium by reducing photosynthetic activity and primary production due to the colourization of the water. Effluents contain significant level of organic contaminants, which are toxic as they create odour, bad taste, unsighty colour, foaming etc.

Dyes and pigments are widely used in textile, leather, paper, plastic, paints, printing, pharmaceutical, lubricant, cosmetic and other industries. The effluents of these industries are characterized by fluctuating pH with large load of suspended

solids, COD and are laden with colour. The dyes, generally, have complex aromatic structures which provide them physico-chemical, thermal and optical stability i.e., they are stable to light, oxidizing agents and heat. Hence they offer considerable resistance to their biodegradation, causing aesthetic, acute and chronic toxicity problems in receiving waters thus, upsetting aquatic life. Dyes accumulate in sediments at many sites, especially at locations of wastewater discharge, which has an impact on the ecological balance in the aquatic system. Ground water systems are also affected by these pollutants because of leaching from soil (Sharma et al., 1999). Thus, dyes in wastewater have to be removed before it is discharged into a water body or on land. Different dyes used in industry and their effects are given Table 1.6.

Table 1.5. Dyes used in Industry and their possible effects

Dye	Possible Effect
Aniline blue	Bladder carcinogen
Auramine O	Bladder carcinogen and mutagen
Congo red	Highly toxic, mutagen and irritant
Fast green	Animal carcinogen
Indigo carmine	Mutagen
Malachite green	Systemic poison
Orange G	Mutagen
Uranyl nitrate	Radioactive and oxidising agent

Sanganer town, district Jaipur (Rajasthan, India), is famous for its dyeing and printing industries. There are about 400 industries involved in textile printing processes, which discharge effluents into nearby ponds and drains, without any treatment. These effluents contain highly toxic dyes, bleaching agents, salts, acids, and alkalis. Heavy metals like cadmium, copper, zinc, chromium, and iron are also found in the dye effluents. Textile workers are exposed to such waters with no control over the length and frequency of exposure. Further, as the untreated effluents are discharged into the

environment they can cause severe contamination of surface and underground water. Environmental pollution caused by such textile effluents results in adverse effects on flora, fauna, and the general health of not only the textile workers, but also the residents of Sanganer town. Studies clearly indicated that the effluents and the surface water of Amani Shah drainage have high mutagenic activity. Further, the drainage water and the dry bed of the drainage (during summer months) are not fit for agricultural or other recreational purposes. A low level of mutagenicity in the underground water of Sanganer again emphasizes the grave pollution problem existing in the area (mathur et al., 2005).

In addition, some dyes like Malachite green (MG) are highly cytotoxic to mammalian cells and act as a tumor-enhancing agent. These dyes may enter into the food chain and could possibly cause carcinogenic, mutagenic and teratogenic effects on humans.

1.4 TREATMENT METHODS OF DYE BEARING WASTE WATER

The dyestuff industry is one of the heavily polluting industries. The discharge of dye wastewater into the environment causes various pollution problems. Hence the ubiquitous colour needs to be regulated. The new drinking water standards prescribed by the Bureau of Indian Standards (IS 10500) set colour standards at 5 colour units as the desirable limit and 25 colour units as the permissible limit in the absence of alternate source. But removing the colour from effluents is extremely difficult. There is no universally applicable technique for all conditions. Research and development, therefore focuses on sector-specific methods and technologies to remove colour and similar contaminants from different kinds of waste streams. Depending on the quantum, concentration, toxicity, and presence of non biodegradable organics in the industrial wastewater, its treatment may consist of any one or more of the following processes:

- Chemical Processes, enhance the degradation of volatile organic compounds present at low concentrations in contaminated media. These processes offer some distinct advantages over more conventional technologies, which merely, separate and transfer the contaminants from one phase to another

- Physical processes are used to substantially remove floating and settleable solids in wastewater. This process include screening, sedimentation, adsorption, membrane filtration, ion exchange, Irradiation, Electrokinetic coagulation.
- Biological treatment, in which bacteria break down the organic parts of wastewaters; usually accomplished by bringing the wastewater and bacteria together in trickling filters, aerobic, anaerobic or in the activated sludge process.

1.4.1 Chemical Treatment Methods

Various chemical methods are Oxidative processes, H_2O_2-Fe (II) salts (Fentons reagent), Ozonation, Photochemical, Sodium hypochloride (NaOCl), electrochemical destruction. In recent years there has been increasing interest in the use of electrochemical methods for the treatment of wastewaters. The organic and toxic pollutants present in treated wastewaters such as dyes and phenols are usually destroyed by a direct anodic process or by an indirect anodic oxidation via the production of oxidants such as hydroxyl radicals, ozone, etc. Many dyes may be effectively decolorized using chemical oxidizing agents such as chlorine in the form of liquid or gas. Ozone is a more powerful oxidant than chlorine and it is used for oxidizing dye wastewater. Environmentally, H_2O_2 is a friendly oxidant (Daly et al., 2005).

The degradation of organic matter in coloured solutions of different classes of dyes by ozonation in the presence of activated carbon is investigated. The combination of activated carbon with ozone enhanced the decolourization of the solutions and especially the mineralization of the organic matter. Activated carbon acts both as an adsorbent and as a catalyst in the reaction of ozonation (Faria et al., 2005).

Heterogeneous photocatalysis has been considered as a cost effective alternative for the purification of dye containing wastewater. Indeed recent studies have demonstrated that photocatalysis can be used to mineralize organic compounds or degrade dyes using TiO_2 under UV irradiation. Moreover, photocatalysis does not require expensive oxidants and can be carried out at mild temperature and pressure (EPA Hand Book, Advanced Photochemical Oxidation Processes, Dec 1998).

1.4.2 Physical Treatment Methods

Physical treatment methods for the removal of dyes are Membrane filtration, Ion exchange, Electrokinetic coagulation, Adsorption. Surfactants and dyes with high molecular weights are successfully removed by the coagulation/flocculation processes followed by sedimentation, flotation and filtration, respectively. The main advantage of the conventional processes like coagulation and flocculation is decolourization of the waste stream due to the removal of dye molecules from the dye bath effluents, and not due to a partial decomposition of dyes, which can lead to an even more potentially harmful and toxic aromatic compound. The major disadvantage of coagulation/flocculation processes is the production of sludge which results in high disposal costs. However, amount of sludge could be minimized if only a low volume of the highly coloured dye bath could be eliminated by chemical treatment directly after the dyeing process (Golob et al. 2005).

Membrane filtration method has the ability to clarify, concentrate and, most importantly, to separate pollutants continuously from effluent. It has some special features unrivalled by other methods; resistance to temperature, an adverse chemical environment, and microbial attack. The concentrated residue left after separation poses disposal problems, and high capital cost and the possibility of clogging, and membrane replacement are its disadvantages. This method of filtration is suitable for water recycling within a plant if the effluent contains low concentration of pollutants, but it is unable to reduce the dissolved solid content, which makes water re-use a difficult task.

Ion exchange has not been widely used for the treatment of dye-containing effluents (Slokar and Le Marechal, 1998). Advantages of this method include no loss of adsorbent on regeneration, reclamation of solvent after use and the removal of soluble dyes. But this method is not economical as far as the cost is concerned.

Electrokinetic coagulation is an economically feasible method. It involves the addition of ferrous sulphate and ferric chloride, allowing excellent removal of pollutants from wastewaters. Unfortunately, because of high cost of the ferrous sulphate and ferric chloride, this method is not used widely. Production of large amount of sludge occurs, and this results in high disposal costs. Adsorption techniques have gained favor recently due to their efficiency in the removal of pollutants too stable for conventional methods.

Adsorption is a simple and economical method for wastewater treatment. Decolourization is a result of two mechanisms: adsorption and ion exchange and is influenced by many physio-chemical factors, such as, dye/ sorbent interaction, sorbent surface area, particle size, temperature, pH, and contact time. Adsorption is well recognized as a unit operation for the removal of impurities present in trace amounts from wastewater which otherwise cannot be removed efficiently. These include heavy metals, non-biodegradable organic compounds like phenols, toxic substances, dyes etc. It has been used for taste and odour control in water and wastewater treatment. Almost complete removal of impurities with negligible side effects explains its wide application in tertiary treatment stages and polishing stages. A comparative study has been done by Marmagne et al., 1996, for removal of colour and COD using different methods of treatment as coagulation-flocculation, membrane-treatment, activated carbon treatment and ozonation.

1.4.3 Biological Treatment Methods

The removal of colour by using biological treatment is widely used. The use of white rot fungus, strain L-25 (Hamedaani et al., 2007), wood rotting fungus (Zhang et al., 1999), Bjerkandera sp. Strain BOL 13 (Axelsson et al., 2006) has been used for effective colour removal. Other fungi such as, Hirschioporus larincinus, Inonotus hispidus, Phlebia tremellosa and Coriolus versicolor have also been shown to decolorize dye-containing effluent (Banat et al., 1996; Kirby, 1999).

1.5 INDIGO CARMINE: PROPERTIES, USES AND HEALTH EFFECTS

The chemical structure of indigo was determined by Prussian chemist J. F. W. Adolf von Baeyer in 1883. It is normally produced by a synthesis of indoxyl by fusion of sodium phenylglycinate in a mixture of caustic soda and sodamide. Indigo carmine is a blue synthetic coal tar dye, is used in textile industry for dyeing of clothes (blue jeans) and other blue denim, in food industry (typical products include milk deserts, sweets, biscuits), cosmetics industries, as a diagnostic aid (e.g. in kidney function tests) and as a redox indicator in analytical chemistry i.e. as a titrimetric indicator of Cr(II), Sn(II), Fe(III), and Ti(III). Indigo carmine is also used as a photometric detector, and a

biological stain. The molecular structure of Indigo Carmine is shown in Fig 1.1 and properties and health effects of Indigo Carmine are summarized in Table 1.6.

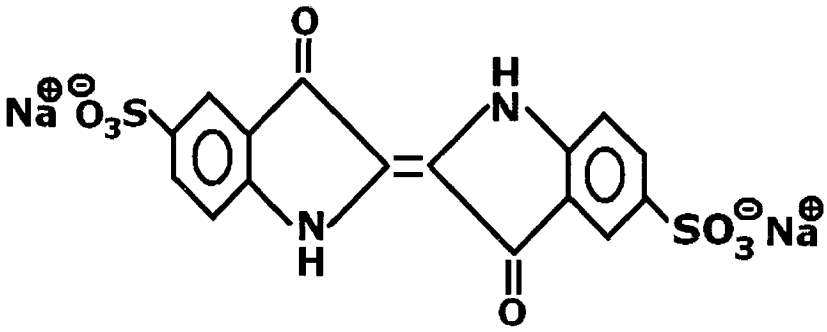

Fig 1.1 Molecular structure of Indigo Carmine

Table 1.6. Properties and health effects of Indigo Carmine.

Chemical Name	Acid Blue 74
Colour Index	73015
Chemical Formula	$C_{16}H_8N_2O_8S_2Na_2$
Molecular Weight	466.35
Appearance	Dark Blue to Purple Powder
Odor	Odorless.
Melting Point	Not available
Vapor Pressure	Not applicable
Boiling Point	Not available
Stability	Stable. Incompatible with nitric acid, chlorates, and other strong oxidizing agents
Hazardous Decomposition Products	May form carbon oxides (CO, CO_2), nitrogen oxides (NO_x), sulfur oxides (SO_x) and some metallic oxides when heated to decomposition (**Prepared by:** Environmental Health & Safety, (U.S.A.)).
Potential Health Effects	There is no data available on the effects of

	this dye on humans. However, tests on laboratory animals have shown that the dye is a mutagen and highly toxic
Inhalation	May cause irritation to the respiratory tract. Symptoms may include coughing and shortness of breath
Ingestion	Causes irritation to the gastrointestinal tract. Symptoms may include nausea, vomiting and diarrhea
Skin Contact	May cause irritation with redness and pain
Eye Contact	Hazardous in case of eye contact (irritant)
LD_{50}	2000 mg/kg [Rat], 2500 mg/kg [Mouse]

1.6 OBJECTIVES OF THE PRESENT STUDY

The objective of this study is to investigate the feasibility of Bagasse Fly Ash (BFA) and Rice Husk Ash (RHA) for the removal of Indigo Carmine dye, which is commonly used in textile industry as well as food industry, from aqueous solution. The whole study deals with various parameters dealing with adsorption and adsorption kinetics. The experiments were carried out to study the following:

1. Characterization of Rice Husk Ash and, Bagasse fly ash which includes particle size distribution, proximate analysis, etc.
2. Study the effect of adsorbent dose, contact time, pH, initial concentration and temperature on the removal of Indigo Carmine from aqueous solution by batch process.
3. Study the kinetics of Indigo Carmine using Lagergren (Pseudo-first-order model), Pseudo second order and Weber Morris equations.
4. Study of equilibrium data for removal efficiency of the adsorbent using Freundlich, Langmuir, Dublin-Redushkevih and Temkin isotherms.

CHAPTER-2

LITERATURE REVIEW

The dyestuff industry is one of the heavily polluting industries. The discharge of dye bearing wastewater into the environment causes various pollution problems by affecting the aquatic flora and fauna, and may cause many water borne diseases. Some dyes are carcinogenic and others after transformations or degradation yield compounds such as aromatic amines, which may be carcinogenic or otherwise toxic as discussed in chapter 1. Hence the ubiquitous colour needs to be regulated. But removing the colour from effluents is extremely difficult. There is no universally applicable technique for all conditions. Research and development, therefore, focuses on sector-specific methods and technologies to remove colour and similar contaminants from different kinds of waste streams. Depending on the quantum, concentration, toxicity, and presence of non biodegradable organics in the industrial wastewater, its treatment may consist of any one or more of the chemical, physical and biological methods.

Various chemical methods used for the treatment of dye bearing wastewaters are Oxidative processes, H_2O_2-Fe (II) salts (Fentons reagent), Ozonation, Photochemical, Sodium hypochloride (NaOCl) and Electrochemical destruction. Physical treatment methods for the removal of dyes are adsorption, membrane filtration, ion exchange, electrokinetic coagulation etc. The removal of colour by using biological treatment is widely used. The use of white rot fungus, strain L-25 (Hamedaani et al., 2007), wood rotting fungus (Zhang et al, 1999), *Bjerkandera* sp. Strain BOL 13 (Axelsson et al., 2006) has been used for effective colour removal. Types of dyes, toxicity of dyes and a critical literature review of all these methods are discussed in this chapter.

2.1 DIFFERENT TYPES OF DYES

2.1.1 ACID DYES

Acid dyes are salts of sulphonic acids consisting very large molecules of linked aromatic rings. Acid dyes usually have a sulphonyl or amino group on the molecule,

hence, are soluble and form coloured anions in water. They are applied in weakly acid medium often vinegar (acetic acid) or citric acid.

Acid dyes have high water solubility and form neutral or slightly alkaline water solution. They have fair to good light fastness. Because of their low affinity for wood fibres, dye retention aids must be used. They are sensitive to heat (migrate on dryers) and are excellent for calender dyeing.

They are used for dying silk, wool and nylon. Acid dyes are thought to fix to fibers by hydrogen bonding. Attachment to the fibre is attributed, to salt formation between anionic groups in the dyes and cationic groups in the fibre. Acid dyes are not substantive to cellulosic fibres. Some acid dyes are used to colour food.

2.1.2 AZO DYES

Azo dyes are derived from amino compounds. They are insoluble dyes that are not applied directly as dyes, but are absorbed on the surface of the substance to be dyed. The colours are not fast. Azo dyes are used for cotton, silk and rayon. Azo dyes became the most important commercial colorants because of their wide colour range, good fastness properties, and tinctorial strength (colour density), which is twice that of the anthraquinones.

2.1.3 BASIC DYES

Basic dyes are water soluble cationic dyes which are mainly applied to acrylic fibres but find some use for wool, and silk. Usually acetic acid is added to the dye bath to help the take up of the dye onto the fibre. A mordant, usually a metallic salt is used to increase the affinity of the fabric for the dye. Basic dyes include the most brilliant of all the synthetic dyes known and are used to produce bright and deep shades with good light and wash. Basic dyes are also used in the coloration of paper.

2.1.4 DIRECT DYES

Chemically direct dyes are salts of complex sulfonic acids. They are soluble in water and have an affinity for a wide variety of fibers. Mordants are not used as direct dyes are capable of forming hydrogen bond with molecules of the fabric and can be applied directly on the fabric. Dyeing is normally carried out in a neutral or slightly

alkaline dye bath, at or near the boil, with the addition of either sodium chloride (NaCl) or sodium sulphate (Na_2SO_4). Direct dyes are used on cotton, paper, leather, wool, silk and nylon. They do not dye acetate rayon and synthetic fibres. Direct dyes can be applied well at low temperatures and are therefore suitable for tie-dyeing and batik work. They are also used as pH indicators and as biological stains. Generally these dyes are used where high wash fastness is not required.

2.1.5 REACTIVE DYES

The dyes contain a reactive group, either a haloheterocycle or an activated double bond, that, when applied to a fibre in a weakly alkaline dye bath, forms a chemical bond with an hydroxyl group on the cellulose fibre dyed and cannot be removed by washing or boiling. The main feature of the dyestuff is its low affinity to cellulose; therefore large amounts of salt are required to force its deposition on the fabric. These dyes are soluble in water and are salted out of solution onto the fiber where they are made to react chemically within the fibers. Reactive dyes are used where bright dyeing with high light and wash fastness is required. Fastness properties are generally good except to chlorine.

2.1.6 SULPHUR DYES

Sulfur dyes are relatively inexpensive; they are insoluble in water and have no affinity for the fiber until reduced with alkaline sulfide compounds. They are applied to the fiber in a reduced state and oxidized within the fiber to an insoluble dye again. Shades in Sulfur dyes are dull; therefore these dyes are used chiefly for black. They are cheap, easy to apply and possess good wash and light fastness and satisfactory for dry crocking. They should be classed as poor for wet crocking and chlorine fastness. An outstanding member of this family is Sulphur black.

2.1.7 VAT DYES

Vat dyes are insoluble compounds and have no affinity for the fibers until reduced with caustic soda and hydro. Because of the high alkali concentration in the dye bath, pure vat dyes cannot be used on animal fibres, (wool, natural silk, and various hairs). Solubilized vat dyes, not requiring the presence of alkali, can be used for dyeing on

animal fibres. Vat dyes are used in cotton dyeing where high wash and boil fastness required. Indigo is one of the most important members of this group. Because they are dyed at low temperatures, they are used in batik dyeing for green shades. Reasonably bright shades can be produced except for brilliant red. Generally vat dyes are the most expensive and are the best class for chlorine fastness.

2.1.8 MORDANT DYES

As the name suggests these dyes require a mordant. This improves the fastness of the dye on the fibre such as water, light and perspiration fastness. The choice of mordant is very important as different mordants can change the final colour significantly. Most natural dyes are mordant dyes and there is therefore a large literature base describing dyeing techniques. The most important mordant dyes are the synthetic mordant dyes (chrome dyes) used for wool, especially useful for black and navy shades. The mordant used is potassium dichromate applied as an after-treatment.

2.1.9 NAPHTHOL DYES

Naphthol dyes are classified as fast dyes, usually slightly cheaper than Vat dyeings; the methods of application are complex and the range of colors limited. Brilliant reds are the most important but Naphthol dyes are also used for maroon, brown and black. Naphthol dyes are insoluble azo dyestuffs that are produced on the fiber by applying a Naphthol to the fiber and then combining it with a diaqotized base or salt at a low temperature to produce an insoluble dye molecule within the fiber. Crocking fastness varies with shades but washing fastness is equal to Vat dyeings, generally with less light fastness than the Vats.

2.1.10 DISPERSE DYES

Disperse dyes are originally developed for the dyeing of cellulose acetate. They are substantially water insoluble. The dyes are finely ground in the presence of a dispersing agent. They can also be used to dye nylon, triacetate, polyester and acrylic fibres. In some cases a dyeing temperature of 130 ^{o}C is required and a pressurised dye bath is used. The very fine particle size gives a large surface area that aids dissolution to

allow uptake by the fibre. The dyeing rate can be significantly influenced by the choice of dispersing agent used during the grinding. Their fastness properties vary with the dye, color and fiber on which they are used; on acrylics their fastness properties are generally inferior to Basic or Acid dyes.

Basically developed for dyeing of acetate fibres, disperse dyes are also used for dyeing of polyamide (Nylon) and acrylic (Orlon & Acrylan) fibres. With the addition of 'carriers' or swelling agents these dyes are also used in dyeing of Polyester (Terylene, Tetron, Dacron, etc.).

2.2 SOURCES OF DYE BEARING WASTE WATER AND ITS TOXICITY

The production of dyes in India has been estimated to be around 60,000 tonnes or about 6.6 per cent of the world production. Most of the dyes being used in different industries have not been evaluated for their impact on health and the environment. Yet, they are widely used by textiles, leather, paper, paints, plastics, printing, pharmaceutical, lubricant, cosmetic industries and food industry. Cotton textile industry wastewater generated by the different production steps (i.e. sizing of fibers, scouring, desizing, bleaching, washing, mercerization, dyeing and finishing) has by-products (hydrolyzed dye), some intact dye, auxiliary chemicals, high pH and temperature. It also contains high concentrations of organic matter, non-biodegradable matter, toxic substances, detergents and soaps, suspended and dissolved solids and alkalinity. Wastewater generation from a typical dyeing facility is estimated at 3800 to 7500 m^3 per day (http://www.p2pays.org/ref/11/10489/sectors73ak.html). The typical sources and quantum of wastewater generated are given in Table.2.1.

Table. 2.1. Sources and quantum of wastewater generated in a typical Textile industry.

S. No	Type of Operation	Spent Liquor (lit/kg of yarn)	WashWater (lit/kg of yarn)	Total (lit/kg of yarn)
1.	Scouring	10-15	30-40	40-55
2.	Bleaching	20-25	40-50	60-75
3.	Dyeing	10-15	100-150	110-165

Source: http://www.wittsenvis.org/news_6_apr03.htm

Dyes and pigments are an environment and health problem as cellulose dyeing uses massive amounts of salt, whose presence in effluent leads to very high quanta of total dissolved solids in the water the effluent is released into. Dyes and colour pigments also contain metals such as copper, nickel, chromium, mercury and cobalt. Metals are difficult to remove from wastewater and may escape the capacities of the effluent treatment system (http://www.centralchronicle.com/20050228/2802303.htm). Moreover, the unused dyes and colour released in effluent from dyeing vats, interferes with the transmission of light in the water body that receives the effluent. This in turn inhibits the photosynthesis activity of aquatic biota besides direct toxic effects on biota.

2.3 COLOUR

Colour measurement and representation

Colour can be defined of two types;

1. **True Colour**

   It is the colour of water from which the turbidity has been removed.

2. **Apparent Colour**

   It not only includes colour due to substance in solution, but also that due to suspended matter. Apparent colour is determined on the original sample without filtration or centrifugation.

The three methods of colour measurement;

1. Visual comparison method.
2. Spectrophotometric method.
3. Tristimulus filter method.

It should be noted that colour is pH dependent and when representing colour, pH should be indicated.

Out of the above methods spectrophotometric method is very useful and efficient in wide range of color solution. We can use it in two ways. First we can give the colour in the Hazen unit. 1 Hazen unit is corresponding to the colour of 1 mg/l solution of Pt-Co. We can make some different unit standard solutions by varying concentration of the Pt-Co solution.

Now we take the transmittance of the solution by spectrophotometer and make a calibration chart. Now the sample is taken, the turbidity is removed and then transmittance is checked. This will give the colour unit of the sample.

Secondly if one do not require colour unit and only change is to be measured then there is no need to prepare calibration chart with Pt-Co solution. The calibration chart can be prepared by the sample only and at any stage we can check the concentration of the sample. The colour can also be represented as the load in kg per tonne of the effluent or kg per tonne of product produced.

2.4 ADSORPTION: BEST AVAILABLE TECHNIQUE FOR REMOVAL OF DYES

The Treatment of textile effluents is of interest due to their toxic and esthetic impacts on receiving waters. While much research has been preformed to develop effective treatment technologies for wastewaters containing dyes, no single solution has been satisfactory for remediating the broad diversity of textile wastes. Human and ecological health concerns have prompted the government to require textile effluent discharges to have increasingly lower color and nitrogen levels.

Many chemical, physical and biological methods are generally used to remove dyes from the industrial effluent. A critical review of all these methods is discussed in this chapter. Physico-chemical processes like flocculation, electro-flotation, precipitation, electro-kinetic coagulation, ion exchange, membrane filtration, electrochemical destruction, irradiation and ozonation are generally used to treat dyes laden wastewater.

As there is a wide range in pH and dyes are highly coloured materials, which are difficult to decompose biologically, conventional Physico-chemical and biological treatment processes are not effective in removing dyes from wastewaters. Moreover all these processes are costly and cannot be used by small industries to treat the wide range of dye wastewater.

By comparing all these methods, adsorption process provides an attractive alternative treatment for dye bearing waste water, especially if the adsorbent is inexpensive and readily available. Adsorption produces a high quality product, and is a process which is economically feasible (Choy et al., 1999).Almost complete removal of

impurities with negligible side effects explains its wide application for the treatment of dye bearing waste water. Granular activated carbon (GAC) is the most popular adsorbent, which has been used with great success. However, GAC is expensive and its regeneration and reuse makes it more costly. Consequently, many investigators have studied the feasibility of using low-cost substances for the removal of various dyes and pollutants from wastewaters.

2.5 LITERATURE REVIEW

Due to lack of adequate literature available on the adsorption of Indigo Carmine (IC) dye, help has been taken from other researcher's work on adsorption of different dyes. The literature followed during the complete dissertation work is presented in Table 2.1 and also briefly explained in the following paragraphs.

Researchers like Kasgoz, 2005, Prado et al., 2003, Fernanda et al., 2002, Othman et al., 2006, have worked on the adsorption of Indigo Carmine using different adsorbents. Kasgoz, 2005, effectively used Aminofunctionalized acrylamide–maleic acid hydrogels to adsorb IC. It was found that almost 70–80% of capacity was saturated within approximately 30 min and the adsorption capacity increased at acidic pH and also in presence of NaCl in dye solution. The Langmuir isotherm model was the best fit for these modified AAM–MA hydrogels–Indigo Carmine system. The highest adsorption capacity (660.8 mg/g) was observed for MH-2 polymer at pH 3.0.

Prado et al., 2003, studied the adsorption of IC on Hydrogels (SiHAPS and SiHAFL). Experimental data was well fit with modified Langmuir equation. The thermodynamic data showed endothermic enthalpic values: 12.31 ± 0.55 and 24.69 ± 1.05 kJ/mol for SiHAPS and SiHAFL surfaces, respectively. Gibbs free energies for two adsorption processes of indigo carmine dye presented negative values, reflecting dye/surface interactions must be accompanied by an increased in entropy values, which are 65 ± 3 and 98 ± 5 J/mol K for SiHAPS and SiHAFL materials, respectively. The adsorption processes for both materials were spontaneous in nature although they presented an endothermic enthalpy for the interaction, resulting in an entropically favored process.

Fernanda et al., 2002, suggested that chitosan can be used as an effective adsorbent for removal of Indigo carmine, IC dye (anionic dye), as its protonated amine groups adsorb the anionic species strongly from diluted solutions. It was shown that the increase in the temperature has decreased the adsorption of the dye. The adsorption results were well fitted to both Langmuir and Freundlich adsorption models. The enthalpy of interaction of −23.2 kJ/mol, encountered for all temperature ranges studied, suggests that the IC–chitosan adsorption is an exothermic process. Othman et al., 2006, used ZSM-5 zeolite modified by manganese (Mn/ZSM-5) and lanthanum (La/ZSM-5) for adsorption of IC. It was found that the decolorization activity showed comparably high rates for Mn/ZSM-5 and Mn–La/ZSM-5 samples (100% removal) implying that the adsorption process is more referred to acid-base site pairs where the photocatalytic activity seems to be more restricted to acidic sites. At pH > 3, the decolorization of the IC was negligible. An initial rapid phase for the first 5 min that was found to compromise 92% decolorization.

Many researchers like Krishna and Bhattacharya, 2005, Namasivayam et al., 2005, Wang et al., 2005, Kumar et al., 2005, Vadivelan et al., 2005, etc, have successfully worked on the adsorption of Methylene blue dye using various adsorbents. Krishna and Bhattacharya, 2005, used Neem (Azadirachta indica) leaf powder for adsorption of Methylene blue. It was found that 93% of the dye could be removed by 2 g of the Neem leaf powder from 1 L of an aqueous solution containing 25 mg of the dye at 300 K. The adsorption followed pseudo first order kinetics with a mean rate constant of 3.73×10^{-3} min^{-1} and an intraparticle diffusion rate constant of 6.36×10^{-2} mg g^{-1} $min^{-0.5}$. The experimental data yielded excellent fit with Langmuir and Freundlich isotherm equations. The adsorption of dye was endothermic in nature and was accompanied by an increase in entropy and a decrease in Gibb's free energy in the temperature range of 300 to 330 K.

Fe (III)/Cr (III) hydroxide, an industrial solid waste, was used to adsorb methylene blue and direct red 12B by Namasivayam et al., 2005. It was found that equilibrium adsorption data followed both Langmuir and Freundlich isotherms. The Langmuir adsorption capacity (Q_o) was found to be 5.0 and 22.8 mg dye per g of the adsorbent for direct red 12B and methylene blue, respectively. Adsorption followed

second order rate kinetics and was favored in acidic pH for direct red and in alkaline pH for methylene blue.

Wang et al., 2005, used fly ash and red mud as effective adsorbents. It was found that methylene blue adsorption on both the adsorbents was endothermic in nature with change in enthalpy value at 76.1 and 10.8 KJ/mol, for fly ash and red mud, respectively. Redlich-Peterson model provided the best correlation of experimental data. Temperature has a significant effect on adsorption for red mud while less influence for fly ash.

Fly ash was used as an adsorbent by Kumar et al., 2005, and it was observed that maximum color removal obtained at a pH of 8. Equilibrium data were represented well by a Langmuir isotherm equation with a monolayer sorption capacity of 5.718 mg/g. Sorption data were found to follow pseudo-second-order kinetics. The effective diffusion parameter D_i values were estimated at different initial concentrations and the average value was determined to be 2.063×10^{-9} cm^2/s. Vadivelan et al., 2005, used Rice husk as adsorbent. The equilibrium data were found to be well represented by the Langmuir isotherm equation. and the sorption kinetics followed a pseudo-second-order kinetic model. The average external mass transfer coefficient and intraparticle diffusion coefficient was found to be 0.01133 min^{-1} and 0.695358 mg/g $min^{0.5}$. The effective diffusion coefficient, D_i was calculated using the Boyd constant and was found to be 5.05×10^{-04} cm^2/s for an initial dye concentration of 50 mg/L.

Adsorption of Malachite Green (MG) using bottom ash (Gupta et al., 2004), bagasse fly ash (BFA) and activated carbon-commercial grade (ACC) and laboratory grade (ACL) (Mall et al., 2005) and rice husk-based porous carbons (RHCs) (Guo et al., 2003) is briefly given in Table 2.1. Biological treatment was also used for the adsorption of different dyes using live activated sludge system (Basibuyuk et al., 2003), activated sludge biomass (Chu et al., 2002) and activated sludge (Gulnaz et al., 2004) and Chemical catalytic reaction and biological oxidation (Ghoreishi et al., 2003).

Various chemical treatment methods for removal of dyes from wastewaters using TiO_2/SiO_2 photocatalyst (Chun et al., 2001), Electrochemical treatment (Grimau et al., 2006 and Jime´nez et al., 2000), Coagulation/flocculation (Golob et al., 2005), Ozonation in the presence of activated carbon (Faria et al., 2005), Photodegradation (Cisneros et al., 2002), Adsorption and nanofiltration (Chakraborty et al., 2005), were given in Table 2.1.

Table 2.2 Studies on removal of Dyes using various types of adsorbents used for adsorption and other treatment methods

References	Adsorbent	Adsorbate	Operating conditions, Batch/Column	Results and discussion
Kasgoz, 2005	Aminofunctionalized acrylamide–maleic acid hydrogels	Indigo Carmine	Batch	Almost 70–80% of capacity was saturated within approximately 30 min and quite high adsorption capacity was observed. The adsorption capacity increased at acidic pH and also in presence of NaCl in dye solution. The adsorption isotherm models were applied to the experimental data and it was seen that the Langmuir isotherm model was the best fit for these modified AAM–MA hydrogels–indigo carmine system. The highest adsorption capacity (660.8 mg/g) was observed for MH-2 polymer at pH 3.0. Also, the presence of NaCl in initial dye solution increased the adsorption capacity.
Prado et al., 2004	Chitin and chitosan	Indigo Carmine	Batch	Modified Langmuir isotherm model was the best fit for experimental data. The maximum number of moles adsorbed was $1.24 \pm 0.16\times10^{-5}$ and $1.54 \pm 0.03\times10^{-4}$ mol/g for chitin and chitosan, respectively. The thermodynamic data showed exothermic enthalpic values of -40.12 ± 3.52 and -29.25 ± 1.93 kJ/mol for chitin and chitosan, respectively. Gibbs free energies for the two adsorption processes of indigo carmine dye presented a positive value for chitin and a negative one for chitosan, reflecting that dye/surface interactions are thermodynamic favorable for chitosan and non spontaneous for chitin at 298.15 K. The interaction processes were accompanied by an increase of entropy value for chitosan (90 ± 6 J/mol K) and a decrease for chitin (-145 ± 13 J/mol K). Thus, dye/chitosan interaction showed favorable enthalpic and entropic processes, reflecting thermodynamic stability of the formed complex, while dye/chitin interaction showed an exothermic enthalpic value and a highly nonfavorable entropic effect, resulting in a nonspontaneous thermodynamic system.
Fernanda et al., 2002	Chitosan	Indigo Carmine	Batch	The studies were carried out by the batch method from 35 to 50 oC. The adsorption results were well fitted to both Langmuir and

				Freundlich adsorption models. The increase in the temperature decreased the adsorption of the dye. The enthalpy of interaction, −23.2 kJ/mol, when a monolayer of the dye was formed on the chitosan surface, was encountered for all temperature ranges studied. The spontaneity of the interaction is indicated by the change in Gibbs free energy values from −9.1 to −8.2 kJ/mol.
Prado et al., 2003	Hydrogels (SiHAPS and SiHAFL)	Indigo Carmine	Batch	Experimental data was well fit with modified Langmuir equation. The maximum number of moles adsorbed gave $6.82\pm0.12 \times 10^{-4}$ and $2.15\pm0.17 \times 10^{-4}$ mol/g for SiHAPS and SiHAFL, respectively.The thermodynamic data showed endothermic enthalpic values: 12.31 ± 0.55 and 24.69 ± 1.05 kJ/mol for SiHAPS and SiHAFL surfaces, respectively. Gibbs free energies for two adsorption processes of indigo carmine dye presented negative values, reflecting dye/surface interactions must be accompanied by an increased in entropy values, which are 65 ± 3 and 98 ± 5 J/mol K for SiHAPS and SiHAFL materials, respectively. The adsorption processes for both materials were spontaneous in nature although they presented an endothermic enthalpy for the interaction, resulting in an entropically favored process.
Othman et al., 2006	ZSM-5 zeolite modified by manganese (Mn/ZSM-5) and lanthanum (La/ZSM-5)	Indigo Carmine	Batch	The decolorization activity showed comparable high rates for Mn/ZSM-5 and Mn–La/ZSM-5 samples (100% removal) implying that the adsorption process is more referred to acid-base site pairs where the photocatalytic activity seems to be more restricted to acidic sites. At pH > 3, the decolorization of the IC was negligible. An initial rapid phase for the first 5 min that was found to compromise 92% decolorization.
Hachem et al., 2001	P25 Degussa catalyst.	Orange G, Congo Red, Indigo Carmine, Crystal Violet and Methyl	Batch	The kinetics of reaction have been studied and were found to be zero or first order with respect to the dyes. Adsorption was quite fast and the equilibrium concentration was reached within about 45 min. Acid dyes, Orange II, Orange G, Remazol Blue and Indigo Carmine exhibited a low adsorption while cationic dyes, Malachite Green and Crystal Violet were easily adsorbed. The addition of hydrogen

		Yellow		peroxide enhances the rate of degradation, which is of much interest for improving the quantum yield of degradation.
Krishna and Bhattacharya, 2005	Neem (Azadiracht a indica) leaf powder	Methylene blue	Batch	Ninety three percent of the dye could be removed by 2 g of the Neem leaf powder from 1 L of an aqueous solution containing 25 mg of the dye at 300 K. The adsorption followed pseudo first order kinetics with a mean rate constant of $3.73x10^{-3}$ min^{-1} and an intraparticle diffusion rate constant of $6.36x10^{-2}$ mg/g $min^{0.5}$. The experimental data yielded excellent fits with Langmuir and Freundlich isotherm equations. Co= 25 to 70 mg/L. The adsorption of dye was endothermic in nature and was accompanied by an increase in entropy and a decrease in Gibb's free energy in the temperature range of 300 to 330 K.
Namasivayam et al., 2005	Fe (III)/Cr (III) hydroxide, an industrial solid waste	Methylene blue Direct red 12B	Batch	Equilibrium adsorption data followed both Langmuir and Freundlich isotherms. The Langmuir adsorption capacity (Q_o) was found to be 5.0 and 22.8 mg dye per g of the adsorbent for direct red 12B and methylene blue, respectively. Adsorption followed second order rate kinetics. Adsorption was favored in acidic pH for direct red and in alkaline pH for methylene blue. Effect of pH and desorption studies showed that chemisorption seems to be the major mode of desorption.
Chao et al., 2004	Polymeric adsorbents NDA_99, NPA and AMR	Brilliant blue XBR	Batch	The results showed that the pore structure and amino groups of polymers influenced the adsorption capacity. Equilibrium adsorption data was well fitted to Freundlich model. The negative value of Gibbs free energy indicated that the overall adsorption process was spontaneous and thermodynamically favorable.
Wang et al., 2005	Fly ash and red mud	Methylene blue	Batch	Methylene blue adsorption on fly ash and red mud is endothermic reaction with change in enthalpy value at 76.1 and 10.8 KJ/mol, respectively. Redlich-Peterson model provided the best correlation of experimental data. Temperature has a significant effect on adsorption for red mud while less influence for fly ash.
Grabowska et al., 2006	Coal-based mesoporous activated	Congo red	Batch	The mesopore contribution to the total pore volume ranged from 53.4 to 82.1%. The pseudo-second-order kinetic model describes the adsorption of CR on mesoporous activated carbon very well. The

	carbon			correlation coefficients ranged from 0.980 to 0.991. The intraparticle diffusion into small mesopores was found to be the rate-limiting step in the adsorption process. The adsorption of CR was better represented by the Langmuir equation.
Kumar et al., 2005a	Fly ash	Methylene blue	Batch	Maximum color removal was observed at a basic pH of 8. Equilibrium data were represented well by a Langmuir isotherm equation with a monolayer sorption capacity of 5.718 mg/g. Sorption data were fitted to both Lagergren first-order and pseudo-second-order kinetic models and the data were found to follow pseudo-second-order kinetics. The effective diffusion parameter D_i values were estimated at different initial concentrations and the average value was determined to be 2.063×10^{-9} cm^2/s.
Kumar et al., 2005b	Mango seed kernel powder	Methylene blue	Batch	Equilibrium data were found to be well represented by Langmuir isotherm equation. The monolayer sorption capacity of mango seed kernel for methylene blue sorption was found to be 142.857 mg/g at 303 K. The sorption kinetics was found to follow pseudo first order kinetic model. The average effective diffusion coefficient was calculated and found to be 5.66×10^{-4} cm^2/s. Analysis of sorption data using Boyd plot confirms that the external mass transfer as the rate limiting step in the sorption process. The positive value of entropy shows the increased randomness at the solid–liquid interface during the sorption of dye ions onto mango seed kernel particles.
Alkan et al., 2004	Sepiolite	Acid red 57	Batch	Adsorption equilibrium was reached within 1 h. The removal of acid red 57 decreases with pH from 3 to 9 and temperature from 25 to 55 °C, whereas it increases with ionic strength from 0 to 0.5 mol/l. It was found that the Langmuir model appears to fit the isotherm data. Approximately, 21.49% weight loss was observed. The surface area value of sepiolite was 342 m^2/g at 105 °C and it increased to 357 m^2/g at 200 °C. Further increase in temperature caused channel plugging and crystal structure deformation, as a result the surface area values showed a decrease with temperature. The thermodynamic data indicate that acid red 57 adsorption onto sepiolite is characterized by physical adsorption.

Özcan et al., 2004	Na–bentonite and DTMA–bentonite	Acid blue 193	Batch	Results show that a pH value of 1.5 is favorable for the adsorption of Acid Blue 193. The isothermal data could be well described by the Freundlich equation. The dynamical data fit well with the pseudo-second-order kinetic model. The adsorption capacity of DTMA–bentonite (740.5 mg/g) was found to be around 11 times higher than that of Na–bentonite (67.1 mg/g) at 20°C The overall adsorption process was exothermic but it is only spontaneous at 20 °C.
Garg et al., 2005	Indian Rosewood sawdust: a timber industry waste	Basic dye (Methylene blue)	Batch	Optimum pH=7. Higher adsorption percentages were observed at lower concentrations of methylene blue. Experiments were conducted with GAC, SDC (Sulphuric acid treated sawdust (SDC)) and SD(Formaldehyde treated sawdust) at constant adsorbent dosage (0.4 g/ 100 ml), pH (neutral), and temperature (26 °C) for 3 h by varying methylene blue concentrations (50-500 mg/L). GAC has more adsorption efficiency in comparison to SDC and SD at all initial dye concentrations studied. Decolouriztion of wastewater was 100%, 92% and 87.1% by GAC, SDC and SD, respectively, at 50 mg/L dye concentration.
Gupta et al., 2004	Bottom ash	Malachite green (MG)	Batch and column	Maximum uptake of MG took place at a pH of 5.0. It can also be noted that the change in free energy decreases with increase in temperature, which exhibits an increase in adsorption with the rise in temperature. The endothermic nature of the process is once again supported by the positive value of enthalpy change while positive value of entropy change reflects the affinity of the adsorbent material towards MG. Freundlich model fits slightly better than the Langmuir model in the present studies Almost 96% of the dye was recovered when eluted with acetone.
Malik et al., 2004	Mahogany sawdust	Direct dyes.	Batch	The equilibrium data fit well in the Langmuir model of adsorption, showing monolayer coverage of dye molecules at the outer surface of sawdust carbon. The rates of adsorption were found to conform to the pseudo-second-order kinetics with good correlation. The equilibrium adsorption capacity of the sawdust carbon was found to be >300 mg dye per gram of the adsorbent. The most ideal pH for

				adsorption of direct dyes onto sawdust carbon was found to be 3 and below.
Srivastava et al., 2005	Bagasse fly ash (BFA) and activated carbon-commercial grade (ACC) and laboratory grade (ACL)	Malachite green (MG)	Batch	The effective pH was 7.0 for adsorption of MG by the three adsorbents. Equilibrium reached in about 4 h contact time. Optimum BFA, ACC and ACL dosages were found to be 1, 20 and 4 g/l, respectively. The adsorption followed pseudo-second-order kinetics Non-linear error analysis showed that the Freundlich isotherm best-fits the equilibrium data for adsorptive removal of MG by BFA and ACC and Redlich–Peterson best follows the equilibrium data for ACL. Thermodynamic study showed that MG adsorption on BFA was comparable to that obtained with ACC or ACL.
Mall et al., 2005	Bagasse fly ash (BFA) and activated carbon-commercial grade (ACC) and laboratory grade(ACL)	Congo red (CR)	Batch	The effective pH_o was 7.0 for adsorption on BFA. Kinetic studies showed that the adsorption of CR on all the adsorbents was a gradual process. Equilibrium reached in about 4 h contact time. Optimum BFA, ACC and ACL dosages were found to be 1, 20 and 2 g/l, respectively. CR uptake by the adsorbents followed pseudo-second-order kinetics. Error analysis showed that the R–P isotherm best-fits the CR adsorption isotherm data on all adsorbents. The Freundlich isotherm also shows comparable fit. Thermodynamics showed that the adsorption of CR on BFA was most favourable in comparison to activated carbons.
Mall et al., 2006	Bagasse fly ash (BFA)	Orange-G (OG) and Methyl Violet (MV)	Batch	Effective pH for OG and MV removal were 4 and 9, respectively. Greater percentage of dye was removed with decrease in the initial concentration of dyes, and increase in amount of adsorbent used. Kinetic study showed that the adsorption of dyes on BFA was a gradual process. Quasiequilibrium reached in 4 h. Pseudo-second-order rate equation was able to provide realistic description of adsorption kinetics. Freundlich equation is found to best represent the equilibrium data for OG-BFA system while Redlich-Peterson

				equation better fits the data for MV-BFA system. Thermodynamic study showed that adsorption of MV on BFA (with a more negative Gibbs free energy value) is more favored among the dyes studied.
Órfão et al., 2006	Chemically modified activated carbons	Reactive dye (Rifafix Red 3BN, C.I. reactive red 241)	Batch	The kinetic curves were fitted using the second-order model. The respective rate constants seemed to diminish progressively with the initial concentration for the more diluted solutions tested, reaching a constant value at higher concentrations, which was dependent on the experimental system under consideration (adsorbent and pH). Langmuir model provided the best fit for the equilibrium data. It was also shown that the optimal adsorption condition for all the activated carbons tested corresponds to solution pH values not higher than the pHpzc of the adsorbents, which may be interpreted by taking into account the electrostatic forces present. The maximum adsorption capacities were at pH 2 and 7.
Vadivelan et al., 2005	Rice Husk	Methylene blue	Batch	The equilibrium data were found to be well represented by the Langmuir isotherm equation. The monolayer sorption capacity of rice husk for methylene blue sorption was found to be 40.5833 mg/g at room temperature (32 °C) and the sorption kinetics were found to follow a pseudo-second-order kinetic model. The sorption process was be controlled by both surface and pore diffusion with surface diffusion at the earlier stages followed by pore diffusion at the later stages. The average external mass transfer coefficient and intraparticle diffusion coefficient was found to be 0.01133 min^{-1} and 0.695358 mg/g $min^{0.5}$. Boyd plot confirms that external mass transfer is the rate limiting step in the sorption process. The effective diffusion coefficient, Di was calculated using the Boyd constant and was found to be 5.05×10^{-04} cm^2/s for an initial dye concentration of 50 mg/L.
Hoda et al., 2006	Activated Carbon	Acid Blue 45, Acid Blue 92,	Batch	It was found that the adsorption process of these dyes onto ACC follows the pseudo-second-order model. Concentrations of dyes in

	Cloth (ACC)	Acid Blue 120 and Acid Blue 129		aqueous solution were reduced by a factor of approximately 217 for AB45, 25 for AB92, 10 for AB120 and 91 for AB129 over the course of adsorption. Freundlich model is good for representing the adsorption isotherm data of the dyes studied. These results indicate that pH of dye solutions is not a determining factor for the trend observed in kinetic and equilibrium data for the adsorption of dyes.
Guo et al., 2003	Rice husk-based porous carbons (RHCs)	Malachite green	Batch	Equilibrium is achieved in about 90 min at 25 °C with an adsorbent dose of 0.8g/l and an adsorbate concentration of 1.2 mmol/l. The adsorption was increased with pH. The increase in adsorption with temperature (20-80 °C) is may be due to the increase of the intraparticle diffusion rate of sorbate ions into the pores at higher temperature as diffusion is an endothermic process. The results obtained under various experimental conditions were found to follow the Freundlich adsorption isotherm.
Basibuyuk et al., 2003	Live activated sludge system	Basic dye (Maxilon Red BL-N)	Batch	According to the results obtained, the initial part of the adsorption followed a first-order process, controlled by film diffusion. The kinetics of sorption have been analyzed by three kinetic models, the first order Lagergren model, apseudo second order model and the second order model. Co=25, 50, 75, 100, 125, 150 and 200 mg/l. The contact time was 120 min. Maxilon Red bound to the sludge well and the maximum removal capacity was 123.2 mg/g.
Batzias et al., 2004	Calcium chloride treated beech sawdust	Methylene blue and Red basic 22	Batch and continuous	The results showed that the $CaCl_2$ treatment of the beech sawdust enhances its adsorption properties. The Freundlich adsorption capacity K_F (batch studies) for methylene blue increased by 28% for pretreatment at 23 °C and 98% for pretreatment at 100 °C. The K_F value for red basic 22 increased by 14 and 30% for pretreatment at 23 and 100 °C, respectively. The adsorption capacity coefficient N according to the Bohart–Adams bed depth service model (column studies) for methylene blue increased by 8% for pretreatment at 23 °C and 28% for pretreatment at 100 °C. The N value for red basic 22 increased by 5 and 30% for the same pretreatments, respectively.
Gupta et al., 2003	Waste carbon	Basic red	Batch	Optimum conditions are 1.0 g/l of activated carbon, 10.0 g/l of activated slag and pH of 6.0. Equilibrium was attained in about 6–8

	slurries and blast furnace slag			h. Both the Freundlich and Langmuir models could be used to fit the data and estimate model parameters. The thermodynamic parameters indicated that the dye adsorption was spontaneous and endothermic in nature. The analysis of the kinetic data showed the uptake of basic red on the prepared adsorbents to be first order.
Liversidge et al., 1997	Linseed cake	Basic blue 41	Batch	The Langmuir equation described the adsorption well. The enthalpy of adsorption was found to be endothermic and the capacity of the linseed cake for the dye decreased with increasing temperature. The linseed cake was compared with peat and it was found that it had a greater capacity for the dyestuff than peat.
Chu et al., 2002	Activated sludge biomass	Basic blue 3 , Basic violet 3, Basic red 18, Basic yellow 24, Basic red 29, Basic blue 47 and Basic blue 54	Batch	Dose=0.2g/100ml. The experimental results of COD removal (%) showed that for various basic dyes, adsorption by biomass was not only feasible but also effective. The kinetics of adsorption followed first-order processes, controlled by film diffusion. The effects of temperature on adsorption of Basic Violet 3 dye were studied and adsorption capacity decreased with increasing temperature. The process was exothermic in nature and the activation energy was 3.27 kcal /mol.
Gulnaz et al., 2004	Activated sludge	Basic red 18 and Basic blue 9	Batch	The activated sludge had the highest dye uptake capacity, having the monolayer adsorption capacity 285.71 and 256.41 mg g−1 for Basic Red 18 and Basic Blue 9, respectively, at pH value of 7.0 and 20 °C. The equilibrium data fixed very well with both the Langmuir and Freundlich models.
Sun et al., 2003	Modified peat–resin particle	Basic Magenta and Basic Brilliant green	Batch	Co=100-400mg/l, Agitation speed=200-500rpm, particle size=0.8-5mm, The adsorption isotherm showed that the adsorption of basic dyes on modified peat–resin particle deviated from the Langmuir and Freundlich equations. The pseudo-first order, pseudo-second order and intraparticle diffusion models were used to fit the experimental data. The change of agitation speed did not cause significant difference of intraparticle diffusion parameter in experimental conditions.
Gupta et al., 1992	Coal, fly ash,	Omega Chrome Red	Batch	Low adsorbate concentration, the low temperature, and an acidic medium favor the dye removal process. The process of uptake

	wollastonite, and china clay	ME		follows first-order adsorption rate expression and obeys Langmuir's model of adsorption. The removal process is also partially diffusion controlled.
McKay et al., 1980	Sorbsil silica	Astrazone blue	Batch	Equilibrium time increases with increasing in concentration. Adsorption increases with decrease in particle size. The rate-controlling step is mainly intraparticle diffusion. Adsorption increased with increase in temp. However adsorption capacity decreased with increase in time.
Ghoreishi et al., 2003	Chemical catalytic reaction and biological oxidation	Direct, basic and reactive colors.	-	The optimum dosage for treatment of actual wastewater was found to be 50–60 mg/l for catalyst bisulfite and 200–250 mg/l for sodium borohydride. Finally, a bench-scale experimental comparison of this technique with other reported combined chemical–biological methods showed higher efficiency and lower cost for the new technique. The results of this study indicate that a combined reduction–biological treatment method is a viable technique to effectively decrease the color, BOD, COD and TSS by 74–88%, 97–100, 76–83 and 92–97%, respectively. The major difference between this newly developed technique with other conventional methods is the key step of converting non-biodegradable dyes into biodegradable materials via reduction reaction with sodium borohydride as the reducing agent and bisulfite as the catalyst. The main economic advantage of this system is the lack of a serious sludge disposal problem and consequently much less operating cost.
Chun et al., 2001	TiO_2/SiO_2 photocatalyst	Reactive yellow KD-3G-, reactive red 15. reactive red 24,	-	Greater than 90% of color removal of most dyes solution was achieved after 20-30 min. treatment. With the decolorization, COD and TOC in wastewater were also reduced from 60%to 85%depending the dye. It was found that bod in wastewater was increased after photooxidation. This indicates that the biodegradability of the wastewater can be enhanced by photocatalytic oxidation. The BOD/COD of wastewater was generally more than 0.30 when their color disappeared completely. The result implies that the optimal exposing time to photocalatysis process is the period for complete decolorization. The photocatalysis

				process could be an alternative for decolorization and further colour removal of dyes from wastewater as pre- or post –treatment of conventional biological process.
Grimau et al., 2006	Electrochemical treatment	Reactive Orange 4	-	The electrochemical treatment with Ti/PtO_x anodes provides better decolourisation results when the reactive dyebath effluents contain NaCl than when the dyeing electrolyte is Na_2SO_4. The pH of the effluents does not have a significant influence on the electrochemical decolourisation. A TOC removal of 81% was obtained when high current density was applied for a prolonged treatment with recirculation. This treatment required a high electrical consumption.
Golob et al., 2005	Coagulation /flocculation	Reactive and acid dyes	-	The coagulation/flocculation method was studied as a wastewater treatment technique for the decolourization of residual dyebath effluents after dyeing cotton/polyamide blends using reactive and acid dyes. It was discovered that a combination of aluminium sulphate and a cationic organic flocculant yields an effective treatment for residual dyebath wastewaters since almost complete decolourization was achieved, TOC, COD, AOX, BOD and the anionic surfactants were reduced and the biodegradability was increased.
Jime´nez et al.,2000	Electrochemical treatment	Azo, methine, indigo , natural and arylmethane	-	It was found that the novel (in this application) diamond electrode is efficient in studying the degradation of various dyes. Possible fragmentation and molecule moiety rearrangement are proposed as a result of the electrochemical treatment.
Daly et al., 2005.	By reaction with hydrogen peroxide	Direct Green 28 and Direct Blue 78	-	It is used in the current work to oxidize and decolorize two of the direct dyes that fulfill an outstanding demand. The oxidation reaction of Direct Green 28 showed a first order kinetics for $[H_2O_2]$ and zero-order kinetics for [Dye]. The oxidation reaction of Direct Blue 78 showed a first order kinetics for both [dye] and [Cu (II)] and a zero-order kinetics for $[H_2O_2]$.
Faria et al., 2005	Ozonation in the presence of	CI Acid blue 113, CI Reactive red	-	Under the experimental conditions used in this work, activated carbon was not capable of completely removing the colour of the solutions in reasonable time. On the other hand, ozonation quickly

	activated carbon	241 and CI Basic red 14		decolourised all the solutions, but satisfactory removal of TOC was never achieved by this process. The combination of activated carbon with ozone enhanced the decolourisation of the solutions and especially the mineralization of the organic matter. Activated carbon acts both as an adsorbent and as a catalyst in the reaction of ozonation.
Cisneros et al., 2002	Photodegradation	Azo dye, Hispamin Black CA,	-	An advanced oxidation treatment, UV/H_2O_2, was applied to an azo dye, Hispamin Black CA. A strongly absorbing solution was completely decolorized after 35 min of treatment, and after 60 min an 82% reduction of the total organic carbon (TOC) was obtained. It has been found that the degradation rate increased until an optimum value, beyond which the reagent exerted an inhibitory effect. The degradation rate was also function of pH.
Tan et al., 2000	Chemical precipitation method using Magnesium chlorid	The reactive dye, Brill Blue EBRA	-	The results show that $MgCl_2$ is capable of removing more than 90% of the colouring material at a pH of 11 and a dose of 4 g $MgCl_2$/l of dye solution. $MgCl_2$ is shown to be more effective in removing reactive dye than alum and PAC in terms of settling time and amount of alkalinity required. The treatment of the industrial waste has shown a reduction of 88% in COD and 95% of suspended solids.
Chakraborty et al., 2005	Adsorption and nanofiltration	Reactive red CNN and reactive black B	-	A combination of adsorption and nanofiltration (NF) was adopted for the treatment of a textile dye house effluent containing a mixture of two reactive dyes. The effluent stream was first treated in a batch adsorption process with sawdust as an adsorbent to reduce the dye concentration of the effluent by about 83% for Dye 1 and 93% for Dye 2. The effluent from the adsorption unit was passed through an NF unit for the removal of the remaining small amount of dyes and to recover the associated chemicals (mainly salt) in the effluent stream. The dyes remaining after this step were less than 1 ppm. The percentage removal of COD was greater than 99%.

CHAPTER-3

ADSORPTION FUNDAMENTALS

3.1 GENERAL

Adsorption is a surface phenomenon. The adsorption operations exploit the ability of certain solids preferentially to concentrate specific substances from solution onto their surfaces. The solute accumulated is called the adsorbate or solute and the adsorbing substance is the adsorbent. In the water purification, adsorbents are used to remove organic impurities, particularly those that are non-biodegradable or associated with taste, colour, and odour. Although adsorption is applied in low concentration, recent physical-chemical processes use adsorption as a primary technique to remove soluble organics from the wastewater. The adsorption is called physical adsorption when the bonding forces are relatively weak intermolecular forces like van der Waal's forces and, chemical when the bonding forces are strong like chemical bonding. During adsorption, the solid adsorbent becomes saturated or nearly saturated with the adsorbate. To recover the adsorbate and allow the adsorbent to be reused, it is regenerated by desorbing the adsorbed substances (i.e. the adsorbates).

3.1.1 Physical Adsorption vs. Chemisorption

Adsorption processes can be classified as physical adsorption (van der Waals adsorption) and chemisorption (activated adsorption) depending on the type of forces between the adsorbate and the adsorbent. In physical adsorption, the individuality of the adsorbate and the adsorbent are preserved. In chemisorption, there is a transfer or sharing of electron, or breakage of the adsorbate into atoms or radicals, which are bound separately.

Physical adsorption of a gas occurs when the inter-molecular attractive forces between molecules of the solid adsorbent and the gas are greater than those between molecules of the gas itself. In effect, the resulting adsorption is like condensation, which is exothermic and thus is accompanied by the release of heat, similar in magnitude to the heat of condensation. Physical adsorption occurs quickly and may be monomolecular

(unimolecular) layer or monolayer, or two, three or more layers thick (multi-molecular). As physical adsorption takes place, it begins as a monolayer. It can then become multi-layer, and then, if the pores are close to the size of the molecules, more adsorption occurs until the pores are filled with adsorbate. Accordingly, the maximum capacity of a porous adsorbent can be more related to the pore volume than to the surface area.

In contrast, chemisorption is monolayer, involves the formation of chemical bonds between the adsorbate and adsorbent, often with a release of heat much larger than the heat of condensation. Chemisorption from a gas generally takes place only at temperatures greater than 200 °C, and may be slow and irreversible.

Most commercial adsorbents rely on physical adsorption; while catalysis relies on chemisorption. A comparison between physical adsorption and chemical adsorption is given in Table 3.1.

Table 3 .1. Comparison of Physical and Chemical Adsorption

Sl. No.	Physical Adsorption	Chemical Adsorption
1.	Van der Wall's adsorption	Activated adsorption
2.	Heat of adsorption = 5 kcal/mol	Heat of adsorption = 20-100 kcal/mol
3.	Adsorption occurs only at temperature less than the boiling point of the adsorbate	Adsorption can occur even at higher temperature
4.	No activation energy is involved in the adsorption process	Activation energy may be involved
5.	Adsorption occurs in mono and multi layers	Adsorption occurs almost in mono layer
6.	Quantity adsorbed per unit mass is high i.e. entire surface is participating	Quantity adsorbed per unit mass is low i.e. only active surface sites are important
7.	Rate of adsorption controlled by mass transfer resistance	Rate of adsorption controlled by resistance reaction

3.1.2 Intra-particle Diffusion Process

The rate of adsorption is determined by the rate of transfer of the adsorbate from the bulk solution to the adsorption sites within the particles. This can be broken conceptually into a series of consecutive steps.

1. Diffusion of adsorbate across a stationary solvent film surrounding each adsorbent
2. Diffusion through the macro pore
3. Diffusion through micro pore
4. Adsorption at an appropriate site

It is assumed that the fourth step occurs very rapidly in comparison to the second step. If the system is agitated vigorously, the exterior diffusion film around the adsorbent will be very thin, offering negligible resistance to diffusion. So, it can be assumed that the main resistance to adsorption shall lie in the pore diffusion step. Weber and Morris while referring to the rate limiting step of organic materials uptake by granulated activated carbon in the rapidly mixed batch system propose the term "intra-particle transport" which comprises of surface diffusion and molecular diffusion. Several researchers have shown that surface diffusion is the dominant mechanism and is the rate-determining step. A functional relationship common to most of the treatments of intra-particle transport is that the uptake varies almost proportionally with the square root of time.

3.1.3 Stages in Adsorption Process

Adsorption is thought to occur in three stages, as the adsorbate concentration increases.

Stage I: First, a single layer of molecules builds up over the surface of the solid. This monolayer may be chemisorbed and is associated with a change in free energy that is a characteristic of the forces that hold it.

Stage II: As the fluid concentration is further increased, second, third etc., layers are formed by physical adsorption; the number of layers which can form are limited by the size of the pores.

Stage III: Finally, for adsorption from the gas phase, capillary condensation may occur in which capillaries become filled with condensed adsorbate, when its partial pressure reaches a critical value relative to the size of the pore.

3.2 ADSORPTION ISOTHERMS

When a solution is contacted with a solid adsorbent, molecules of adsorbate get transferred from the fluid to the solid until the concentration of adsorbate in solution as well as in the solid phase are in equilibrium. At equilibrium, equal amounts of solute eventually are being adsorbed and desorbed simultaneously. This is called adsorption equilibrium. The equilibrium data at a given temperature are represented by adsorption isotherm and the study of adsorption is important in a number of chemical processes ranging from the design of heterogeneous chemical reactors to purification of compounds by adsorption.

Many theoretical and empirical models have been developed to represent the various types of adsorption isotherms. Langmuir, Freundlich, Brunauer-Emmet-Teller (BET), Redlich-Peterson (R-P) etc. are most commonly used adsorption isotherm models for describing the dynamic equilibrium. The isotherm equations used for the study are described follows:

3.2.1 Langmuir Isotherm

This equation based on the assumptions that:

1. Only monolayer adsorption is possible.
2. Adsorbent surface is uniform in terms of energy of adsorption.
3. Adsorbed molecules do not interact with each other.
4. Adsorbed molecules do not migrate on the adsorbent surface

The adsorption isotherm derived by Langmuir for the adsorption of a solute from a liquid solution is

$$Q_e = \frac{Q_m K_A C_e}{1 + K_A C_e} \tag{3.1}$$

where,

Q_e = Amount of adsorbate adsorbed per unit amount of adsorbent at equilibrium.

Q_m = Amount of adsorbate adsorbed per unit amount of adsorbent required for monolayer adsorption (limiting adsorbing capacity).

K_A = Constant related to enthalpy of adsorption.

C_e = Concentration of adsorbate solution at equilibrium.

The Langmuir isotherm can be rearranged to the following linear forms:

$$\frac{C_e}{Q_e} = \frac{1}{K_A Q_m} + \frac{C_e}{Q_m} \tag{3.2}$$

or

$$\frac{1}{Q_e} = \left(\frac{1}{K_A Q_m}\right)\left(\frac{1}{C_e}\right) + \left(\frac{1}{Q_m}\right) \tag{3.3}$$

3.2.2 Freundlich Isotherm

The heat of adsorption in many instances decreases in magnitude with increasing extent of adsorption. This decline in heat of adsorption is logarithmic, implying that adsorption sites are distributed exponentially with respect to adsorption energy. This isotherm does not indicate an adsorption limit when coverage is sufficient to fill a monolayer .The equation that describes such isotherm is the Freundlich Isotherm, given as

$$Q_e = K_F C_e^{\frac{1}{n}} \tag{3.4}$$

where ,

K_F and n are the constants

C_e = the concentration of adsorbate solution at equilibrium

by taking logarithm on both sides, this equation is converted into a linear form:

$$\ln Q_e = \ln K_F + \frac{1}{n} \ln C_e \tag{3.5}$$

Thus a plot between ln Q_e and ln C_e is a straight line. The Freundlich equation is most useful for dilute solutions over small concentration ranges. It is frequently applied

to the adsorption of impurities from a liquid solution on to the activated carbon. A high K_F and high 'n' value is an indication of high adsorption through out the concentration range. A low K_F and high 'n' indicates a low adsorption through out the concentration range. A low 'n' value indicates high adsorption at strong solute concentration.

3.2.3 Temkin Isotherm

It is given as

$$q_e = \frac{RT}{b}\ln(K_T C_e) \tag{3.10}$$

which can be linearized as:

$$q_e = B_1 \ln K_T + B_1 \ln C_e \tag{3.11}$$

where $B_1 = \frac{RT}{b}$

Temkin isotherm contains a factor that explicitly takes into the account of adsorbing species-adsorbent interactions. This isotherm assumes that (i) the heat of adsorption of all the molecules in the layer decreases linearly with coverage due to adsorbent-adsorbate interactions, and that (ii) the adsorption is characterized by a uniform distribution of binding energies, up to some maximum binding energy (Temkin and Pyzhev, 1940; Kim et al. 2004). A plot of q_e versus $\ln C_e$ enables the determination of the isotherm constants B_1 and K_T from the slope and the intercept, respectively. K_T is the equilibrium binding constant (l/mol) corresponding to the maximum binding energy and constant B_1 is related to the heat of adsorption.

3.2.4 Dubinin-Radushkevich (D-R) Isotherm [Dubinin and Radushkevich, 1947] :

It is given as

$$q_e = q_s \exp(-B\varepsilon^2) \tag{3.12}$$

where, q_s is the D-R constant and ε can be correlated as

$$\varepsilon = \mathrm{RT}\ln\left(1+\frac{1}{\mathrm{C_e}}\right) \tag{3.13}$$

The constant B gives the mean free energy E of sorption per molecule of sorbate when it is transferred to the surface of the solid from infinity in the solution and can be computed using the relationship $E = 1/\sqrt{2B}$. [Hasany and Chaudhary, 1996].

3.3 ADSORPTION PRACTICES

Adsorption systems are run either on batch or on continuous basis. Following text gives a brief account of both types of systems as in practice.

3.3.1 Batch Adsorption Systems

In a batch adsorption process the adsorbent is mixed with the solution to be treated in a suitable reaction vessel for the stipulated period of time, until the concentration of adsorbate in solution reaches an equilibrium value. Agitation is generally provided to ensure proper contact of the two phases. After the equilibrium is attained the adsorbent is separated from the liquid through any of the methods available like filtration, centrifugation or settling. The adsorbent can be regenerated and reused depending upon the need.

3.3.2 Continuous Adsorption Systems

The continuous flow processes are usually operated in fixed bed adsorption columns. These systems are capable of treating large volumes of waste wasters and are widely used for treating domestic and industrial wastewaters. They may be operated either in the up flow columns or down flow column. Continuous counter current columns are generally not used for wastewater treatment due to operational problems.

Fluidized beds have higher operating costs hence are not common in use. Wastewater usually contains several compounds which have different properties and which are adsorbed at different rates. Biological reactions occurring in the column may also function as filter bed, retaining solids entering with the feed. As a result of these and other complicating factors, laboratory or pilot plant studies on specific wastewater to be treated should be carried out. The variables to be examined include type of adsorbent, liquid feed rate, solute concentration in feed and height of adsorbent bed.

3.4 FACTORS CONTROLLING ADSORPTION

The amount adsorbed by an adsorbent from the adsorbate solution is influenced by a number of factors such as:

1. Initial concentration
2. Temperature

3. pH
4. Contact time
5. Degree of agitation
6. Nature of adsorbent

3.4.1 Initial Concentration

The initial concentration of pollutant has remarkable effect on its removal by adsorption. The amount of adsorbed material increases with the increasing adsorbate concentration as the resistance to the uptake of the adsorbate from solution decreases with increasing solute concentration. Percent removal increases with decreasing concentrations.

3.4.2 Temperature

Temperature is one of the most important controlling parameter in adsorption. Adsorption is normally exothermic in nature and the extent and rate of adsorption in most cases decreases with increasing temperature of the system. Some of the adsorption studies show increased adsorption with increasing temperature. This increase in adsorption is mainly due to increase in number of adsorption sites caused by breaking of some of the internal bonds near the edge of the active surface sites of the adsorbents.

3.4.3 pH

Adsorption from solution is strongly influenced by pH of the solution. The adsorption of cations increases while that of the anions decreases with increase in pH. The hydrogen ion and hydroxyl ions are adsorbed quite strongly and therefore the adsorption of other ions is affected by pH of solution. Change in pH affects the adsorptive process through dissociation of functional groups on the adsorbent surface active sites. This subsequently leads to a shift in reaction kinetics and equilibrium characteristics of adsorption process. It is an evident observation that the surface adsorbs anions favorably at lower pH due to presence of H^+ ions, whereas the surface is active for the adsorption of cations at higher pH due to the deposition of OH^- ions.

3.4.4 Contact Time

The studies on the effect of contact time between adsorbent and adsorbate have significant importance. In physical adsorption, most of the adsorbate species are adsorbed on the adsorbent surface with in short contact time. The uptake of adsorbate is fast in the initial stages of the contact period and becomes slow near equilibrium. Strong chemical binding of adsorbate with adsorbent requires a longer contact time for the attainment of equilibrium. Available adsorption results reveal that the uptake of heavy metals is fast at the initial stages of the contact period, and there after it becomes slow near equilibrium.

3.4.5 Degree of Agitation

Agitation in batch adsorbers is most important to ensure proper contact between the adsorbent and the solution. At lower agitation speed, the stationary fluid film around the particle is thicker and the process is mass transfer controlled. With the increase in agitation this film decreases in thickness and the resistance to mass transfer due to this film reduces and after a certain point the process becomes intra particle diffusion controlled. Whatever is the extent of agitation the solution inside the process remain unaffected and hence for intraparticle mass transfer controlled process agitation has no effect on the rate on the adsorption.

3.4.6 Nature of Adsorbent

Many solids are used as adsorbents to remove the impurities from fluids. Commercial adsorbents generally have large surface area per unit mass. Most of the surface area is provided by a network of small pores inside the particles. Common industrial adsorbents for fluids include activated carbon, silica gel, activated alumina, molecular sieves etc. Adsorption capacity is directly proportional to the exposed surface. For the non-porous adsorbents, the adsorption capacity is directly proportional to the particle size diameter whereas for porous materials it is practically independent of particle size.

Activated carbon is the most widely used adsorbent for water purification. In the manufacture of activated carbon, organic materials such as coal nutshells, bagasse is first pyrolysed to a carbonaceous residue. Larger channels or pores with diameter 1000 Å are called macro pores. Most of the surface area for adsorption is provided by micropores, which are arbitrarily defined as pores with diameter from 10-1000 Å.

CHAPTER-4

EXPERIMENTAL PROGRAMME

4.1 GENERAL

In the present study, rice husk ash (RHA) and bagasse fly ash (BFA) have been utilized for the treatment of Indigo Carmine (IC) bearing aqueous solution. Experimental details of the study have been presented in this chapter. These details include characterization of adsorbents and batch adsorption studies on RHA and BFA.

4.2 CHARACTERIZATION OF ADSORBENT

The physico-chemical characteristics of the RHA and BFA were determined using standard procedures as discussed below:

4.2.1 Proximate Analysis

Proximate analysis of the RHA and BFA were carried out using the procedure as per IS 1350:1984.

4.2.2 Density

The Bulk density of RHA and BFA were determined using MAC bulk density meter.

4.2.3 Particle Size Analysis

Particle size analysis of the RHA and BFA was made using standard sieve as per IS 2720 (Pt 4): 1985.

4.2.4 Surface area measurement

The specific surface area, pore volume and pore diameter of the sample were measured by N_2 adsorption isotherm using an ASAP 2010 micrometric instrument and by Brunauer-Emmett-Teller (BET) method, using the software of micromeritics, Nitrogen was used as cold bath.

4.2.5 Scanning Electron Micrograph (SEM)

SEM analysis of RHA and BFA were carried out before and after the adsorption of IC from aquous solution by using LEO 435 VP Scanning electron microscope.

4.3 ADSORBATE

A.R. grade Indigo Carmine (IC) dye supplied HiMedia Laboratories Pvt. Limited, India was used as adsorbate. Synthetic wastewater solutions of IC of desired concentrations (50–1000 mg/l) were prepared by dissolving accurately weighed quantity of $C_{16}H_8N_2O_8S_2Na_2$ in distilled water.

4.3.1 Analytical measurement

The determination of the concentration of IC was done by finding out the absorbance characteristic wavelength using UV/VIS spectrophotometer (Perkin Elmer 35). A standard solution of IC was taken and the absorbance was determined at different wavelengths to obtain a plot of absorbance versus wavelength. The wavelength corresponding to maximum absorbance (λ_{max}) was determined from this plot. The λ_{max} for Indigo Carmine was found to be 610 nm λ. Calibration curve was plotted between the absorbance and the concentration of IC solution. The linearity of calibration curve (Fig. 4.1) indicated the applicability of the Lambert-Beer's Law.

4.4 EXPERIMENTAL PROGRAMME

The experimental programme was performed by Batch adsorption studies

4.4.1 Batch Adsorption Experiments

To study the effect of important parameters like initial pH (pH_0), adsorbent dose (m), initial concentration (C_0) and contact time (t) on the adsorptive removal of IC by RHA and BFA, batch experiments were conducted at 30 ± 1 °C. For each experimental run, 100 ml of IC solution of known C_0, pH_0 and a known amount of the adsorbent were taken in a 250 ml stoppered conical flask. This mixture was agitated in a temperature-controlled shaking water bath at a constant speed of 160 rpm at 30 ± 1 °C. Samples were withdrawn at appropriate time intervals. Some RHA and BFA particles remain suspended and do not settle down easily. Therefore, all the samples were centrifuged (Research

Centrifuge, Remi scientific works, Mumbai) at 7000 rpm for 10 minute and analyzed for the residual dye concentration using double beam UV/VIS spectrophotometer. The effect of pH_0 on dye removal was studied over a pH_0 range of 3 to 10. pH_0 was adjusted by the addition of dilute aqueous solutions of H_2SO_4 or NaOH (0.10 M). For the optimum amount of m, a 100 ml dye solution was contacted with different amounts of RHA and BFA till equilibrium was attained. The kinetics of adsorption was determined by analyzing adsorptive uptake of the IC from the aqueous solution at different time intervals. For adsorption isotherms, dye solutions of different concentrations were agitated with the known amount of adsorbent till the equilibrium was achieved. The residual IC concentration of the solution was then determined. Blank experimental runs, with only the adsorbent in 100 ml of distilled water, were conducted simultaneously at similar conditions to account for any colour leached by the adsorbents and adsorbed by glass containers. Batch tests were carried out to compare the adsorptive capacity and intensity of RHA and BFA.

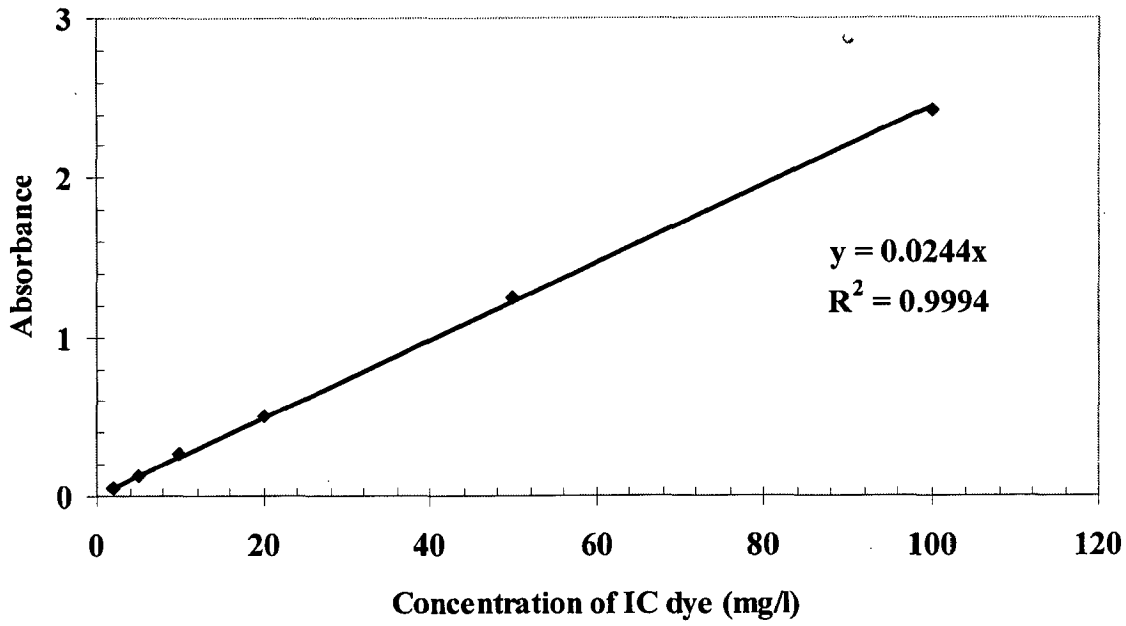

Fig 4.1 Calibration Graph of Indigo Carmine

CHAPTER-5

RESULTS AND DISCUSSION

5.1 GENERAL

The detailed discussion on the results of the experiments conducted is given in this chapter. These results include

- Characterization of Rice husk ash (RHA) and Bagasse fly ash (BFA).
- Batch adsorption studies.

5.2 CHARACTERIZATION OF RICE HUSK ASH AND BAGASSE FLY ASH

Characteristics of RHA and BFA included proximate and particle size analysis. Proximate analysis (Table 5.1) showed that the RHA has higher ash component as compared to BFA, however, amount of fixed carbon is more in BFA. Due to presence of high carbon content, BFA may be treated as organic in nature. The organic nature of BFA imparts porosity to it. The physico-chemical characteristics of the adsorbents given in Table 5.1 show that RHA has higher bulk density as compared to BFA. BFA also has a large surface area of ~237.83 m^2/g which comprises mainly of pore surface area, with average pore diameter of 22.47 A^0 . Each adsorbent has different particle size distribution. This was because of the use of the adsorbents as procured. Particle size is important in systems having external mass transfer resistance. The aqueous dye solution-adsorbents mixture was agitated at the maximum rpm, and the external mass transfer resistance is assumed to be absent. Adsorption of dyes is basically governed by intra-particle surface diffusion, where pore size distribution and surface area are important. Average particle size of RHA and BFA was 150.47 and 460.04 μm, respectively.

For structural characteristics scanning electron micrograph (SEM) analysis was carried out. Scanning electron micrograph photograph (Figs. 5.1a and 5.2a) of RHA and BFA reveal their surface texture and porosity. This photomicrograph shows fibrous structure of BFA. SEM of BFA (Fig. 5.2a) shows fibrous structure with large pore size with strands in each fibre. The size of the fibre and inter fibre space is lesser in RHA (Fig. 5.1a). Number of pores in RHA is lesser than that in BFA. However, the fibrous nature of

the structure of BFA is not so predominant in the micrograph, which may be due to its large size. However, the surface of the RHA and BFA becomes smooth after adsorption of IC as shown in Figs. 5.1b and 5.2b, respectively.

5.3 BATCH ADSORPTION STUDY

In order to study the effect of different parameters the batch operations were performed. Batch adsorption experiments were carried out in 250 ml Stoppard conical flask for removal of IC from synthetic solutions of known concentrations by using RHA and BFA. The effect of various operating parameters, viz. concentration, adsorbent dose, contact time and pH is studied and presented here.

5.3.1. Effect of initial pH (pH_0)

The pH of the solution affects the surface charge of the adsorbent as well as the degree of ionization of the materials present in the solution. The hydrogen ion and hydroxyl ions are adsorbed quite strongly and, therefore, the adsorption of other ions is affected by the pH of the solution. The change of pH affects the adsorptive process through dissociation of functional groups on the active sites of the adsorbent. This subsequently leads to a shift in reaction kinetics and equilibrium characteristics of the adsorption process. It is a common observation that the surface adsorbs anions favorably at lower pH due to presence of H^+ ions, whereas, the surface is active for the adsorption of cations at higher pH due to the deposition of OH^- ions.

pH is also known to affect the structural stability of IC and, therefore, its colour intensity. Hence the effect of pH is studied. Figs 5.3-5.20 show that the colour removal over a pH_0 range of 2 to 10. The percentage removal of IC (anionic dye) is maximum at acidic pH and decreased with further increase in pH. The results obtained are similar to those described by Kasgoz, 2005 over the pH range of 3–8 for IC dye adsorption on MH-2 polymer. As the colour is almost stable at around natural pH ($pH_0 = 5.6$) for RHA and around 3.0 for BFA, all further experiments are conducted by adjusting the pH.

5.3.2 Effect of adsorbent dosage (m)

The effect of m on the removal of IC by RHA and BFA at initial concentration

C_0 = 50 mg/l is shown in Figs. 5.4 and 5.21, respectively. It can be seen that the IC removal increases up to a certain limit and then it remains almost constant. Optimum m was found to be 10 g/l for RHA and 5 g/l for BFA. An increase in the adsorption with the adsorbent dose can be attributed to greater surface area and the availability of more adsorption sites. Further, in all the cases, equilibrium was found to be attained more rapidly at lower adsorbent dosage.

5.3.3 Effect of initial dye concentration (C_0)

The effect of C_0 on the removal of IC by RHA and BFA is shown in Figs. 5.5-5.6 and 5.22-5.23, respectively. It is evident from the Figures, that the amount of IC adsorbed per unit mass of adsorbent (q_e) increased with the increase in C_0 (Figs.5.5 and 5.22), although percentage IC removal decreased with the increase in C_0 (Figs. 5.6 and 5.23). q_e increased with the increase in C_0 as the resistance to the uptake of IC from the solution decreases with the increase in IC concentration. The rate of adsorption also increases with the increase in C_0 due to increase in the driving force.

5.3.4 Effect of contact time (t)

The effect of contact time on the removal of IC by RHA and BFA at C_0=50, 100, 250 and 500 mg/l is given in Figs. 5.7 and 5.24, respectively. The contact time curves show rapid adsorption of IC in the first 30 min, thereafter, the adsorption rate decreases gradually and the adsorption reaches equilibrium in 8 h for RHA and 4 h for BFA (optimum contact time). Increase in contact time up to 7 days showed that the IC removal increases slightly over those obtained for optimum contact time. Aggregation of dye molecules with the increase in contact time makes it almost impossible to diffuse deeper into the adsorbent structure at highest energy sites. This aggregation negates the influence of contact time as the mesopores get filled up and start offering resistance to diffusion of aggregated dye molecules in the adsorbents. This is the reason why an insignificant enhancement in adsorption is effected in 7 days as compared to that in optimum time. Hence further experiments were conducted for optimum contact time only. The curves are single, smooth and continuous leading to saturation. The adsorption curves of contact time

indicate the possible mono-layer coverage of dye on the surface of RHA and BFA (Wong and Yu, 1999; Malik, 2003).

5.3.5 Effect of temperature

Temperature has a pronounced effect on the adsorption capacity of the adsorbents. Figs. 5.13-5.14 and 5.30-31 show the plots of adsorption isotherms, for IC-RHA and IC-BFA systems at 293, 303, 313 and 323 K. It shows that the adsorptivity of IC increases with the increase in temperature. This increase shows that the adsorption process may be by chemisorption. This Figure also shows that at lower adsorbate concentrations, Q_e rises sharply and thereafter the increase is gradual with solute concentration in the solution. Since sorption is an exothermic process, it would be expected that an increase in temperature of the adsorbate-adsorbent system would result in decreased sorption capacity. However, if the adsorption process is controlled by the diffusion process (intraparticle transport-pore diffusion), the sorption capacity will show an increase with an increase in temperatures. This is basically due to the fact that the diffusion process is an endothermic process. With an increase in temperature, the mobility of the IC ions increases and the retarding forces acting on the diffusing ions decrease, thereby increasing the sorptive capacity of adsorbent. The increase in IC sorption capacity of the other adsorbents with the increase in temperature has also been reported by other investigators (Krishna and Bhattacharyya, 2003; Prado et al., 2003).

5.3.6 Effect of NaCl concentration

Generally wastewaters from various industries contain salts like NaCl in large quantities. Hence a series of adsorption experiments were carried out in presence of different concentrations of NaCl to find its effect on the adsorption capacity of BFA. Fig.5.24 shows the influence of the amount of the NaCl on the adsorption capacity of BFA. The concentration of NaCl was varied between 0 and 0.1 M and Indigo Carmine concentration was 50 mg/l. As seen from fig.11, the adsorption capacity of BFA decreased in the presence of NaCl in solution. The adsorption capacity of BFA was 9.9172 mg/g for distilled water and it decreased to 8.5573 mg/g for the solution containing 0.1 M NaCl.

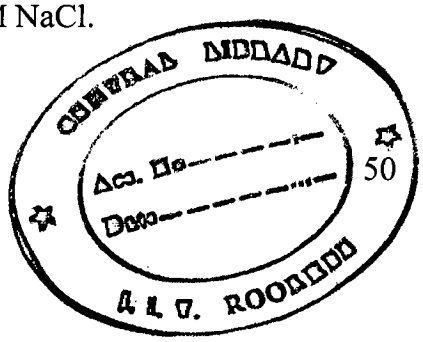

5.4 ADSORPTION KINETICS STUDY

5.4.1 Pseudo-first-order model:

The pseudo-first-order equation is given as

$$\frac{dq_t}{dt} = k_f(q_e - q_t) \tag{5.1}$$

where, q_t is the amount of adsorbate adsorbed at time t (mg/g), q_e is the adsorption capacity at equilibrium (mg/g), k_f is the pseudo-first-order rate constant (min^{-1}), and t is the contact time (min). The integration of Eq. (1) with the initial condition, q_t=0 at t=0 leads to following equation (Ho and McKay, 2000).

$$\log(q_e - q_t) = \log q_e - \frac{k_f}{2.303}t \tag{5.2}$$

The values of adsorption rate constant (k_f) for IC adsorption on RHA and BFA at C_0=50, 100, 250 and 500 mg/l were determined from the plot of log (q_e – q_t) against t (Figs. 5.9 and 5.26). The k_f values are given in Table 5.2 and 5.6.

5.4.2 Pseudo-second-order model:

The pseudo-second-order model is represented as (Ho and McKay, 1999):

$$\frac{dq_t}{dt} = k_S(q_e - q_t)^2 \tag{5.3}$$

Where, k_S is the pseudo-second-order rate constant (g/mg/min). Integrating Eq (5.3) and noting that q_t=0 at t=0, the following equation is obtained:

$$\frac{t}{q_t} = \frac{1}{k_S q_e^2} + \frac{1}{q_e}t \tag{5.4}$$

The initial sorption rate, h (mg/g/min), at $t \to 0$ is defined as

$$h = k_S q_e^2$$

Figs. 5.10 and 5.27 shows the plot of t/q_t versus t for RHA and BFA, respectively, at C_0=50, 100, 250 and 500 mg/l. The q_e is obtained from the slope of the plot and the h value is obtained from the intercept. Since q_e is known from the slope, k_S can be

determined from the h value. The k_S and h values as calculated from the Figures are listed in Table 5.2 and 5.6 for both the adsorbents. The calculated correlation coefficients are also closer to unity and also $q_{e,calc}$ and $q_{e,\ expt}$ values are almost same for pseudo-second-order kinetics than that for the pseudo first-order kinetic model. Therefore the sorption can be approximated more appropriately by the pseudo-second-order kinetic model. It can be seen that the BFA has higher h and q_e values for IC adsorption.

5.5 INTRA-PARTICLE DIFFUSION STUDY

5.5.1 Weber-Morris intra-particle diffusion equation :

The possibility of intra-particle diffusion was explored by using the intra-particle diffusion model:

$$q_t = k_{id} t^{1/2} + I \tag{5.5}$$

Where, k_{id} is the intra-particle diffusion rate constant (mg/g $min^{1/2}$) and I is the intercept (mg/g). Plot of q_t versus $t^{1/2}$ should be a straight line with a slope k_{id} and intercept I when adsorption mechanism follows the intra-particle diffusion process. Figs. 5.11 and 5.28 present a plot of q_t versus $t^{1/2}$ at C_0=50, 100, 250 and 500 mg/l for IC adsorption on RHA and BFA, respectively. The values of I (Table 5.2 and 5.6), gives an idea about the thickness of the boundary layer, i.e., the larger the intercept the greater is the boundary layer effect (Allen and Brown, 1995). The deviation of straight lines from the origin (Figs. 5.11 and 5.28) may be because of the difference between the rate of mass transfer in the initial and final stages of adsorption. Further, such deviation of straight line from the origin indicates that the pore diffusion is not the sole rate-controlling step. The values of intra-particle diffusion rate parameters are given in Tables 5.2 and 5.6 for RHA and BFA, respectively.

5.5.2 Bangham's equation: Bangham's equation (Aharoni et al., 1979) is given as

$$\log\log\left(\frac{C_0}{C_0 - q_t m}\right) = \log\left(\frac{k_0 m}{2.303V}\right) + \alpha \log(t) \tag{5.6}$$

where V is the volume of the solution (ml), and α (<1) and k_0 are constants. The double logarithmic plot, according to Eq. 5.6, did not yield satisfactory linear curves for the IC removal by the adsorbents (Figs. 5.12 and 5.29). This shows that the diffusion of adsorbate into the pores of the sorbent was not the only rate-controlling step (Tutem et al., 1998). It may be that both the film and pore diffusion were important to different extents in the removal process.

5.6 ADSORPTION EQUILIBRIUM STUDY

To optimize the design of an adsorption system for the adsorption of adsorbates, it is important to establish the most appropriate correlation for the equilibrium curves. Various isotherm equations have been used to describe the equilibrium characteristics of adsorption.

5.6.1 Freundlich and Langmuir Isotherms:

Linearised form of Freundlich and Langmuir isotherm equations are given as

$$\ln Q_e = \ln K_F + \frac{1}{n}\ln C_e \quad \text{(Linear form)} \tag{5.7}$$

$$\frac{C_e}{Q_e} = \frac{1}{K_A Q_m} + \frac{C_e}{Q_m} \quad \text{(Linear form)} \tag{5.8}$$

Figs. 5.15 an-5.32 shows the Freundlich isotherm plots (ln Q_e versus ln C_e) for adsorption of IC, respectively, onto RHA and BFA at 293, 303, 313 and 323 K. Langmuir isotherm plot (C_e/Q_e versus C_e) are shown in Figs. 5.16 and 5.33, respectively for adsorption onto RHA and BFA. Freundlich and Langmuir isotherm parameter along with linear and non-linear correlation coefficients are given in Tables 5.3 and 5.7, respectively. The Q_m values for both the adsorbents increase with temperature indicating endothermic nature of adsorption. Though adsorption is generally exothermic, but when it is controlled by diffusion of adsorbates into adsorbent, then it may be endothermic. This is due to the endothermicity of the diffusion process. At all temperatures, Freundlich isotherm represents a better fit of the experimental data for RHA and BFA. The essential characteristics of a Langmuir isotherm can be expressed in terms of a dimensionless

factor, R_L, which describes the type of pattern and is defined as $R_L=1/(1 + K_A C_0)$ indicates the nature of adsorption as

If	$R_L > 1$	Unfavorable
	$R_L = 1$	Linear
	$0 < R_L < 1$	Favourable
	$R_L = 0$	Irreversible

The value of R_L is found to be less than 1 for adsorption of IC on RHA and BFA, so adsorption onto both the adsorbents is favorable. The values of 1/n were also found to be less than 1 showing favourable nature of adsorption (Faust and Aly, 1978).

5.6.2 Temkin Isotherm: It is given as

$$q_e = \frac{RT}{b}\ln(K_T C_e) \tag{5.9}$$

which can be linearized as:

$$q_e = B_1 \ln K_T + B_1 \ln C_e \tag{5.10}$$

where $B_1 = \frac{RT}{b}$

Temkin isotherm contains a factor that explicitly takes into the account adsorbing species-adsorbent interactions. This isotherm assumes that (i) the heat of adsorption of all the molecules in the layer decreases linearly with coverage due to adsorbent-adsorbate interactions, and that (ii) the adsorption is characterized by a uniform distribution of binding energies, up to some maximum binding energy (Temkin and Pyzhev, 1940; Kim et al. 2004). A plot of q_e versus $\ln C_e$ enables the determination of the isotherm constants B_1 and K_T from the slope and the intercept, respectively. K_T is the equilibrium binding constant (l/mol) corresponding to the maximum binding energy and constant B_1 is related to the heat of adsorption. Figs. 5.17 and 5.34 show the Temkin isotherm plot. The Temkin isotherm parameters listed in Tables 5.3 and 5.7. It shows better only after Freundlich and Langmuir isotherms.

5.6.3 Dubinin-Radushkevich (D-R) Isotherm: It is given as (Dubinin and Radushkevich, 1947)

$$q_e = q_s \exp(-B\varepsilon^2) \tag{5.11}$$

where, q_s is the D-R constant and ϵ^2 can be correlated as

$$\varepsilon = \mathrm{RT} \ln\left(1 + \frac{1}{\mathrm{C_e}}\right) \tag{5.12}$$

The constant B gives the mean free energy E of sorption per molecule of sorbate when it is transferred to the surface of the solid from infinity in the solution and can be computed using the following relationship (Hasany and Chaudhary, 1996):

$$E = 1/\sqrt{2B}$$

D-R isotherm plots at 293, 303, 313 and 323 K are shown in Figs. 5.18 and Figs. 35, respectively. The estimated values of the D-R constants for the adsorption of IC are shown in Tables 5.3 and 5.7. It may be observed that the sorption energy value is the lowest for adsorption of IC at lower temperatures. The values of correlation coefficients are the lowest in comparison to the values for all other isotherms investigated. Thus, the D-R equation does not represent the experimental data satisfactorily.

5.7 ERROR ANALYSIS

The use of R^2 is limited to solving linear forms of isotherm equation, which measure the difference between experimental data and theoretical data in linear plots only, but not the errors in isotherm curves. Purely, from a comparison of the correlation coefficients (R^2 values) for the linearized models, it can be seen that higher weightage is given to the higher C_e value data points, thus giving a better fit correlation to the higher C_e value date points. Due to the inherent bias resulting from linearization, error functions of non-linear regression basin are employed to evaluate the isotherm constants and compare them with the less accurate linearized analysis values. Five different error functions of non-linear regression basin were employed in this study to find out the best-fit isotherm model to the experimental equilibrium data.

5.7.1 The Sum of the Squares of the Errors (SSE)

This error function, SSE is given as

$$SSE = \sum_{i=1}^{n} \left(q_{e,calc} - q_{e,\exp}\right)_i^2 \tag{5.13}$$

Here, $q_{e,cal}$ and $q_{e,\exp}$ are, respectively, the calculated and the experimental value of the equilibrium adsorbate solid concentration in the solid phase (mg/g) and n is the number of data points. This most commonly used error function, SSE has one major drawback in that it will result in the calculated isotherm parameters providing a better fit at the higher end of the liquid phase concentration range. This is because of the magnitude of the errors, which increase as the concentration increases. The values of SSE are given in Tables 5.4 and 5.8, both for RHA and BFA, respectively.

5.7.2 The Sum of the Absolute Errors (SAE)

SAE is given as

$$SAE = \sum_{i=1}^{n} \left|q_{e,calc} - q_{e,\exp}\right|_i \tag{5.14}$$

The isotherm parameters determined by this method provide a better fit as the magnitude of the errors increase, biasing the fit towards the high concentration data. The values of SAE are given in Tables 5.4 and 5.8, both for RHA and BFA, respectively.

5.7.3 The Average Relative Error (ARE)

ARE (Kapoor and Yang, 1989) is given as

$$ARE = \frac{100}{n} \sum_{i=1}^{n} \left| \frac{(q_{e,\exp} - q_{e,calc})}{q_{e,\exp}} \right|_i \tag{5.15}$$

This error function attempts to minimize the fractional error distribution across the entire concentration range. The values of ARE are given in Tables 5.4 and 5.8, both for RHA and BFA, respectively.

5.7.4 The Hybrid Fractional Error Function (HYBRID)

HYBRID is given as

$$HYBRID = \frac{100}{n-p}\sum_{i=1}^{n}\left[\frac{(q_{e,\exp}-q_{e,calc})}{q_{e,\exp}}\right]_i \tag{5.16}$$

This error function was developed (Porter and McKay, 1999) to improve the fit of the ARE method at low concentration values. Instead of n as used in ARE, the sum of the fractional errors is divided by (n-p) where p is the number of parameters in the isotherm equation. The values of HYBRID error functions are given in Tables 5.4 and 5.8, both for RHA and BFA, respectively.

5.7.5 Marquardt's Percent Standard Deviation (MPSD)

MPSD has been used by a number of researchers in the field (Wong et al., 2004, Seidel and Gelbin, 1988, Ng et al, 2003) to test the adequacy and accuracy of the model fit with the experimental data. It has some similarity to the geometric mean error distribution, but was modified by incorporating the number of degrees of freedom. This error function is given as

$$100\sqrt{\frac{1}{n-p}\sum_{i=1}^{n}\left(\frac{(q_{e,meas}-q_{e,calc})}{q_{e,meas}}\right)_i^2} \tag{5.17}$$

The values of MPSD error functions are given in Tables 5.4 and 5.8, both for RHA and BFA, respectively.

5.7.6 Choosing best-fit isotherm based on error analysis:

The values of the five error functions are presented in Tables 5.4 and 5.8. By comparing the results of the values of the error functions, it is found that Freundlich isotherm best-fitted the isotherm data for IC adsorption on RHA and BFA at almost all temperatures. It may, however, be noted that the error analysis values and the non-linear correlation coefficients, R^2 are comparable for Freundlich and Langmuir isotherms. Hence any one of the isotherms could be used for IC adsorption on RHA and BFA.

5.8 THERMODYNAMIC STUDY

The Gibbs free energy change of the adsorption process is related to the equilibrium constant by the classic Van't Hoff equation

$$\Delta G^0 = -RT \ln K \tag{5.18}$$

According to thermodynamics, the Gibbs free energy change is also related to the entropy change and heat of adsorption at constant temperature by the following equation:

$$\Delta G^0 = \Delta H^0 - T\Delta S^0 \tag{5.19}$$

Combining above two equations, we get

$$\ln K = \frac{-\Delta G^0}{RT} = \frac{\Delta S^0}{R} - \frac{\Delta H^0}{R}\frac{1}{T} \tag{5.20}$$

where ΔG^0 is the free energy change (kJ/mol), ΔH^0 is the change in enthalpy (kJ/mol), ΔS^0 is the entropy change (kJ/mol K), T is the absolute temperature (K) and R is the universal gas constant (8.314 J/mol K). Thus ΔH^0 can be determined by the slope of the linear Van't Hoff plot i.e. as $\ln K$ versus $(1/T)$, using equation:

$$\Delta H^0 = \left[R\frac{d \ln K}{d(1/T)} \right] \tag{5.21}$$

Van't Hoff's plot for Freundlich and Langmuir isotherm models for IC-RHA and IC-BFA systems are given in Figs. 5.19 and 5.36, respectively. ΔG^0, ΔH^0 and ΔS^0 as calculated from Freundlich and Langmuir models are given in Table 5.5 and 5.9, respectively, for adsorption of IC onto RHA and BFA. The positive ΔH^0 value confirms the endothermic nature of the overall-sorption process. The adsorption process in the solid-liquid system is a combination of two processes: (a) the desorption of the molecules of solvent (water) previously adsorbed and (b) the adsorption of adsorbate species. The IC ions have to displace more than one water molecule for their adsorption and this results in the endothermicity of the adsorption process.

The positive value of ΔS^0 suggests increased randomness at the solid/solution interface with some structural changes in the adsorbate and adsorbent and an affinity of the RHA and BFA towards IC. Also, positive ΔS value corresponds to an increase in the

degree of freedom of the adsorbed species (Raymon, 1988). Other researchers have shown the increase in entropy for adsorption of IC on Chitosan (90±6 J/mol K) (Prado et al., 2004) and on SiHAPS (65±3 J/mol K) and SiHAFL (98±5 J/mol K) materials, respectively (Prado et al., 2003). ΔG^0 values were negative indicating that the sorption process led to a decrease in Gibbs free energy. Negative ΔG^0_{ads} indicates the feasibility and spontaneity of the adsorption process.

FIGURES

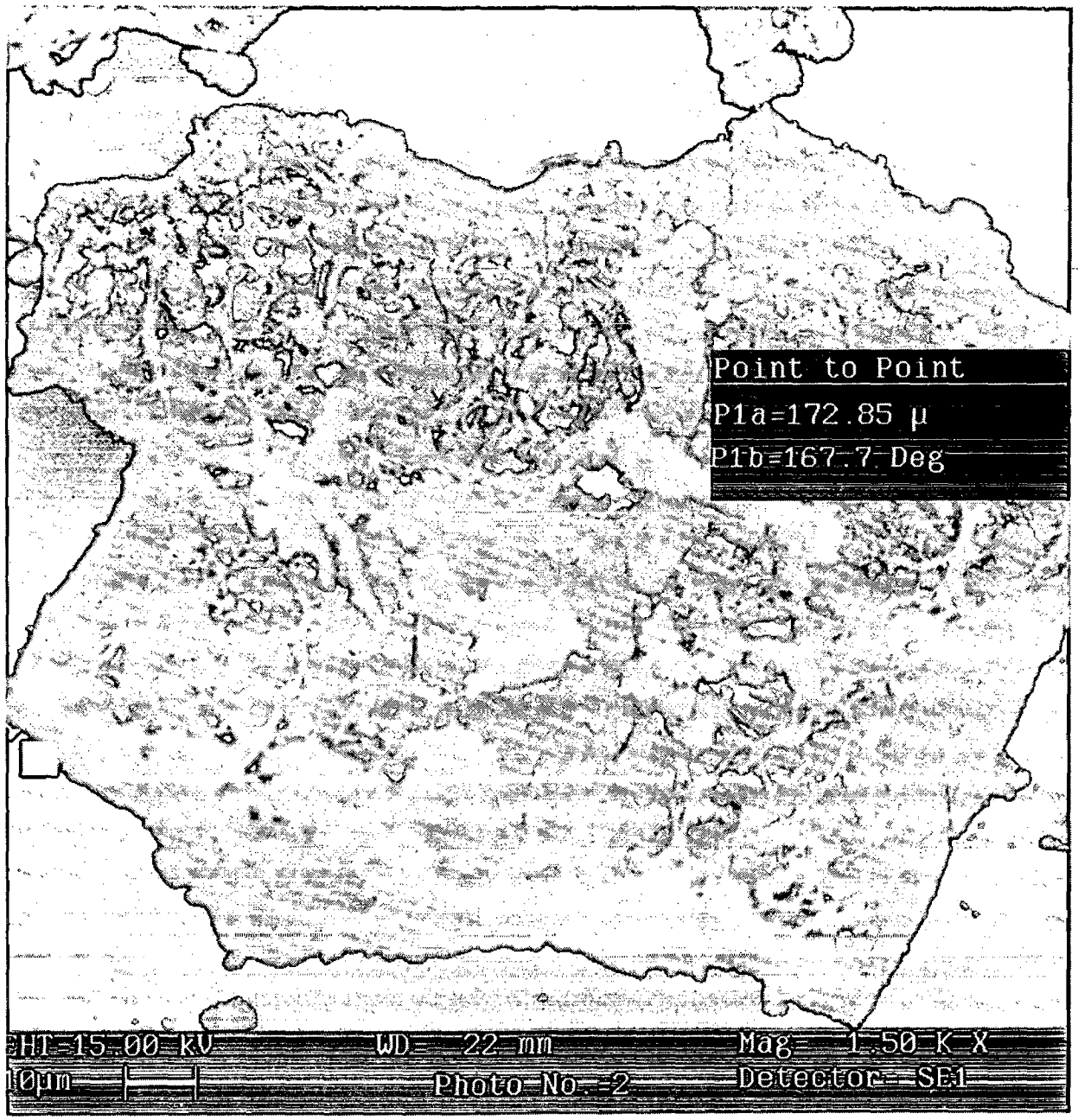

Fig 5.1a. Scanning electron micrograph of Rice husk ash before adsorption at 1500 X magnification

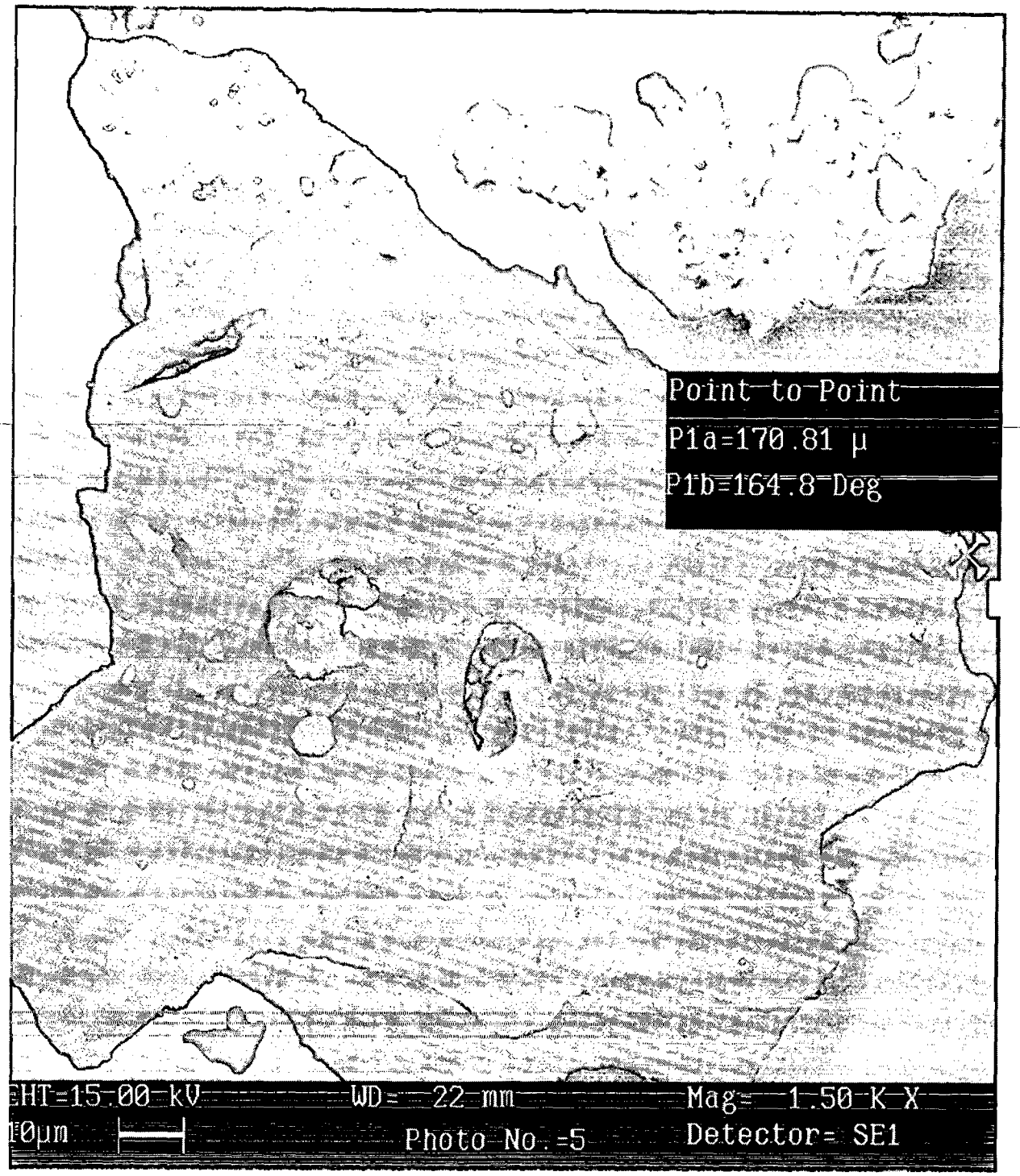

Fig 5.1b. Scanning electron micrograph of Rice husk ash after adsorption at 1500 X magnification

Fig 5.2a. Scanning electron micrograph of Bagasse fly ash before adsorption at 10000 X magnification

Fig 5.2b. Scanning electron micrograph of Bagasse fly ash after adsorption at 10000 X magnification

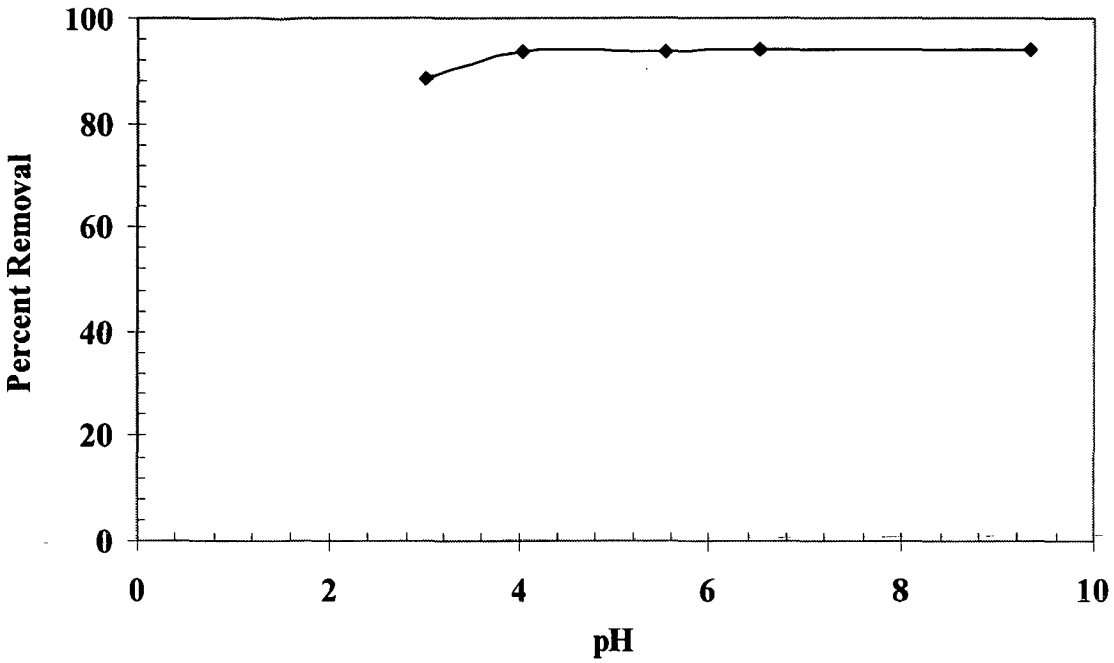

Fig. 5.3. Effect of pH on the adsorption of IC using RHA as adsorbent (T = 303 K, t =6 h, C_0 = 50 mg /l, RHA dose =10 g /l).

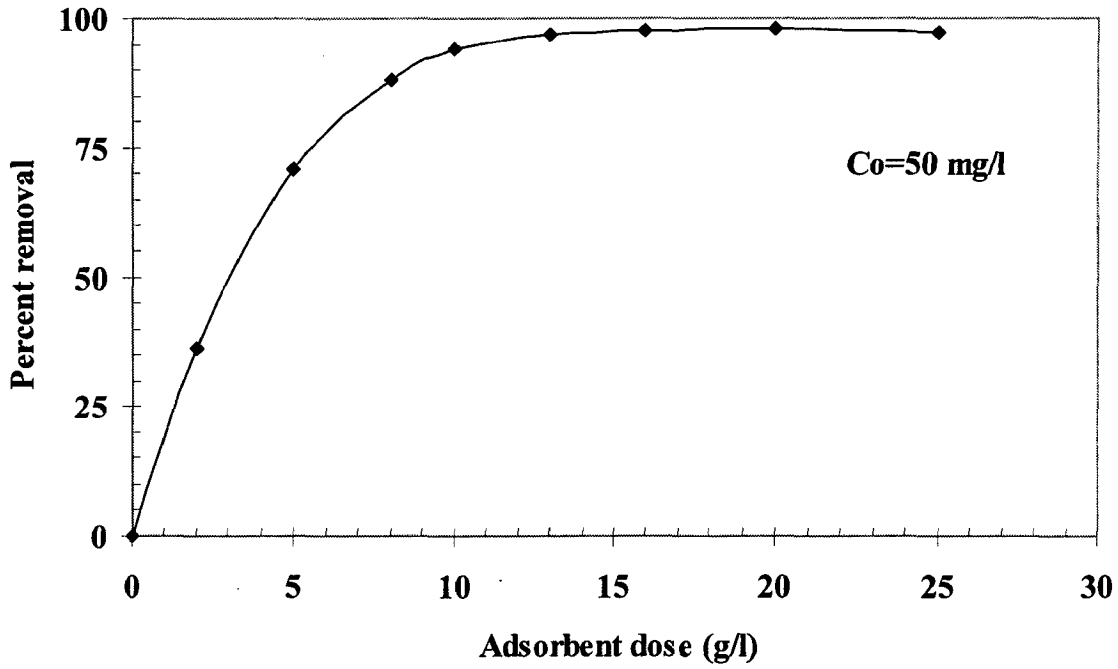

Fig. 5.4. Effect of adsorbent dose on the adsorption of IC by RHA (T = 303 K, t = 6 h, C_0 = 50 mg/l).

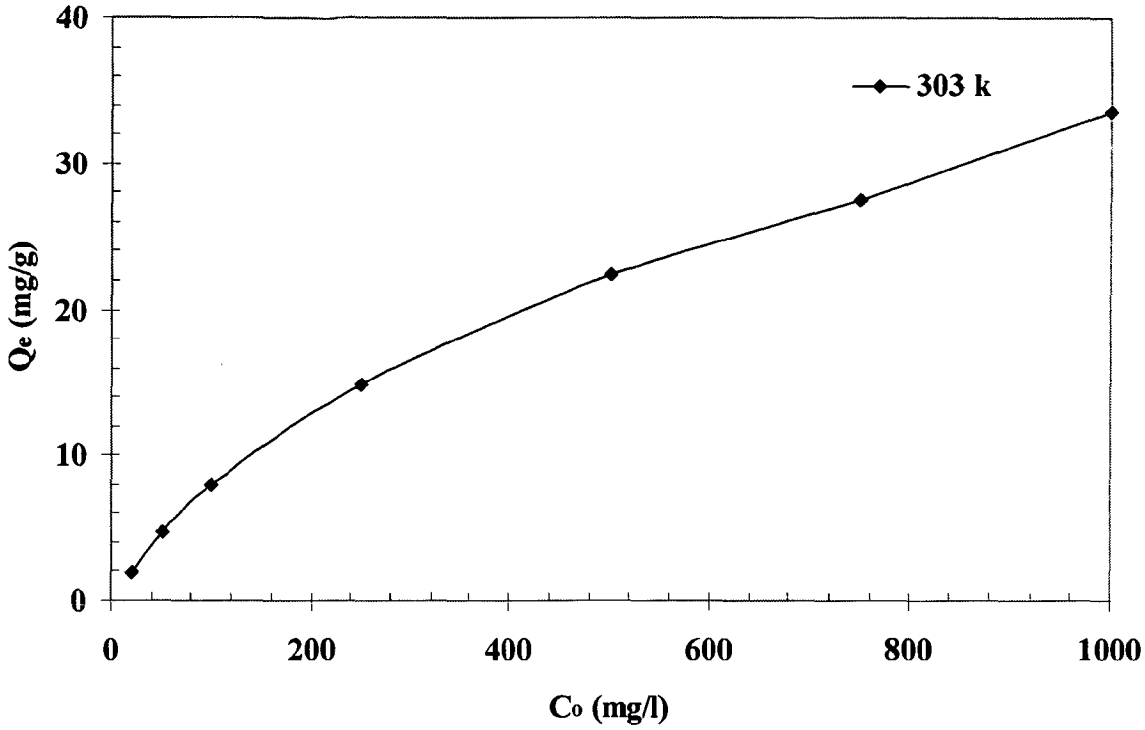

Fig. 5.5. . Effect of initial dye concentration, C_0 on the adsorption capacity of RHA (T = 303 K, t = 8 h, C_0 = 50 mg/l).

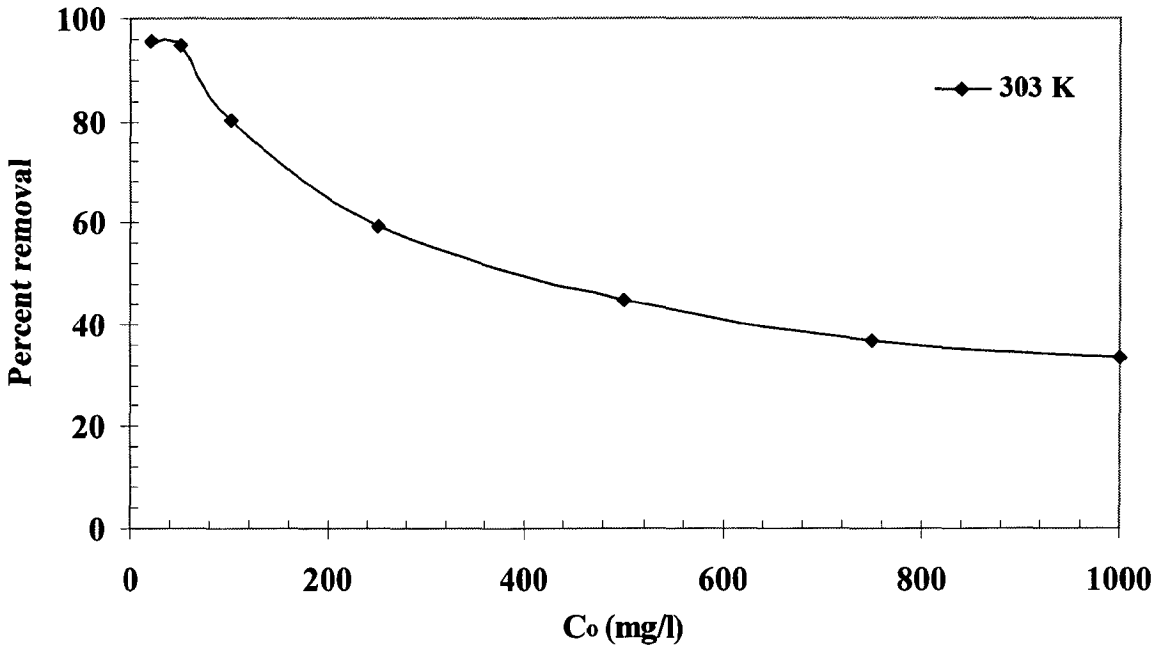

Fig. 5.6. Effect of initial dye concentration, C_0 on the percent removal capacity of RHA (T = 303 K, t = 8 h, C_0 = 50 mg/l).

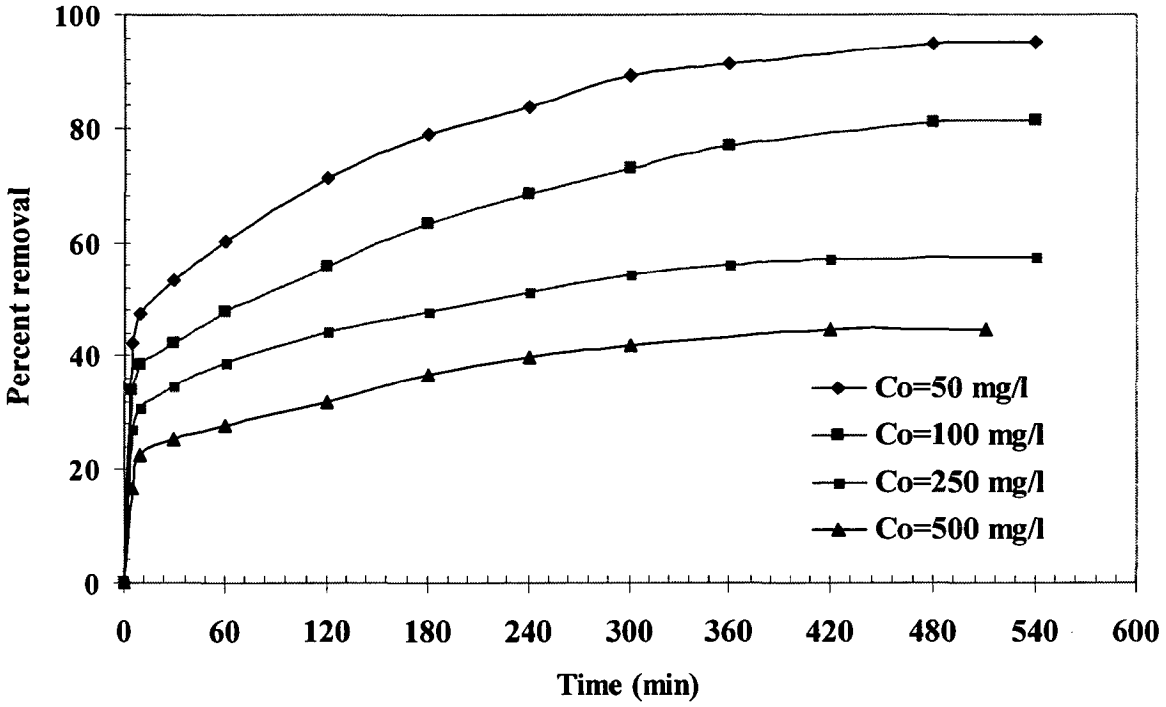

Fig. 5.7. Effect of contact time on percent removal of IC (T= 303 K, C_0 = 50, 100, 250 and 500 mg/l, RHA dose =10 g/l).

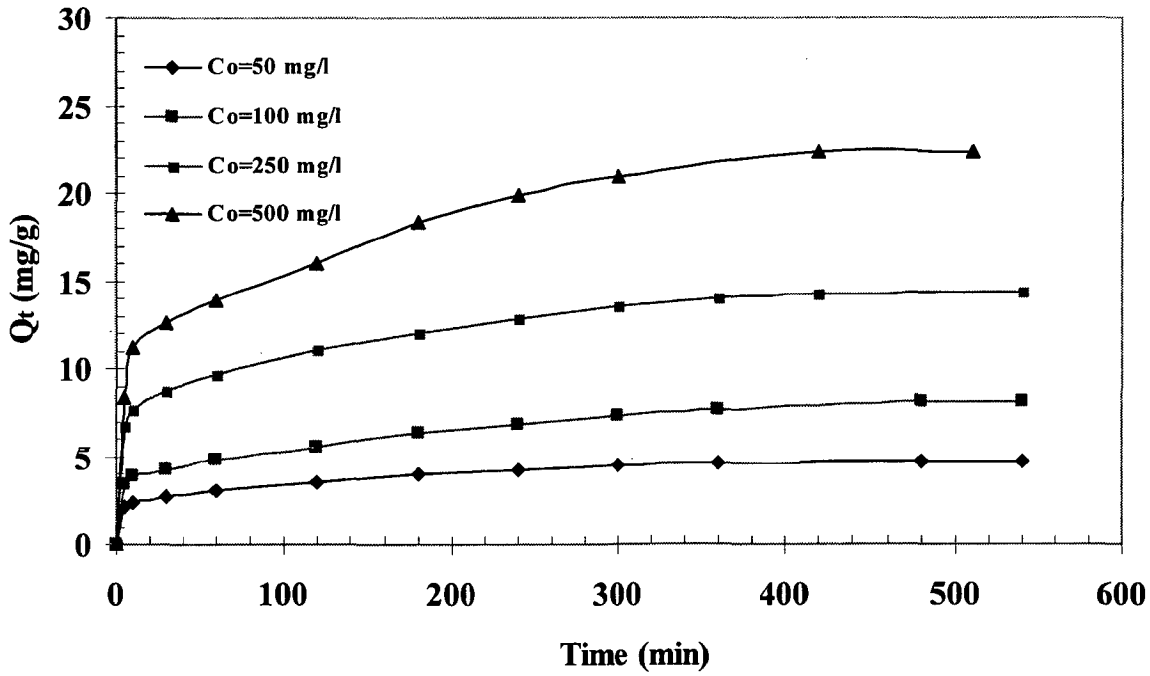

Fig. 5.8. Effect of contact time on adsorption of IC (T= 303 K, C_0 = 50, 100, 250 and 500 mg/l, RHA dose =10 g/l).

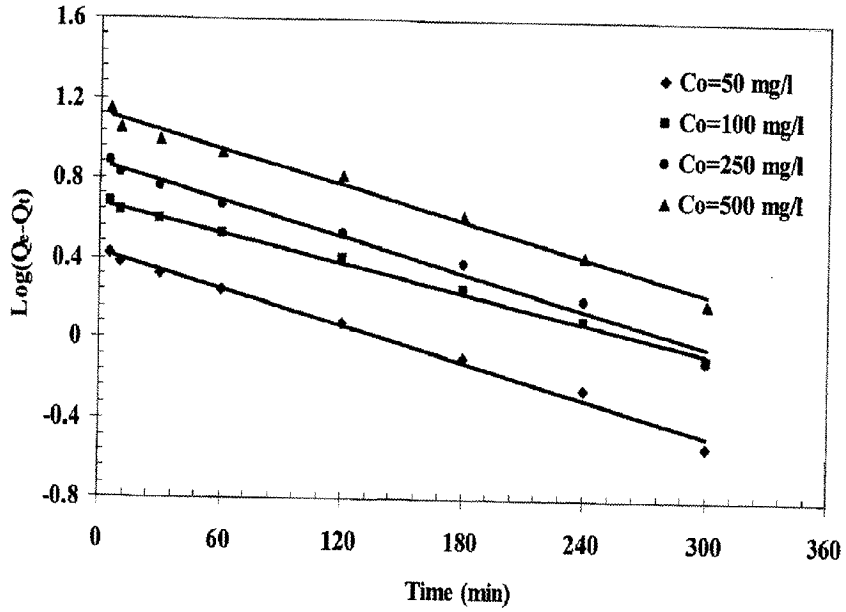

Fig. 5.9. First Order Kinetics for the removal of IC (T= 303 K, C_0 = 50, 100, 250 and 500 mg/l, RHA dose =10 g/l).

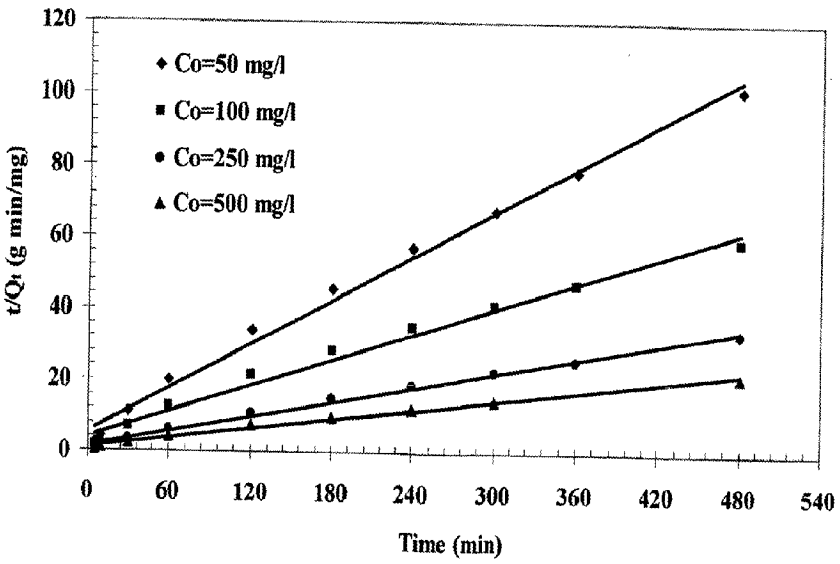

Fig. 5.10. Pseudo second-order kinetic plot for the removal of IC (T = 303 K, C_0 = 50, 100, 250 and 500 mg/l, RHA dose =10 g/l).

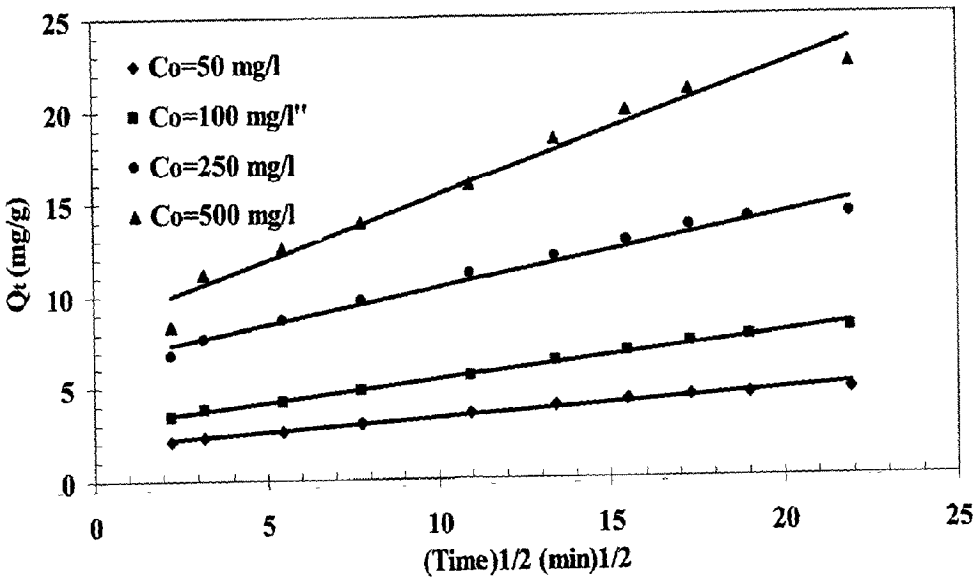

Fig. 5.11. Weber and Morris intra-particle diffusion plot for the removal of IC (T = 303 K, C_0 = 50, 100, 250 and 500 mg/l, RHA dose =10 g/l).

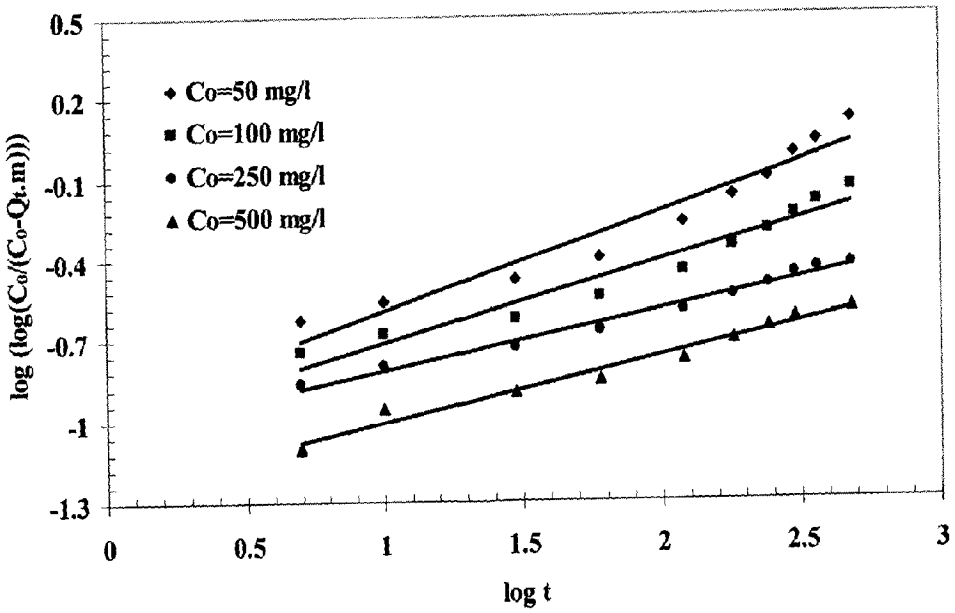

Fig. 5.12. Bangham plot for the removal of IC (T = 303 K, C_0 = 50, 100, 250 and 500 mg/l, RHA dose =10 g/l).

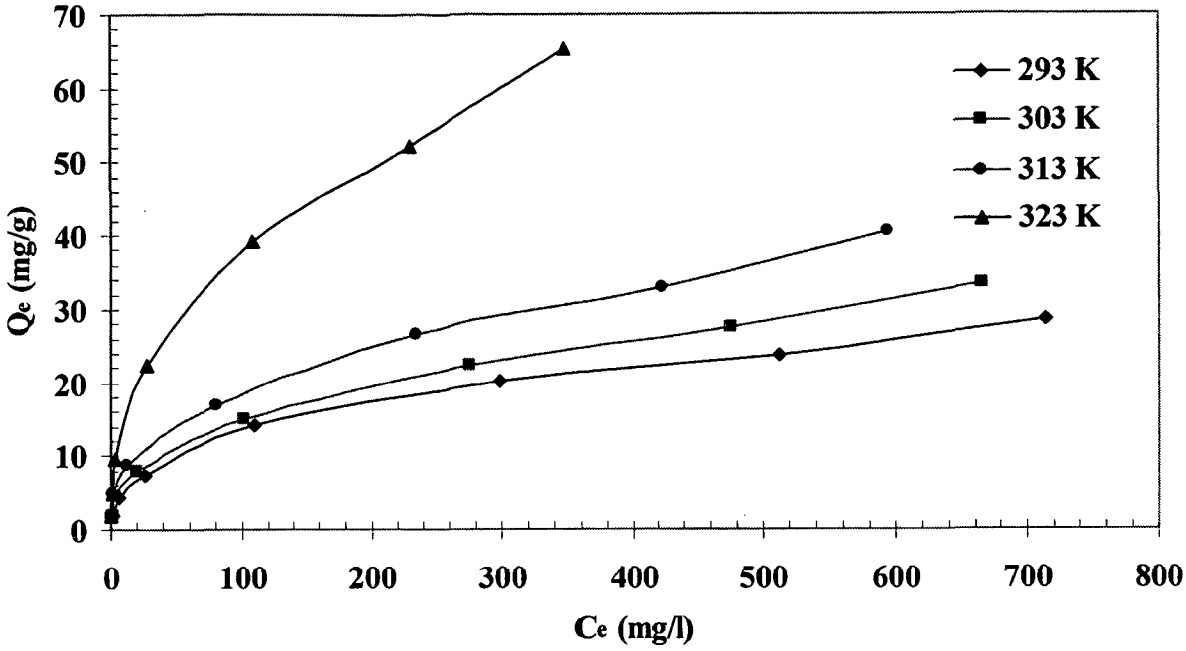

Fig. 5.13. Equilibrium adsorption isotherms at different temperatures for IC-RHA system (t=8h, m=10g/l).

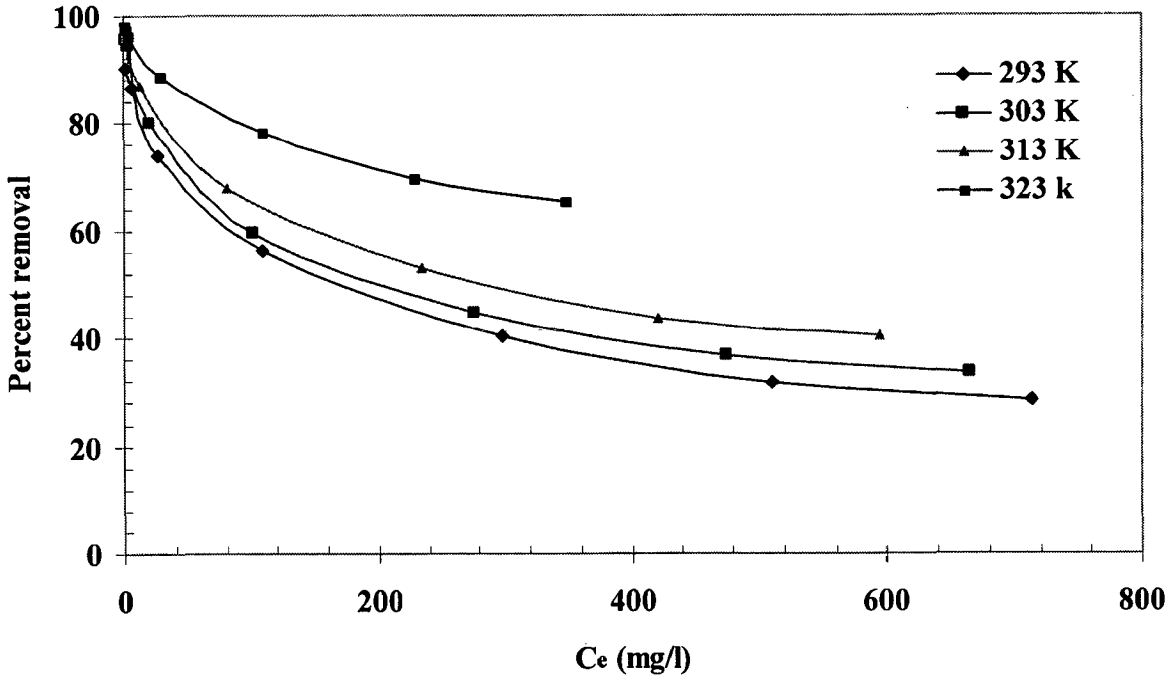

Fig. 5.14. Effect of initial concentration on percent removal of IC by RHA at different temperatures (t=8 h, m=10 g/l).

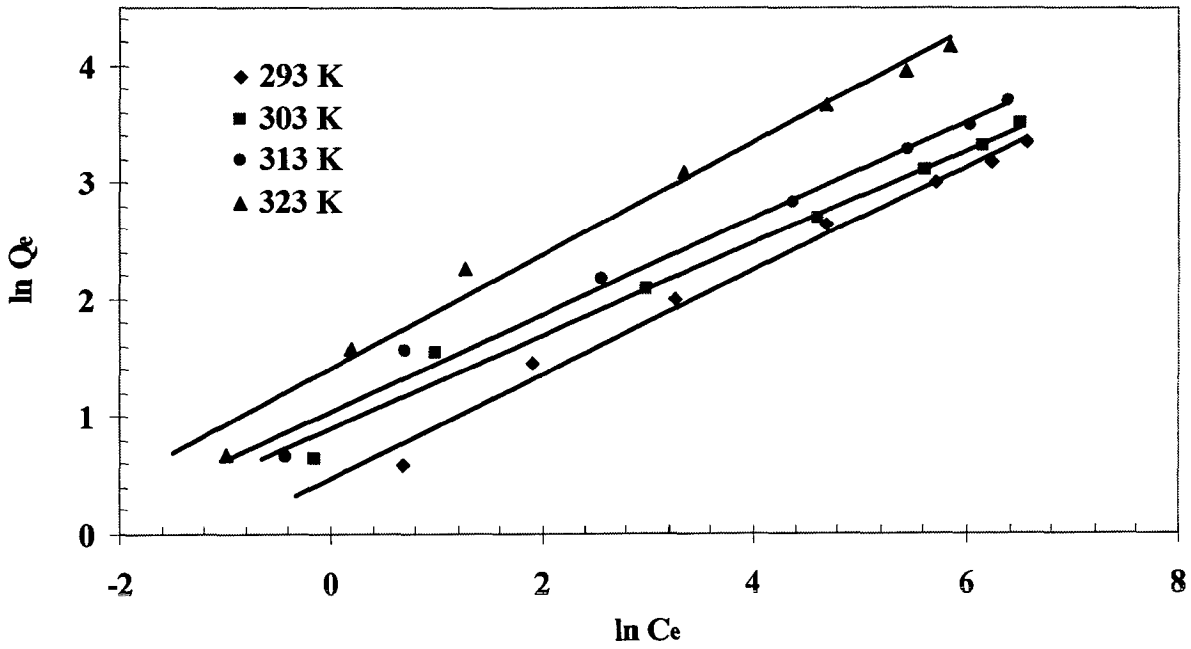

Fig. 5.15. Freundlich isotherm plots for the removal of IC at 293, 303, 313 and 323 K (t=8 h, RHA dose = 10 g/l).

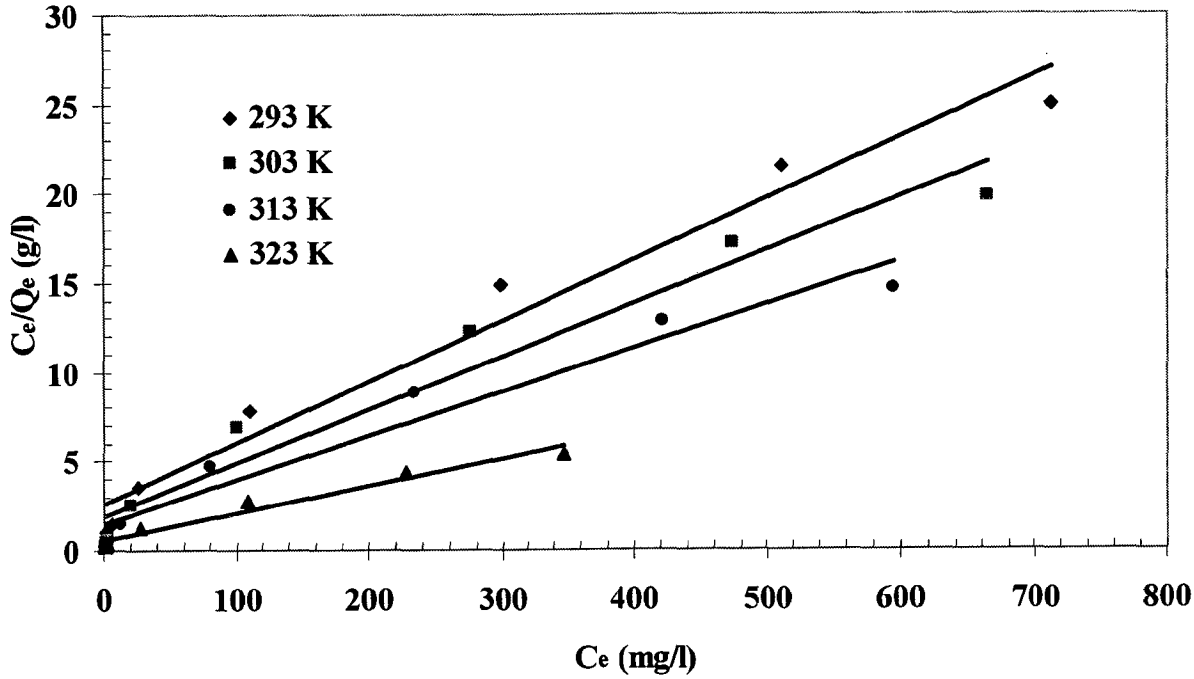

Fig. 5.16. Langmuir isotherm plots for the removal of IC at 293, 303, 313 and 323 K (t=8 h, RHA dose = 10 g/l).

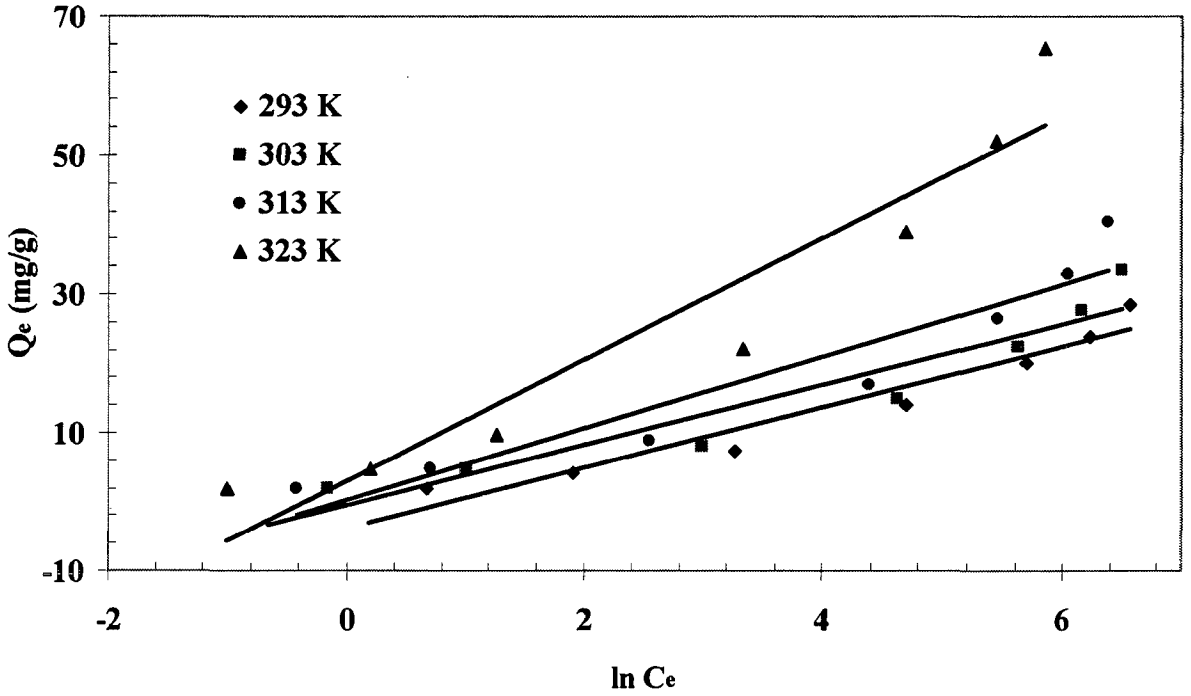

Fig. 5.17. Temkin isotherm plots for the removal of IC at 293, 303, 313 and 323 K (t=8 h, RHA dose = 10 g/l).

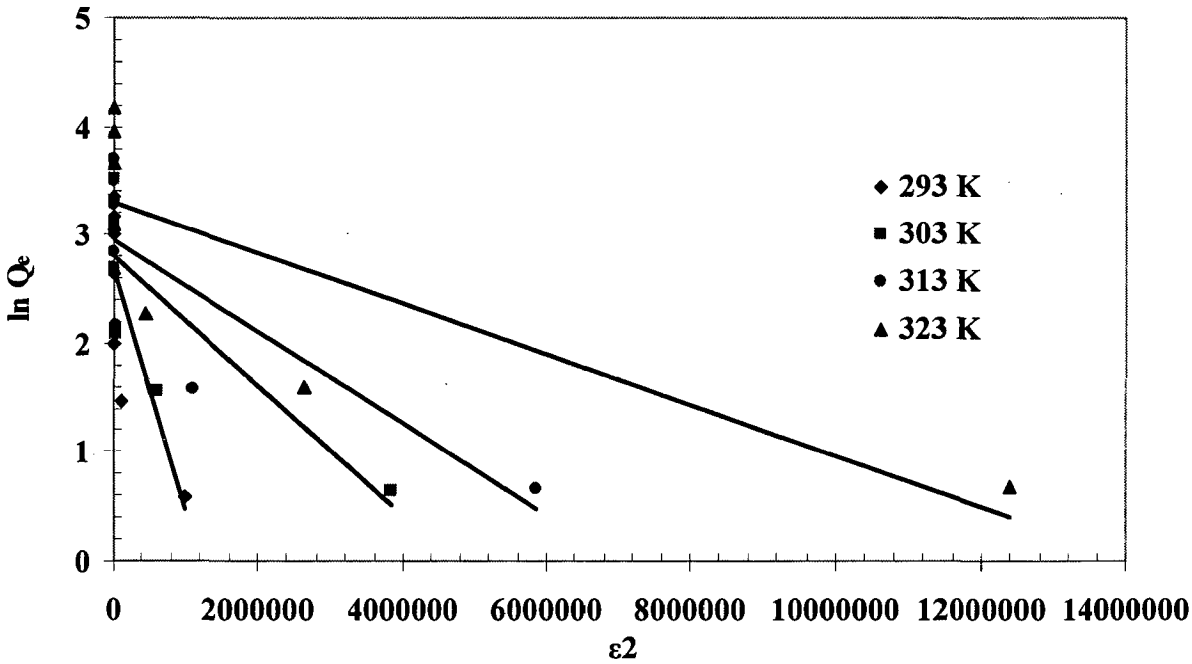

Fig. 5.18. D-R isotherm plots for the removal of IC at 293, 303, 313 and 323 K (t=8 h, RHA dose = 10 g/l).

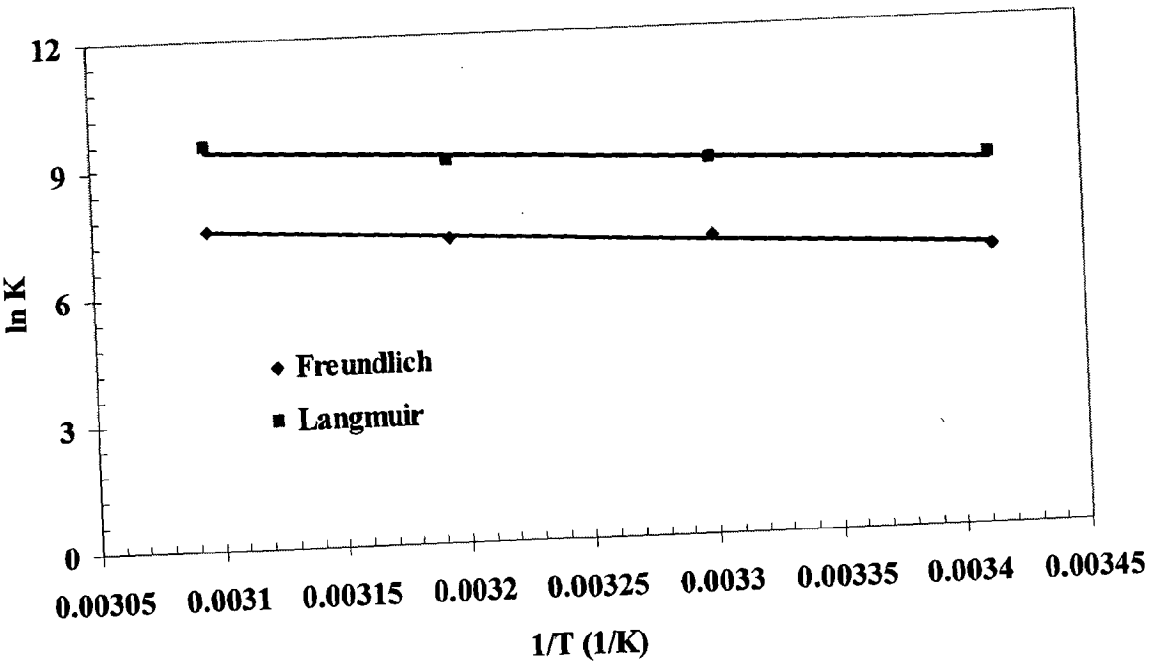

Fig. 5.19. Vant Hoff's plot for various isotherm models.

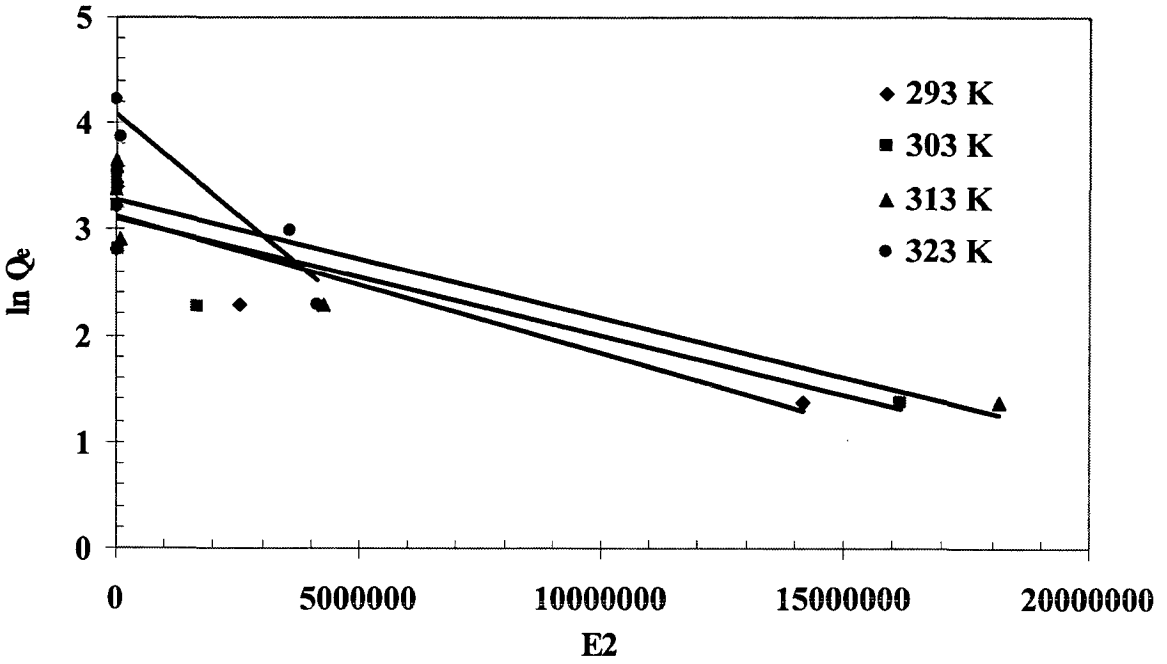

Fig. 5.36. D-R isotherm plots for the removal of IC at 293, 303, 313 and 323 K (t=4 h, BFA dose = 5 g/l).

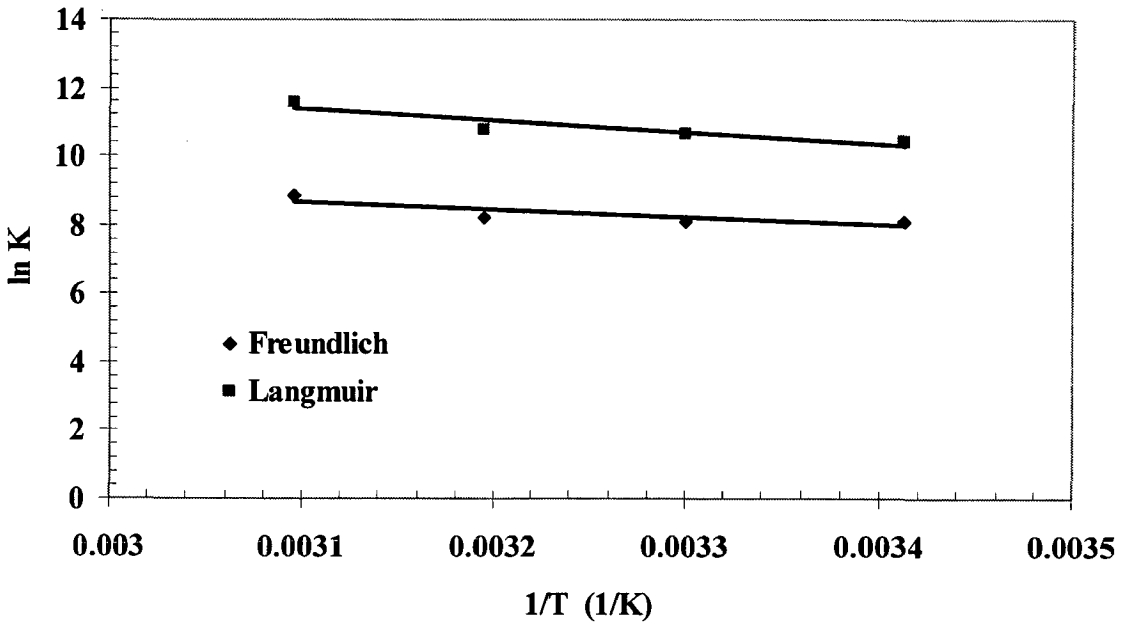

Fig. 5.37. Van't Hoff's plot for various isotherm models.

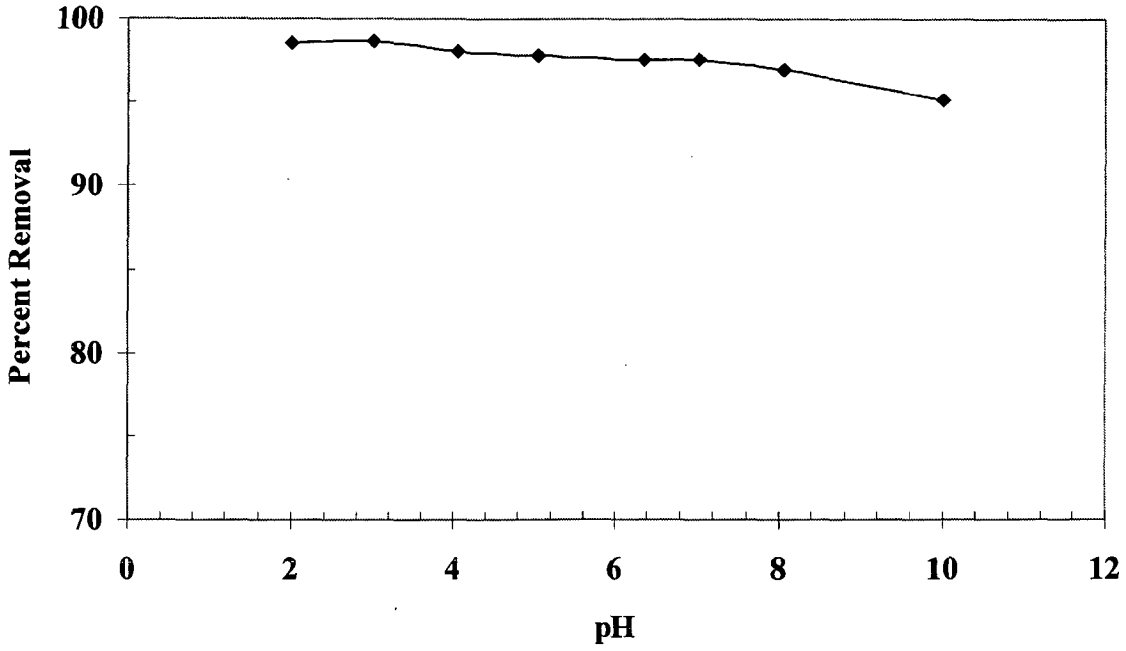

Fig. 5.20. Effect of pH on the adsorption of IC by adsorbent as BFA (T= 303 K, t = 4 h, C_0 = 50 mg/l, BFA dose = 5 g/l).

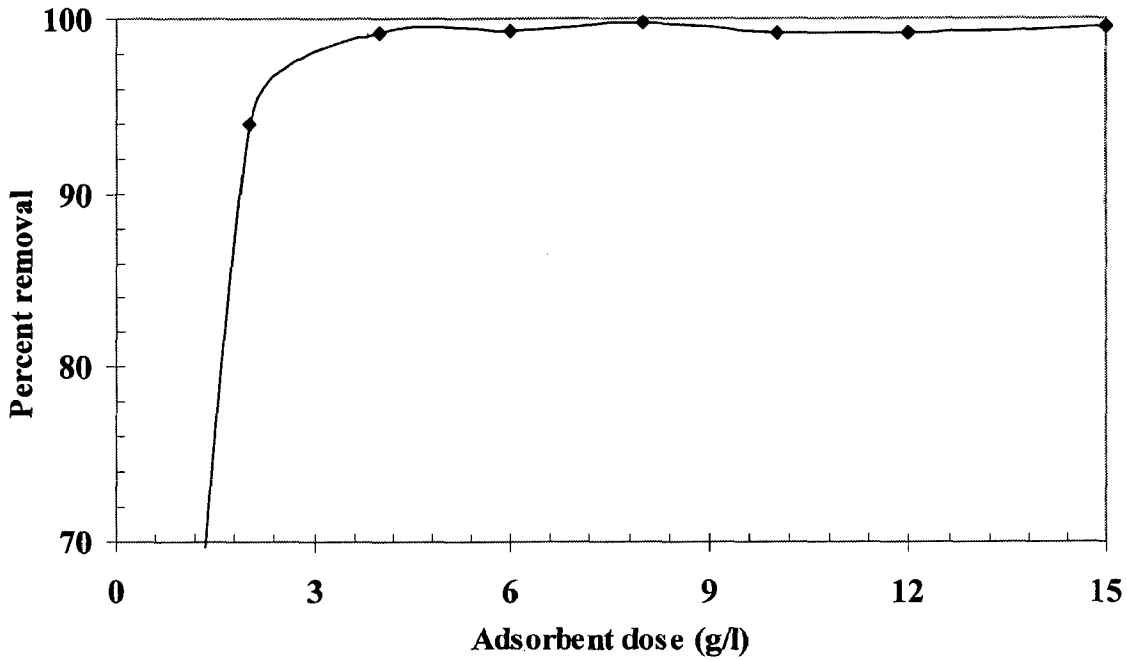

Fig. 5.21. Effect of adsorbent dose on the adsorption of IC by BFA (T = 303 K, t = 4 h, C_0 = 50 mg/l).

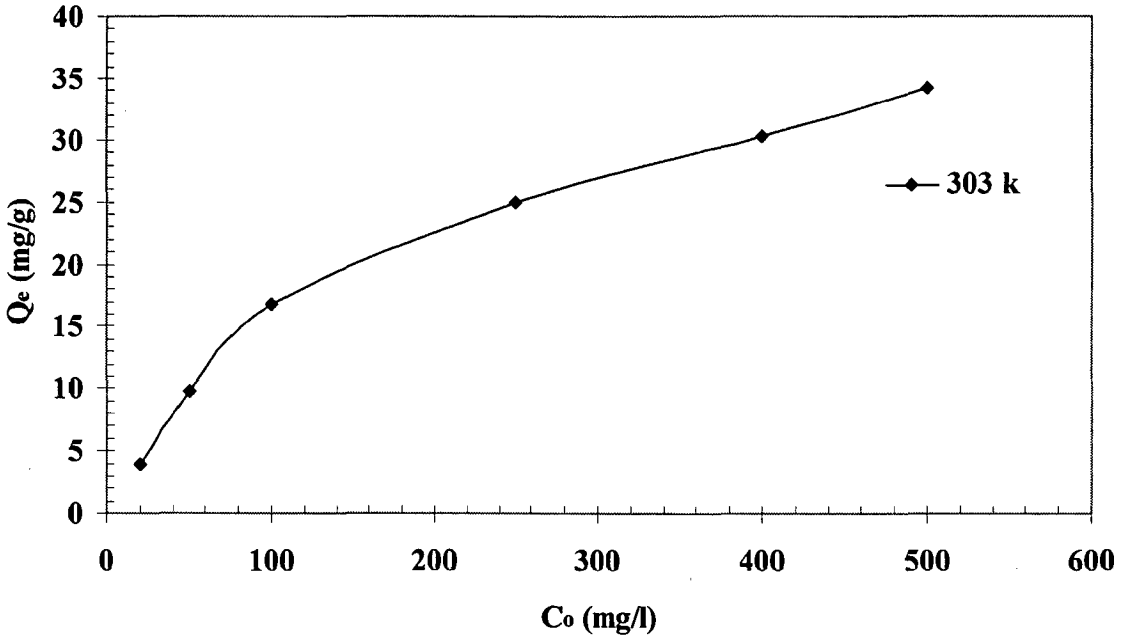

Fig. 5.22. Effect of initial concentration, C_0 on the adsorption capacity of BFA (T = 303 K, t = 4 h, C_0 = 50 mg/l).

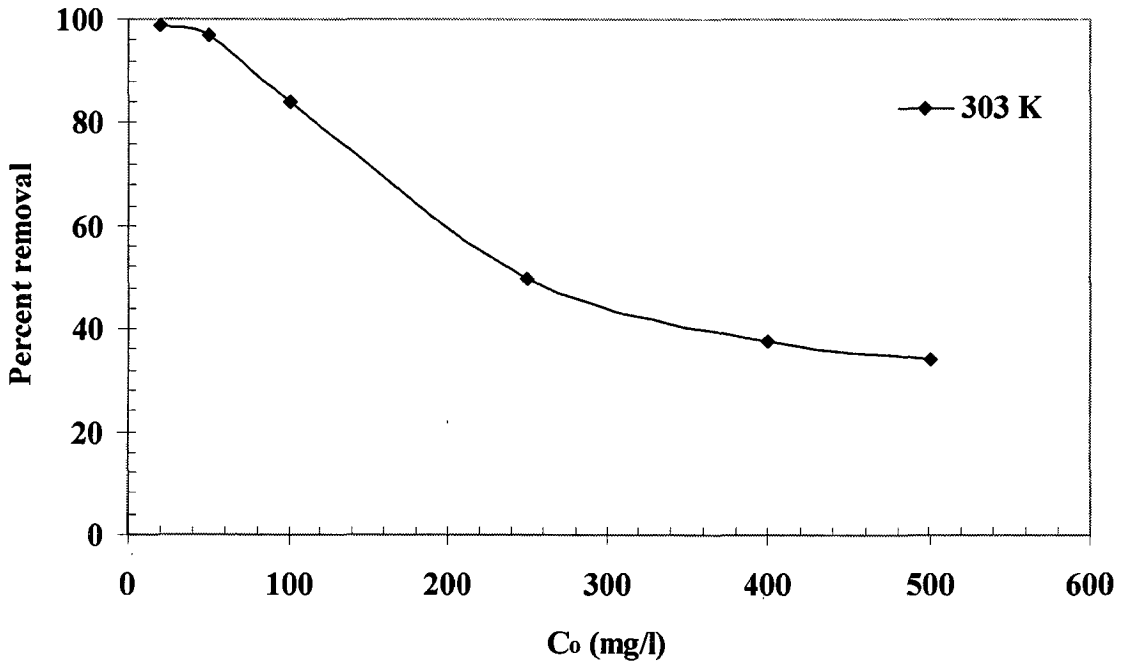

Fig. 5.23. Effect of initial concentration, C_0 on the percent removal capacity of BFA (T = 303 K, t = 4 h, C_0 = 50 mg/l).

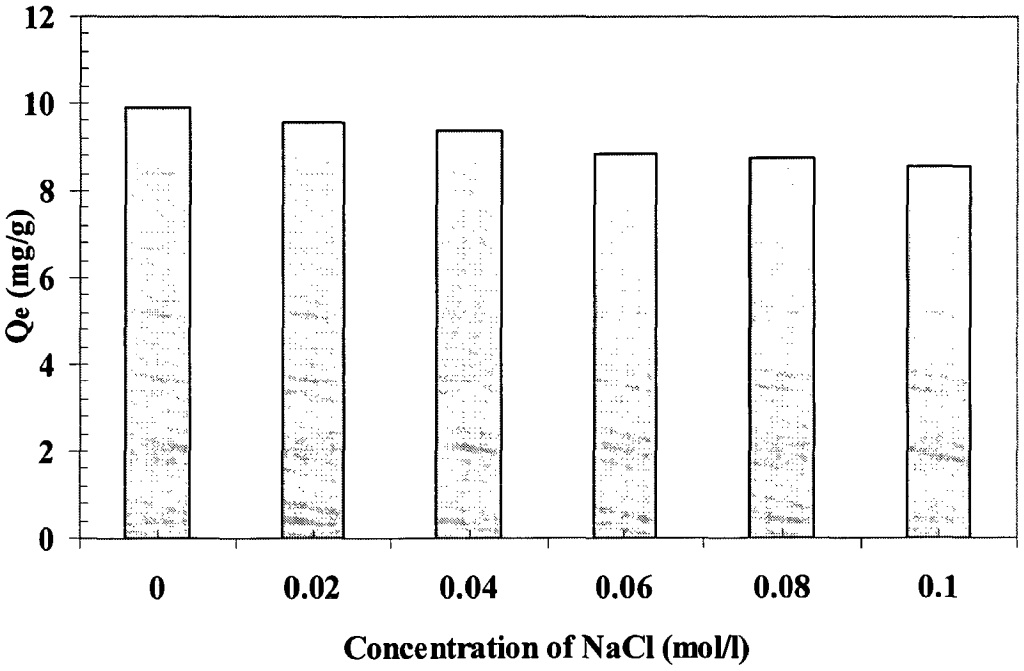

Fig. 5.24. Effect of NaCl concentration on the adsorption capacity of BFA (T= 303 K, C_0 = 50 mg/l, BFA dose =5 g/l).

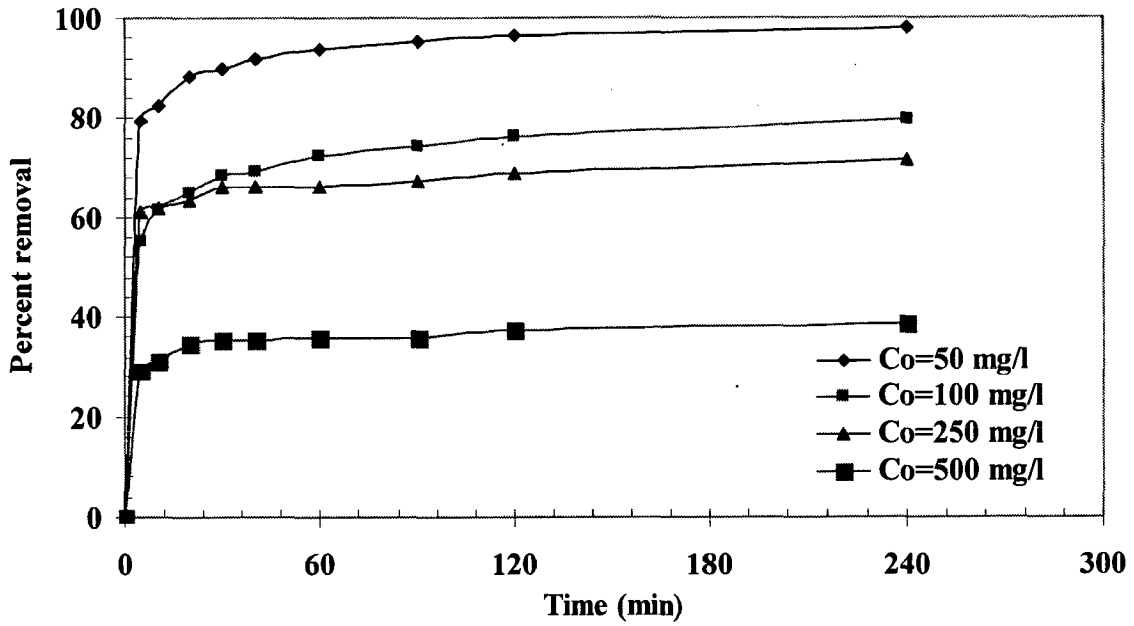

Fig. 5.25. Effect of contact time on percent removal of IC (T= 303 K, C_0 = 50, 100, 250 and 500 mg/l, BFA dose =5 g/l).

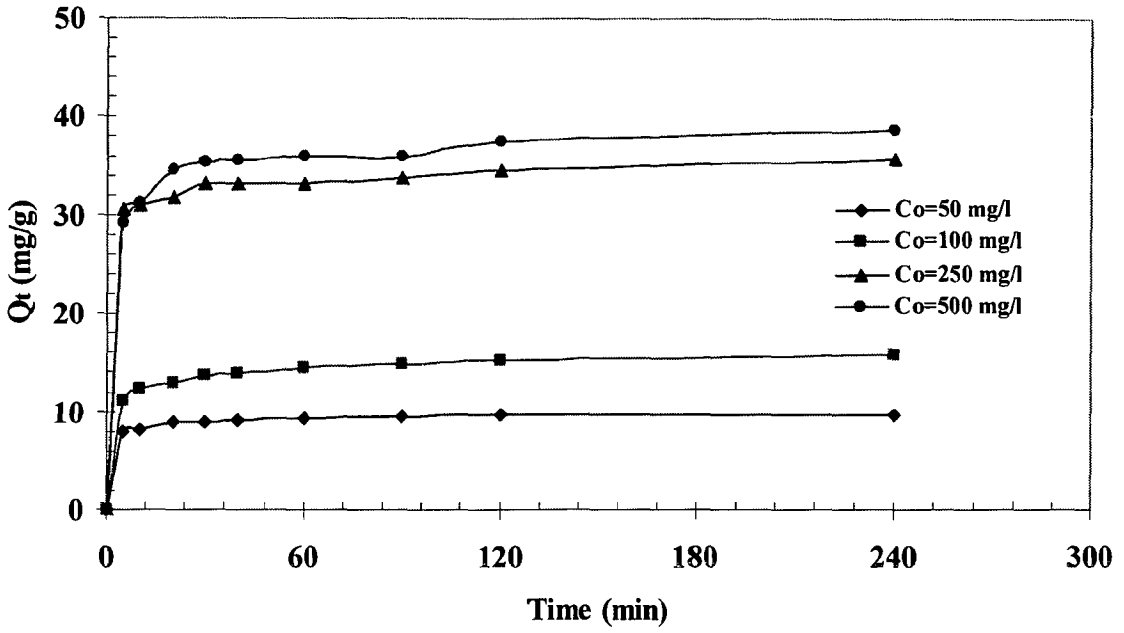

Fig. 5.26. Effect of contact time on adsorption of (T= 303 K, C_0 = 50, 100, 250 and 500 mg/l, BFA dose =5 g/l).

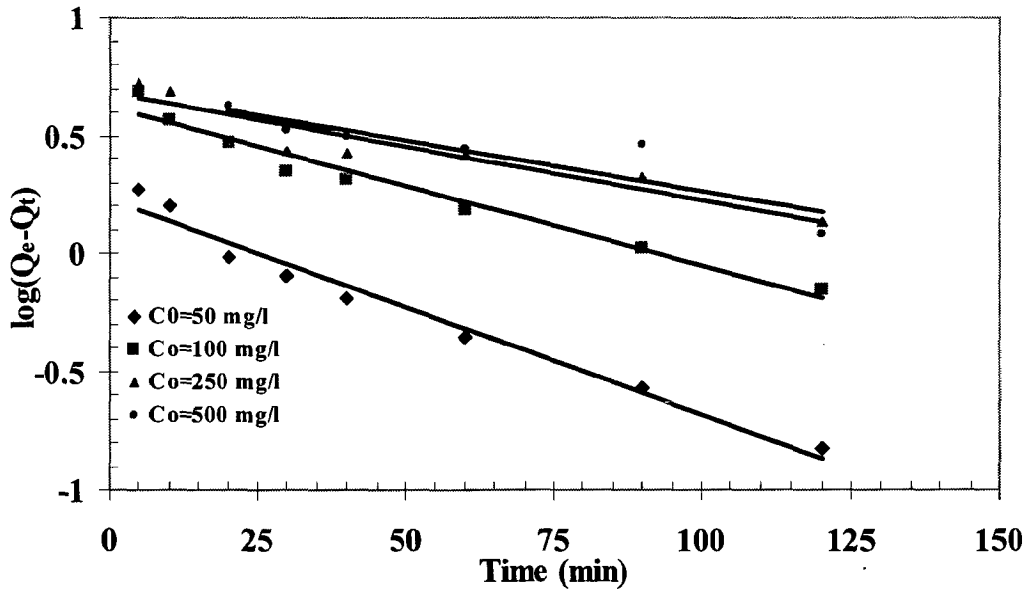

Fig. 5.27. First Order Kinetics for the removal of IC (T = 303 K, C_0 = 50, 100, 250 and 500 mg/l, BFA dose = 5 g/l).

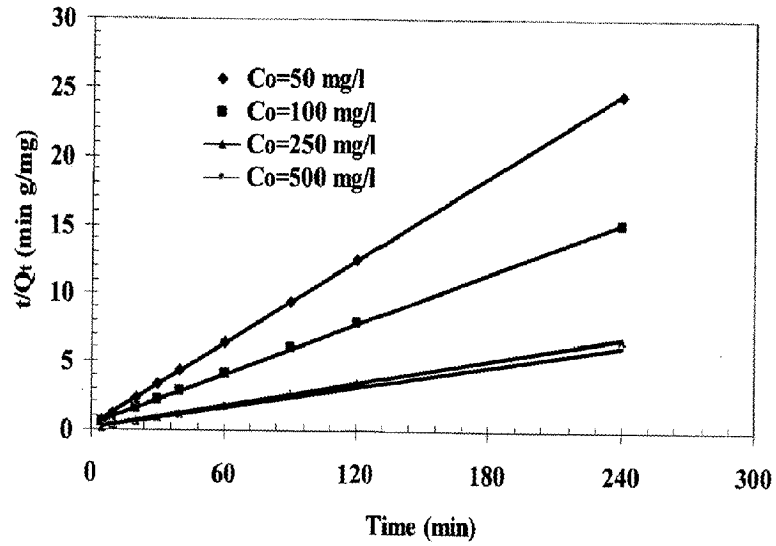

Fig. 5.28. Pseudo second-order kinetic plot for the removal of IC (T = 303 K, C_0 = 50, 100, 250 and 500 mg/l, BFA dose = 5 g/l).

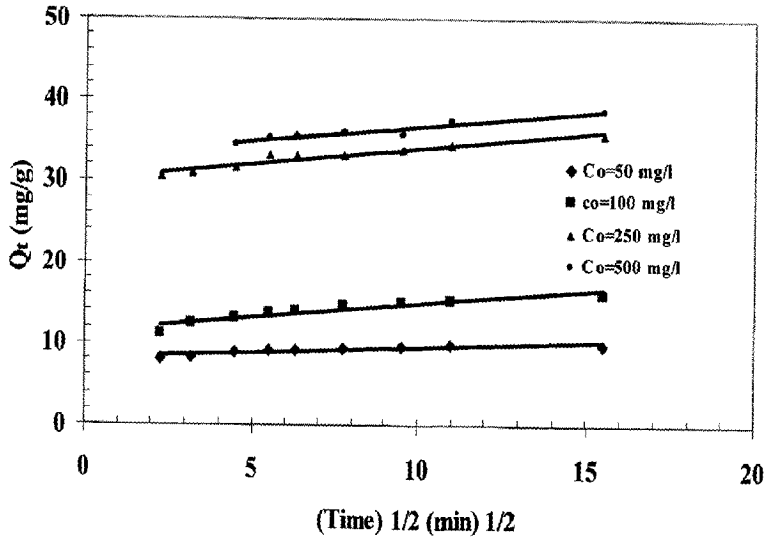

Fig. 5.29. Weber and Morris intra-particle diffusion plot for the removal of IC (T = 303 K, C_0 = 50, 100, 250 and 500 mg/l, BFA dose = 5 g/l).

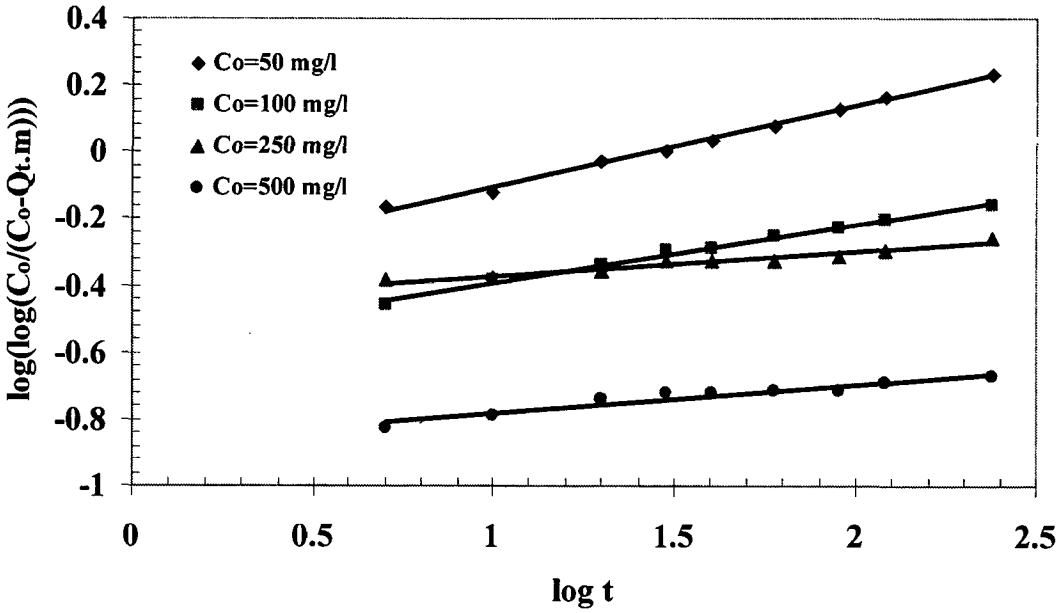

Fig. 5.30. Bangham plot for the removal of (T = 303 K, C_0 = 50, 100, 250 and 500 mg/l, BFA dose = 5 g/l).

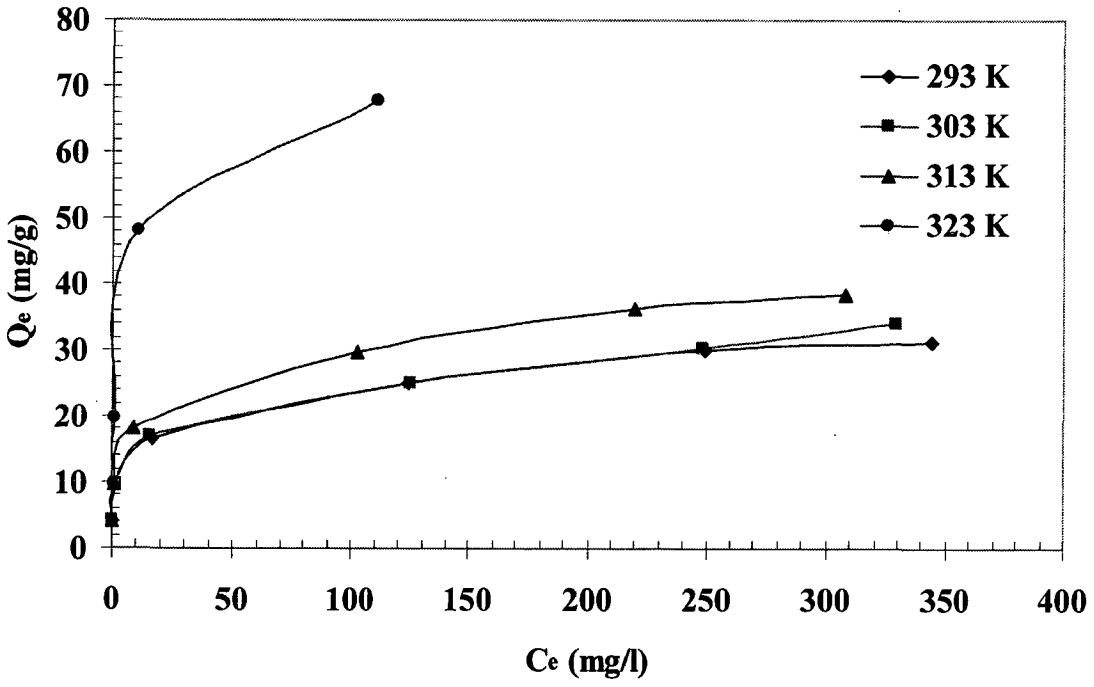

Fig. 5.31. Equilibrium adsorption isotherms at different temperatures for IC-BFA system (t=4h, m=5g/l).

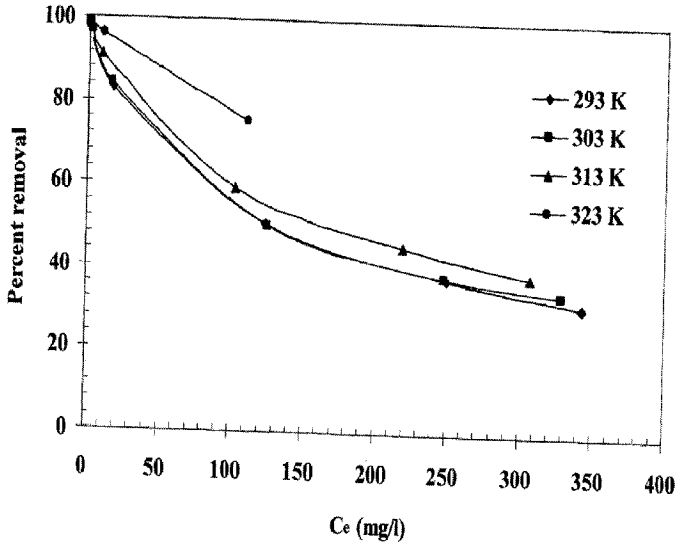

Fig. 5.32. Effect of initial concentration on percent removal of IC by BFA at different temperatures (t=4 h, m=5 g/l).

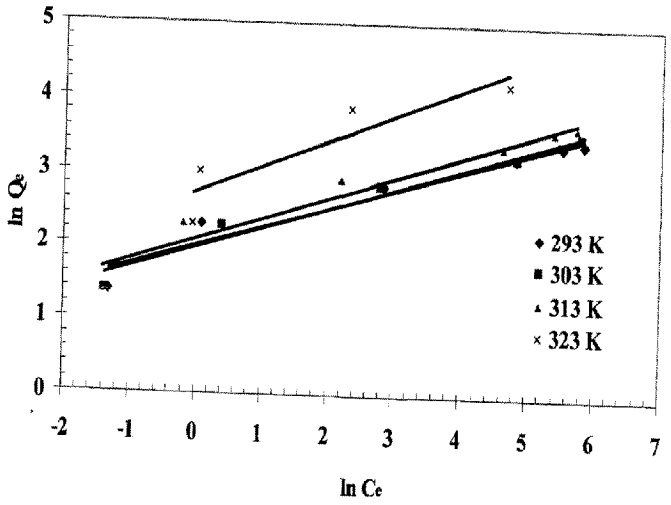

Fig. 5.33. Freundlich isotherm plots for the removal of IC at 293, 303, 313 and 323 K (t=4 h, BFA dose = 5 g/l).

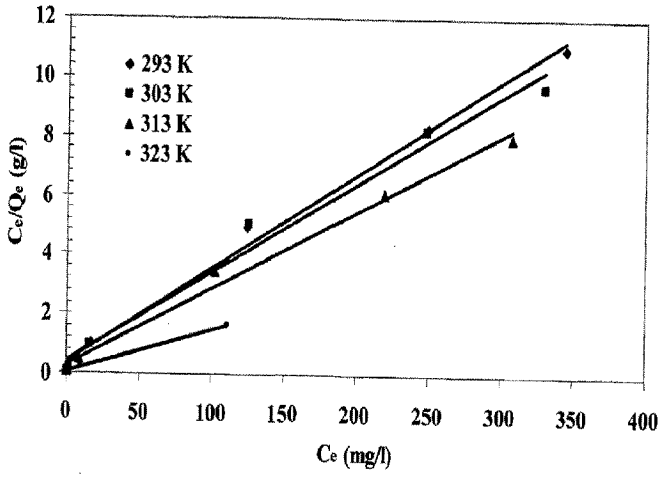

Fig. 5.34. Langmuir isotherm plots for the removal of IC at 293, 303, 313 and 323 K (t=4 h, BFA dose = 5 g/l).

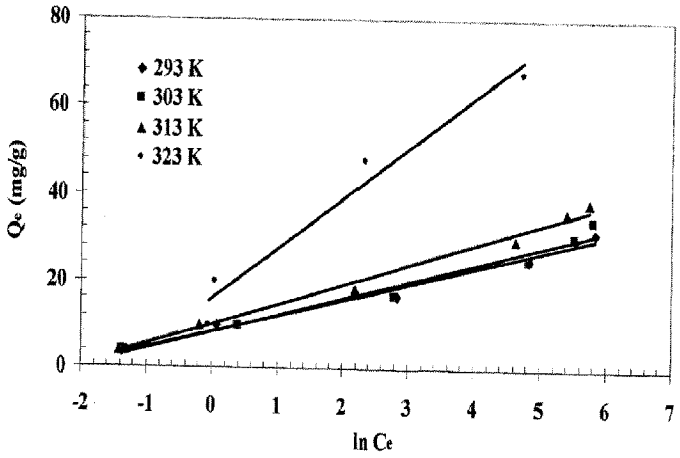

Fig. 5.35. Temkin isotherm plots for the removal of IC at 293, 303, 313 and 323 K (t=4 h, BFA dose = 5 g/l).

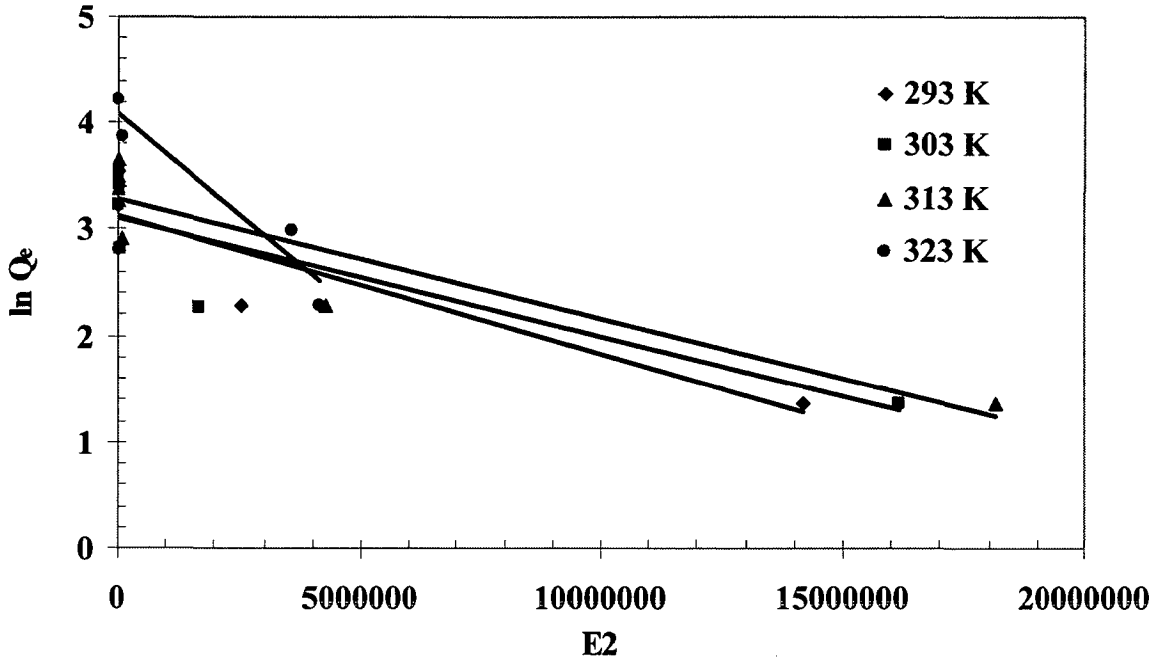

Fig. 5.36. D-R isotherm plots for the removal of IC at 293, 303, 313 and 323 K (t=4 h, BFA dose = 5 g/l).

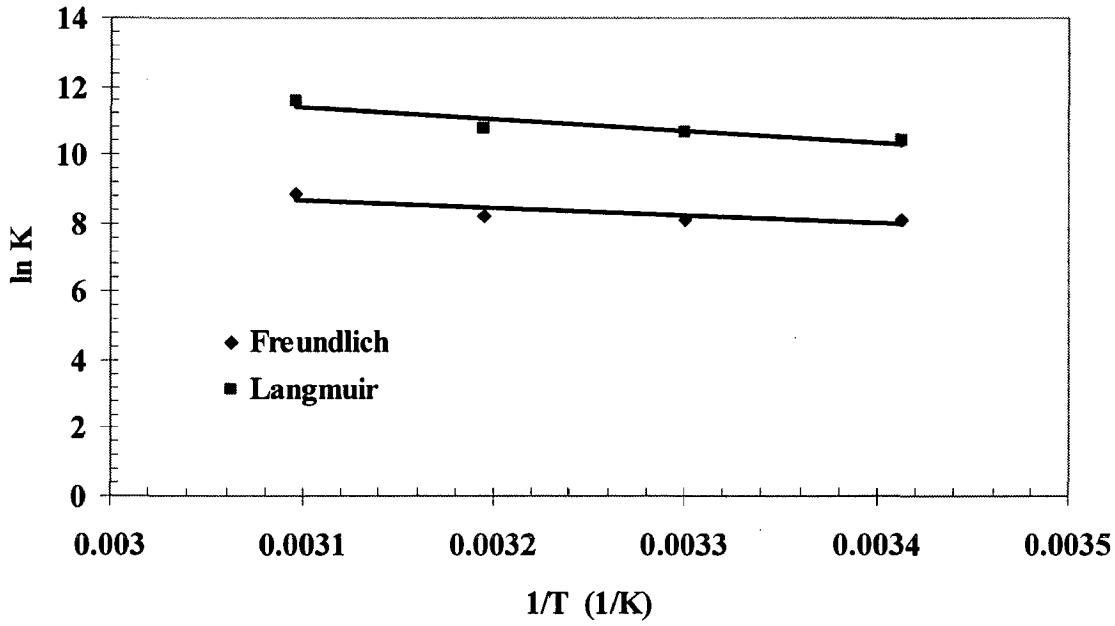

Fig. 5.37. Van't Hoff's plot for various isotherm models.

CHAPTER-6

CONCLUSION AND RECOMMENDATION

6.1 CONCLUSIONS

The following major conclusions can be drawn from the present work are given below:

1. Surface area, pore volume, average pore diameter and average particle size of rice husk ash (RHA) were found to be 65.36 m^2/g, 0.0566 cm^3/g, 34.66 Å and 150.47 μm,, respectively. For bagasse fly ash (BFA), the respective values were 237.83 m^2/g, 0.1337 cm^3/g, 22.47 Å and 460.04 μm.
2. SEM of BFA shows fibrous structure with large pore size with strands in each fibre. Number of pores in RHA is lesser than that in BFA. Surface of the RHA and BFA becomes smooth after adsorption of Indigo Carmine (IC).
3. Percent removal of IC increases with the increase in adsorbent dose for both RHA and BFA up to a certain limit and then remains almost constant. However, Percent removal decreases with increase in Indigo Carmine concentration for both the adsorbents.
4. Change in natural pH of the IC solution caused colour removal due to the structural changes being effected in the dye-molecules. Adsorption of IC on RHA and BFA is maximum in acidic pH range.
5. Effect of initial IC concentration on removal by RHA and BFA shows that for any contact time the percent removal decreases with increase in initial concentration of IC.
6. Kinetic study shows that adsorption of IC on RHA and BFA follows the second order kinetics for both RHA and BFA.
7. Weber-Morris plot reveals that the intraparticle transport (pore diffusion) is not the only rate-controlling step.
8. Freundlich isotherm best-fitted the isotherm data for IC adsorption on RHA and BFA at almost all temperatures, However, the non-linear correlation coefficients,

R^2 and the error analysis values are nearly similar for the Freundlich and Langmuir isotherms and hence any one of the isotherms could be used for IC adsorption on RHA and BFA.

9. Adsorption capacity of RHA and BFA for IC removal increases with increase in temperature for both the adsorbents, showing the endothermic nature of adsorption. The energy of adsorption reveals that it is a transitional state adsorption.
10. The results prove that adsorption processes for both RHA and BFA were spontaneous in nature although they represented an endothermic enthalpy for the interaction, resulting in an entropically favored process and hence can be used as potential adsorbents for the removal of IC.
11. It was seen that use of BFA as an adsorbent for the removal of IC was more economical and feasible than RHA because of its high fixed carbon percent and large surface area.

6.2 RECOMMENDATIONS

1. RHA and BFA from different sugar mills shall be characterized for physical-chemical parameters and surface characteristics to arrive at average values for use in design.
2. Equilibrium adsorption data shall be obtained for mixed dye concentration range encountered in industries.
3. Costing of the adsorption based on industrial scale treatment system shall be carried out to popularize the adsorption technique with RHA and BFA.

REFERENCES

[1] Alkan M., Demirbas O.Z., Sermet C., Mehmet., "Sorption of acid red 57 from aqueous solution onto sepiolite", Journal of Hazardous Materials B, 116 (2004), 135–145.

[2] Allen, P.A., Brown, J., Chem. Technol. Biotechnol., 62 (1995), 170.

[3] Axelsson J., Nilsson U., Terrazas E., Aliaga T.A., and Welander U., "Decolorization of the textile dyes Reactive Red 2 and Reactive Blue 4 using Bjerkandera sp. Strain BOL 13 in a continuous rotating biological contactor reactor", 39 (2006), 32-37.

[4] Banat I.M., Nigam P., Singh D., Marchant R., "Microbial decolorization of textile-dyecontaining effluents: A review", Bioresource Technology, 58 (1996), 217-227.

[5] Basibuyuk M., Forster C.F., "An examination of the adsorption characteristics of a basic dye (Maxilon Red BL-N) on to live activated sludge system", Process Biochemistry, 38 (2003), 1311-1316.

[6] Batzias F.A., Sidiras D.K., "Dye adsorption by calcium chloride treated beech sawdust in batch and fixed-bed systems", Journal of Hazardous Materials B, 114 (2004), 167–174.

[7] Bhattacharyya, K.G., Sharma, A., J. "Adsorption of Pb(II) from aqueous solution by Azadirachta indica (Neem) leaf powder.", Journal of Hazardous Materials B,113 (2004), 97–109.

[8] Chakraborty S., De S., Basu J.K., Gupta S.D., "Treatment of a textile effluent: application of a combination method involving adsorption and nanofiltration", Desalination, 174 (2005), 73-85.

[9] Chao L., Zhaoyang L., Aimin L., Wei L., Zhenmao J., Jinlong C., Quanxing Z., "Adsorption of reactive dyes onto polymeric adsorbents: effect of pore structure and surface chemistry group of adsorbent on adsorptive properties", Separation and Purification Technology, 44 (2005), 115-120.

[21] Ghoreishi S.M., Haghighi R., "Chemical catalytic reaction and biological oxidation for treatment of non-biodegradable textile effluent", Chemical Engineering Journal, 95 (2003), 163–169.

[22] Golob V., Vinder A., Simonic M., "Efficiency of the coagulation/flocculation method for the treatment of dyebath effluents", Dyes and Pigments, 67 (2005), 93-97.

[23] Grabowska E.L., Gryglewicz G.Z., "Adsorption characteristics of Congo Red on coal-based mesoporous activated carbon" Dyes and Pigments (2006), Article in press.

[24] Grimau V.L., Gutie´rrez M.C., "Decolourisation of simulated reactive dyebath effluents by electrochemical oxidation assisted by UV light", Chemosphere, 62 (2006), 106–112.

[25] Gulnaz O., Kayaa A., Matyar F., Arikan B., "Sorption of basic dyes from aqueous solution by activated sludge", Journal of Hazardous Materials, 108 (2004), 183–188.

[26] Gupta G. S., Shukla S. P., "Toxic Effects of Omega Chrome Red ME and Its Treatment by Adsorption", Ecotoxicology and Environmental Safety, 24 (1992), 155-163.

[27] Gupta V.K., Ali, Suhas, Mohan D., "Equilibrium uptake and sorption dynamics for the removal of a basic dye (basic red) using low-cost adsorbents", Journal of Colloid and Interface Science, 265 (2003), 257–264.

[28] Gupta V.K., Mittal A., Krishnan L., Gajbe V., "Adsorption kinetics and column operations for the removal and recovery of malachite green from wastewater using bottom ash", Separation and Purification Technology, 40 (2004), 87–96.

[29] Guo Y., Yang S., Fu W., Qi J., Li R., Wang Z., Xu H., "Adsorption of malachite green on micro- and mesoporous rice husk-based active carbon", Dyes and Pigments, 56 (2003), 219–229.

[30] Hachem C., Bocquillon F., Zahraa O., Bouchy M., "Decolourization of textile industry wastewater by the photocatalytic degradation process", Dyes and Pigments, 49 (2001), 117–125.

[31] Hamedaani H.R.K., Sakurai A., Sakakibara M., "Decolorization of synthetic dyes by a new manganese peroxidase-producing white rot fungus", Dyes and Pigments, 72 (2007), 157-162.

[32] Hasany, S.M., Chaudhary, M.H., Appl. Radiat. Isot. 47 (1996) 467.

[33] Hoda N., Bayram E., Ayranci E., "Kinetic and equilibrium studies on the removal of acid dyes from aqueous solutions by adsorption onto activated carbon cloth", Journal of Hazardous Materials (2006), Article in press.

[34] Ho Y.S., McKay G., "Pseudo-second order model for sorption processes", Process Biochemistry, 34 (1999), 451-465.

[35] Jime´nez M.M.D., Gonza´lez M.P.E., Gonza´lez A.G., Cid A.A.P., "Electrochemical treatment of textile dyes and their analysis by high-performance liquid chromatography with diode array detection", Journal of Chromatography A, 889 (2000), 253–259.

[36] Kapoor A., Yang R.T., "Correlation of equilibrium adsorption data of condensible vapours on porous adsorbents", Gas Separation & Purification, 3 (1989), 187-192.

[37] Kas,g¨oz H., "Aminofunctionalized acrylamide–maleic acid hydrogels: Adsorption of indigo carmine", Colloids and Surfaces A: Physicochem. Eng. Aspects, 266 (2005), 44–50.

[38] Kim, Y., Kim, C., Choi, I., Rengraj, S., Yi, J., Environ. Sci. Technol. 38 (2004), 924.

[39] Kirby, N., "Bioremediation of textile industry wastewater by white rot fungi", DPhil Thesis, University of Ulster, Coleraine, UK., (1999).

[40] Kumar K.V., Kumaran A., "Removal of methylene blue by mango seed kernel powder", Biochemical Engineering Journal, 27 (2005b), 83–93.

[41] Kumar K.V., Ramamurthi V., Sivanesan S., "Modeling the mechanism involved during the sorption of methylene blue onto fly ash", Journal of Colloid and Interface Science ,284 (2005a), 14–21.

[42] Liversidge R.M., Lloyd G.J., Wase D.A.J., Forster C.F., "Removal of Basic Blue 41 dye from aqueous solution by linseed cake", Process Biochemistry, 32 (1997), 473-477.

[43] Malik P.K., "Dye removal from wastewater using activated carbon developed from sawdust: adsorption equilibrium and kinetics", Journal of Hazardous Materials, 113 (2004), 81-88.

[44] Mall I.D., Srivastava V.C., Agarwal N.K., Mishra I.M., "Removal of congo red from aqueous solution by bagasse fly ash and activated carbon: Kinetic study and equilibrium isotherm analyses", Chemosphere, 61 (2005b), 492–501.

[45] Mall I.D., Srivastava V.C., Agarwal N.K., "Removal of Orange-G and Methyl Violet dyes by adsorption onto bagasse fly ash-kinetic study and equilibrium isotherm analyses",Dyes and Pigments, 69 (2006), 210-223.

[46] Marechal A.M.L., Slokar Y.M., Taufer T., "Decoloration of Chlorotriazine Reactive Azo Dyes with H_2O_2/UV.", Dyes and Pigments, 33 (1997), 281-298.

[47] Mathur N., Bhatnagar P., Nagar P., Bijarnia M.K., "Mutagenicity assessment of effluents from textile/dye industries of Sanganer, Jaipur (India): a case study", Ecotoxicology and Environmental Safety, 61 (2005), 105–113.

[48] McKay G., Otterburn M. S., Sweeney A. G., "The removal of colour from effluent using various adsorbents-IV. silica: Equilibria and column studies" Water Research, 14 (1980), 21-27.

[49] Namasivayam C., Sumithra S., "Removal of direct red 12B and methylene blue from water by adsorption onto Fe (III)/Cr (III) hydroxide, an industrial solid waste", Journal of Environmental Management, 74 (2005), 207–215.

[50] Órfão J.J.M., Silva AI.M., Pereira J.C.V., Barata S.A., Fonseca I.M., Faria P.C.C., Pereira M.F.R., "Adsorption of a reactive dye on chemically modified activated carbons—Influence of Ph", Journal of Colloid and Interface Science, 296 (2006), 480–489.

[51] Othman I., Mohamed R.M., Ibrahim I.A., Mohamed M.M., "Synthesis and modification of ZSM-5 with manganese and lanthanum and their effects on decolorization of indigo carmine dye", Applied Catalysis A: General, 299 (2006), 95–102.

[52] Özcan A.S., Erdem B., Özcan A., "Adsorption of Acid Blue 193 from aqueous solutions onto Na–bentonite and DTMA–bentonite", Journal of Colloid and Interface Science, 280 (2004), 44–54.

[53] Porter, J.F., McKay, G., Choy, K.H., Chem. Eng. Sci. 54 (1999), 5863.

[54] Prado A.G.S., Miranda B.S., Jacintho G.V.M., "Interaction of indigo carmine dye with silica modified with humic acids at solid/liquid interface", Surface Science, 542 (2003), 276–282.

[55] Prado A.G.S., Torres J.D., Faria E.A., Dias S.C.L., "Comparative adsorption studies of indigo carmine dye on chitin and chitosan", Journal of Colloid and Interface Science, 277 (2004), 43–47.

[56] Seidel A., Gelbin D., "On applying the ideal adsorbed solution theory to multicomponent adsorption equilibria of dissolved organic components on activated carbon", Chemical Engineering Science, 43, (1988), 79-88.

[57] Slokar Y.M., Marechal A.M.L., "Methods of Decoloration of Textile Wastewaters", Dyes and Pigments, 37 (1998), 335-356.

[58] Srivastava V.C., Mall I.D., Agarwal N.K., Mishra I.M., "Adsorptive removal of malachite green dye from aqueous solution by bagasse fly ash and activated carbon-kinetic study and equilibrium isotherm analyses", Colloids and Surfaces A: Physicochem. Eng. Aspects, 264 (2005), 17–28.

[59] Sun Q., Yang L., "The adsorption of basic dyes from aqueous solution on modified peat–resin particle", Water Research, 37 (2003), 1535–1544.

[60] Tan B.H., Teng T.T., Omar A.K.M., "Removal of dyes and industrial dye wastes by Magnesium chloride", Wat. Res., 34 (2000), 597-601.

[61] Temkin, M.J., Pyzhev, V., Acta Physiochim. URSS 12 (1940), 217.

[62] Tutem, E., Apak, R., Unal, C.F., Water Research 32 (1998), 2315.

[63] Vadivelan V., Kumar K.V., "Equilibrium, kinetics, mechanism, and process design for the sorption of methylene blue onto rice husk", Journal of Colloid and Interface Science, 286 (2005), 90–100.

[64] Wang S., Boyjoo Y., Choueib A., Zhu Z.H., "Removal of dyes from aqueous solution using fly ash and red mud", Water Research, 39 (2005), 129-138.

[65] Wong, Y.C., Szeto, Y.S., Cheung, W.H., McKay, G., Process Biochem., 39 (2004), 693.

[66] Zhang F., Knapp J.S., Tapley K.N., "Decolourisation of cotton bleaching effluent with wood rotting fungus", Water Research, 33 (1999), 919-928.

[67] http://www.centralchronicle.com/20050228/2802303.htm

[68] http://www.agriculture-industry-india.com/agricultural-commodities/dye.html

[69] http://www.cpcb.nic.in

[70] http://www.sciencelab.com/xMSDS-FD_C_Blue_2-9924015

[71] http://physchem.ox.ac.uk/MSDS/IN/indigo_carmine.html

[72] http://www.proscitech.com.au/catalogue/msds/c111.pdf

[73] http://www.p2pays.org/ref/11/10489/sectors73ak.html

TABLES

Table 5.1. Characteristics of RHA and BFA.

Characteristics	RHA	BFA
Proximate analysis		
Moisture (%)	0.74	5.65
Ash (%)	88.0	54.75
Volatile matter (%)	5.37	6.70
Fixed Carbon (%)	5.90	32.90
Bulk density (kg/m^3)	104.9	88.29
Average particle size (μm)	150.47	460.04
Surface area of pores (m^2/g)		
(i) BET	65.36	237.83
(ii) BJH		
(a) adsorption cumulative	52.34	62.29
(b) desorption cumulative	26.61	36.19
BJH cumulative pore volume (cm^3/g)		
(i) Single Point Total	0.0566	0.1337
(ii) BJH adsorption	0.0566	0.0526
(iii) BJH desorption	0.0388	0.0508
Average pore diameter (Å)		
(i) BET	34.66	22.47
(ii) BJH adsorption	43.27	33.77
(iii) BJH desorption	58.33	56.12

Table 5.2. Kinetic parameters for the removal of Indigo Carmine by RHA (pH_0 = natural, T = 303 K, C_0 = 50, 100, 250 and 500 mg/l, RHA dose = 10 g/l).

Pseudo-first-order					
C_o (mg/l)	$Q_{e,\ expt}$ (mg/g)	$Q_{e,\ calc}$ (mg/g)	k_f (1/min)	R_1^2 (linear)	R_2^2 (non-linear)
50	4.754	2.675	0.0069	0.9987	-0.9532
100	8.120	4.750	0.0057	0.9949	-0.9340
250	14.365	7.476	0.0069	0.9843	-0.9897
500	22.479	12.987	0.0057	0.9822	-0.9771

Pseudo-second-order						
C_o (mg/l)	$Q_{e,\ expt}$ (mg/g)	$Q_{e,\ calc}$ (mg/g)	h (mg/g min)	k_S (g/mg min)	R_1^2 (linear)	R_2^2 (non-linear)
50	4.754	4.861	0.183	0.0077	0.9931	0.9965
100	8.120	8.278	0.249	0.0036	0.9868	0.9933
250	14.36	14.598	0.637	0.0029	0.9943	0.9971
500	22.479	22.936	1.009	0.0019	0.9901	0.9950

Bangham				
C_o (mg/l)	k_0 (g)	α	R_1^2 (linear)	R_2^2 (non-linear)
50	2.539	0.366	0.9376	0.9683
100	2.231	0.302	0.9403	0.9697
250	2.109	0.222	0.9843	0.9921
500	1.282	0.245	0.9755	0.9877

Intra-particle diffusion				
C_o (mg/l)	k_{id} (mg/g $min^{1/2}$)	I (mg/g)	R_1^2 (linear)	R_2^2 (non-linear)
50	0.140	1.927	0.9842	0.9920
100	0.246	2.939	0.9947	0.9973
250	0.392	6.458	0.9794	0.9896
500	0.697	8.372	0.9678	0.9837

Table 5.3. Isotherm parameters for removal of Indigo Carmine by RHA (pH_0 = natural, T = 293, 303, 313 and 323 K, t = 8 h, C_0 = 20-1000 mg/l, RHA dose =10 g/l).

Freundlich constants				
T (K)	K_F ((mg/g)/(mg/l)$^{1/n}$)	$1/n$	R_1^2 (linear)	R_2^2 (non-linear)
293	1.602	0.4453	0.9879	0.9939
303	2.470	0.3962	0.984	0.9919
313	2.859	0.4122	0.9858	0.9928
323	4.103	0.4831	0.9856	0.9927

Langmuir constants					
T (K)	K_L (l/mg)	Q_m (mg/g)	R_L	R_1^2 (linear)	R_2^2 (non-linear)
293	0.013	29.239	0.6030	0.9710	0.9854
303	0.015	33.557	0.5695	0.9550	0.9772
313	0.017	40.322	0.5333	0.9544	0.9769
323	0.029	65.789	0.4074	0.9594	0.9795

Dubnin-Radushkevih constants				
T(K)	Q_s (mg/g)	E (kJ/mol)	R_1^2 (linear)	R_2^2 (non-linear)
293	14.444	500.00	0.6478	-0.8048
303	16.444	912.87	0.6698	-0.8184
313	19.106	1118.03	0.6748	-0.8214
323	26.816	1581.14	0.6600	-0.8124

Temkin constants				
T (K)	K_T (l/mg)	B_1	R_1^2 (linear)	R_2^2 (non-linear)
293	0.410	4.3936	0.9391	0.9690
303	0.887	4.3623	0.8973	0.9472
313	1.043	5.2116	0.8997	0.9485
323	1.437	8.7568	0.9112	0.9546

Table 5.4. Values of five different error analyses of isotherm models for adsorption of Indigo Carmine by RHA (pH_0 =natural, T= 293, 303, 313 and 323 K, t = 8 h, C_0 = 20-1000 mg/l, RHA dose =10 g/l).

293 K					
	SSE	**SAE**	**ARE**	**HYBRID**	**MPSD**
Freundlich	7.234	5.886	8.820	-0.768	12.491
Langmuir	32.812	13.340	22.702	13.150	35.873
D-R	419.941	43.720	54.776	-29.791	90.100
Temkin	38.604	13.580	33.541	19.981	71.651
303 K					
	SSE	**SAE**	**ARE**	**HYBRID**	**MPSD**
Freundlich	3.604	4.428	8.032	-1.052	14.043
Langmuir	77.682	20.142	32.337	19.515	51.270
D-R	563.489	50.801	54.878	-24.357	83.921
Temkin	89.421	21.703	42.697	21.655	79.536
313 K					
	SSE	**SAE**	**ARE**	**HYBRID**	**MPSD**
Freundlich	5.392	5.479	8.926	-1.083	14.653
Langmuir	114.092	25.025	34.385	20.608	51.595
D-R	865.466	62.396	58.840	-31.211	92.892
Temkin	131.890	26.051	49.123	29.020	96.673
323 K					
	SSE	**SAE**	**ARE**	**HYBRID**	**MPSD**
Freundlich	43.502	13.649	11.750	-1.509	17.614
Langmuir	247.611	36.045	46.783	18.606	45.732
D-R	2632.921	106.748	78.939	-54.945	127.780
Temkin	326.547	39.755	72.920	59.555	174.161

Table 5.5. Thermodynamic parameters for adsorption of IC by RHA.

Isotherm	$-\Delta G^0$ (kJ/mol K)				ΔH^0 (kJ/mol)	ΔS^0 (J/mol K)
	293 K	303 K	313K	323K		
Freundlich	16.12	17.76	18.72	20.29	23.37	135.06
Langmuir	21.25	22.32	23.44	25.55	19.66	138.97

Table 5.6. Kinetic parameters for the removal of IC by BFA (pH=3.0, T =303 K, C_0 = 50, 100, 250 and 500 mg/l, BFA dose = 5 g/l).

Pseudo-first-order					
C_o (mg/l)	$Q_{e,expt}$ (mg/g)	$Q_{e,calc}$ (mg/g)	k_f (1/min)	R_1^2 (linear)	R_2^2 (non-linear)
50	9.804	1.253	0.021	0.9746	-0.9123
100	15.944	1.864	0.0151	0.9654	-0.9032
250	35.787	1.984	0.010	0.9047	-0.8896
500	38.688	2.008	0.011	0.8162	-0.9034

Pseudo-second-order						
C_o (mg/l)	$Q_{e,expt}$ (mg/g)	$Q_{e,calc}$ (mg/g)	h (mg/g min)	k_S (g/mg min)	R_1^2 (linear)	R_2^2 (non-linear)
50	9.804	9.881	3.905	0.039	0.9999	0.9999
100	15.944	16.129	3.133	0.012	0.9993	0.9996
250	35.787	35.842	11.682	0.009	0.9994	0.9996
500	38.688	39.062	9.310	0.006	0.9993	0.9996

Bangham				
C_o (mg/l)	k_0 (g)	α	R_1^2 (linear)	R_2^2 (non-linear)
50	20.546	0.2436	0.9939	0.9969
100	12.529	0.1734	0.9943	0.9971
250	16.494	0.0728	0.9567	0.9781
500	6.858	0.0642	0.8968	0.94697

Intra-particle diffusion				
C_o (mg/l)	k_{id} (mg/g $min^{1/2}$)	I (mg/g)	R_1^2 (linear)	R_2^2 (non-linear)
50	0.136	8.073	0.8083	0.8990
100	0.342	11.345	0.8766	0.9362
250	0.385	30.142	0.9346	0.9667
500	0.431	32.310	0.8603	0.9275

Table 5.7. Isotherm parameters for removal of IC by BFA (pH=3.0, T = 293, 303, 313 and 323 K, t = 4 h, C_0 = 20-500 mg/l, BFA dose =5 g/l).

Freundlich constants				
T(K)	K_F ((mg/g)/(mg/l)$^{1/n}$)	$1/n$	R_1^2 (linear)	R_2^2 (non-linear)
293	7.230	0.2624	0.9500	0.9746
303	7.023	0.2751	0.9691	0.9844
313	8.032	0.2869	0.9489	0.9741
323	15.157	0.3544	0.8366	0.9147
Langmuir constants				
T (K)	K_L (l/mg)	Q_m (mg/g)	R_L	R_1^2 (linear)	R_2^2 (non-linear)
293	0.092	31.546	0.1788	0.9938	0.9968
303	0.071	33.557	0.2197	0.9839	0.9919
313	0.101	38.461	0.1650	0.9922	0.9961
323	0.227	70.422	0.0809	0.9994	0.7209
Dubnin-Radushkevih constants				
T (K)	Q_s (mg/g)	E (kJ/mol)	R_1^2 (linear)	R_2^2 (non-linear)
293	22.585	2.232	0.8290	-0.9105
303	22.256	2.232	0.7681	-0.8763
313	26.698	2.232	0.8339	-0.9131
323	58.933	1.118	0.924	-0.9612
Temkin constants				
T (K)	K_T (l/mg)	B_1	R_1^2 (linear)	R_2^2 (non-linear)
293	9.897	3.705	0.9830	0.9914
303	7.752	3.967	0.9696	0.9846
313	8.436	4.674	0.9872	0.9935
323	4.066	11.527	0.9641	0.9819

Table 5.8. Values of five different error analyses of isotherm models for adsorption of Indigo Carmine by BFA (pH=3.0, T = 293, 303, 313 and 323 K, t = 4 h, C_0 = 20-500 mg/l, BFA dose = 5 g/l).

293 K					
	SSE	**SAE**	**ARE**	**HYBRID**	**MPSD**
Freundlich	14.814	8.406	12.421	-2.006	20.236
Langmuir	80.281	12.512	27.610	30.602	54.300
D-R	234.65	33.873	35.937	-22.477	51.086
Temkin	10.651	7.122	7.366	-1.023	10.186
303 K					
	SSE	**SAE**	**ARE**	**HYBRID**	**MPSD**
Freundlich	12.748	8.177	10.801	-1.319	16.110
Langmuir	87.464	19.471	31.568	31.522	55.310
D-R	325.826	37.641	34.993	-16.317	54.732
Temkin	21.463	9.253	10.850	4.753	18.520
313 K					
	SSE	**SAE**	**ARE**	**HYBRID**	**MPSD**
Freundlich	29.708	12.239	15.055	-2.565	23.196
Langmuir	88.849	17.337	28.430	32.195	52.764
D-R	361.213	40.291	33.171	-16.602	49.519
Temkin	12.993	8.106	8.089	3.170	11.208
323 K					
	SSE	**SAE**	**ARE**	**HYBRID**	**MPSD**
Freundlich	387.401	35.606	30.110	-9.641	46.217
Langmuir	2946.666	96.214	71.611	143.222	102.312
D-R	201.046	25.427	19.146	3.704	28.400
Temkin	1088.359	63.652	83.560	-167.122	156.775

Table 5.9. Thermodynamic parameters for adsorption of IC by BFA.

Isotherm	$-\Delta G^0$ (kJ/mol K)				ΔH^0 (kJ/mol)	ΔS^0 (J/mol K)
	293 K	303 K	313K	338K		
Freundlich	19.72	20.46	21.41	23.80	18.67	129.92
Langmuir	25.35	26.86	28.00	31.07	27.93	181.01

APPENDIX-A

Table A-1. Calibration curve for Indigo Carmine.

Sl. No.	Concentration (mg/l)	Absorbance
1.	0	0.0000
2.	2	0.0500
3.	5	0.1246
4.	10	0.2692
5.	20	0.5079
6.	50	1.2501
7.	100	2.4182

Table A-2. Effect of pH on the removal of IC with an initial concentration of 50 mg/l at 303 K using RHA.

Sl. No.	pH	RHA % Removal
1.	3.00	88.52
2.	4.03	93.54
3.	5.54	93.85
4.	6.51	94.07
5.	9.32	93.95

Table A-3. Effect of pH on the removal of IC with an initial concentration of 50 mg/l at 303 K using BFA.

Sl. No.	pH	BFA % Removal
1.	2.00	98.50
2.	3.01	98.61
3.	4.04	98.09
4.	5.04	97.86
5.	6.36	97.56
6	7.03	97.52
7	8.04	96.95
8	10.00	95.10

Table A-4. Effect of Adsorbent dose on removal of IC using RHA.

Sl. No.	50 (mg/l)	
	Dose (g/l)	% Removal
1.	2	16.71
2.	5	45.62
3.	8	78.64
4.	10	91.09
5.	13	96.68
6.	16	98.23
7.	20	98.49
8.	25	99.34

Table A-5. Effect of Contact time on removal of IC at 303 K using RHA (10 g/l).

Sl. No.	Contact Time (min)	50 mg/l	100 mg/l	250 mg/l	500 mg/l
		% Removal	% Removal	% Removal	% Removal
1.	0	0.00	0.00	0.00	0.00
2.	5	42.05	33.89	26.88	16.63
3.	10	47.29	38.463	30.69	22.41
4.	30	53.27	42.15	34.75	25.20
5.	60	60.20	47.90	38.77	27.82
6.	120	71.15	55.67	44.18	31.88
7.	180	78.96	63.46	47.82	36.64
8.	240	83.77	68.64	51.10	39.67
9.	300	89.19	73.11	54.30	41.88
10.	360	91.368	76.97	55.90	42.70
11.	480	94.87	80.96	57.00	44.71

Table A-6. Lagergren Plot for removal of IC for different initial concentrations at 303 K using RHA (10 g/l).

Sl. No.	Contact Time (min)	50 mg/l	100 mg/l	250 mg/l	500 mg/l
		Log (Q_e-Q_t)	Log (Q_e-Q_t)	Log (Q_e-Q_t)	Log (Q_e-Q_t)
1.	0	-	-	-	-
2.	5	0.4235	0.6749	0.8832	1.1510
3.	10	0.3783	0.6308	0.8254	1.0519
4.	30	0.3202	0.5916	0.7540	0.9946
5.	60	0.2416	0.5223	0.6695	0.93275
6.	120	0.0779	0.4069	0.5210	0.8153
7.	180	-0.0935	0.2488	0.3816	0.6190
8.	240	-0.2471	0.0987	0.2008	0.4221
9.	300	-0.5306	-0.0922	-0.1029	0.1866
10.	360	-0.7303	-0.3737	-0.4096	0.0519
11.	480	-1.9724	-1.6315	-0.9480	-0.9102

Table A-7. Pseudo second order kinetic Plot for removal of IC for different initial concentrations at 303 K using RHA (10 g/l).

Sl. No.	Contact Time (min)	50 mg/l	100 mg/l	250 mg/l	500 mg/l
		t/Q_t (g min/mg)	t/Q_t (g min/mg)	t/Q_t (g min/mg)	t/Q_t (g min/mg)
1.	0	-	-	-	-
2.	5	2.3781	1.4752	0.7439	0.6009
3.	10	4.2287	2.5998	1.3030	0.8921
4.	30	11.2615	7.1171	3.4528	2.3805
5.	60	19.9319	12.5235	6.1903	4.3122
6.	120	33.7288	21.5532	10.8645	7.5269
7.	180	45.5885	28.3629	15.0539	9.8255
8.	240	57.2994	34.9612	18.7843	12.0991
9.	300	67.2670	41.0314	22.0981	14.3248
10.	360	78.8014	46.7707	25.7595	16.8598
11.	480	101.1835	59.2832	33.6793	21.4702

Table A-8. Weber-Morris Plot for removal of IC for different initial concentrations at 303 K using RHA (10 g/l).

Sl. No.	Time $(min)^{0.5}$	50 mg/l	100 mg/l	250 mg/l	500 mg/l
		Q_t (mg/g)	Q_t (mg/g)	Q_t (mg/g)	Q_t (mg/g)
1.	0	0	0	0	0
2.	2.2360	2.1024	3.3893	6.7213	8.3197
3.	3.1623	2.3647	3.8463	7.6741	11.2090
4.	5.4772	2.6639	4.2151	8.6885	12.6024
5.	7.7459	3.0102	4.7909	9.6926	13.9139
6.	10.9544	3.5577	5.5676	11.0450	15.9426
7.	13.4164	3.9483	6.3463	11.9569	18.3197
8.	15.4919	4.1885	6.8647	12.7766	19.8360
9.	17.3205	4.4598	7.3115	13.5758	20.9426
10.	18.9736	4.56844	7.6971	13.9754	21.3524
11.	21.9089	4.7438	8.0967	14.2520	22.3565

Table A-9. Freundlich isotherm for removal of IC at different temperatures with RHA (10 g/l).

Sl. No	293 K		303 K		313 K		323 K	
	ln Q_e	ln C_e	ln Q_e	ln C_e	ln Q_e	ln C_e	ln Q_e	ln C_e
1.	0.5900	0.6724	0.6496	-0.1596	0.6600	-0.4282	0.6745	-0.9973
2.	1.4657	1.9010	1.5536	0.9981	1.5685	0.6952	1.5850	0.1864
3.	1.9996	3.2634	2.0814	2.9879	2.1642	2.5586	2.2666	1.2620
4.	2.6440	4.6941	2.6984	4.6194	2.8322	4.3840	3.1002	3.3311
5.	3.002	5.6993	3.1099	5.6197	3.2797	5.4567	3.6661	4.6915
6.	3.1710	6.2377	3.3157	6.1624	3.4913	6.0443	3.9545	5.4305
7.	3.3550	6.5702	3.5110	6.5000	3.7021	6.3880	4.1781	5.8509

Table A-10. Langmuir isotherm for removal of IC at different temperatures with RHA (10 g/l).

Sl. No	293 K		303 K		313 K		323 K	
	C_e/Q_e (g/l)	C_e (mg/l)	C_e/Q_e (g/l)	C_e mg/l)	C_e/Q_e (g/l)	C_e mg/l)	C_e/Q_e (g/l)	C_e mg/l)
1.	1.0859	1.9590	0.4452	0.8524	0.3368	0.6516	0.1879	0.3688
2.	1.5454	6.6926	0.5737	2.7131	0.4175	2.0041	0.2469	1.2049
3.	3.5390	26.1393	2.4757	19.8442	1.4834	12.9180	0.3662	3.5328
4.	7.7687	109.303	6.8276	101.434	4.7200	80.1639	1.2598	27.9713
5.	14.8346	298.668	12.3034	275.819	8.8199	234.323	2.7882	109.016
6.	21.4703	511.680	17.2321	474.590	12.8464	421.721	4.3755	228.278
7.	24.9070	713.524	19.8653	665.163	14.6713	594.672	5.3266	347.541

Table A-11. Temkin adsorption for removal of IC at different temperatures with RHA (10 g/l).

Sl. No	293 K		303 K		313 K		323 K	
	Q_e (mg/g)	ln C_e	Q_e (mg/g)	ln C_e	Q_e (mg/g)	ln C_e	Q_e (mg/g)	ln C_e
1.	1.8041	0.6724	1.9147	-0.1596	1.9348	-0.4282	1.9631	-0.997
2.	4.3307	1.9010	4.7287	0.9981	4.7996	0.6952	4.8795	0.1864
3.	7.3860	3.2634	8.0156	2.9879	8.7082	2.5586	9.6467	1.2621
4.	14.069	4.6941	14.8565	4.6194	16.9836	4.3841	22.2028	3.3312
5.	20.1332	5.6993	22.4180	5.6197	26.5676	5.4567	39.0983	4.6915
6.	23.8319	6.2377	27.5409	6.1624	32.8278	6.0443	52.1721	5.4305
7.	28.6475	6.5702	33.4836	6.5000	40.5327	6.3880	65.2459	5.8508

Table A-12. Dubin & Raduskevich adsorption isotherm adsorption for removal of IC at different temperatures with RHA (10 g/l).

Sl. No	293 K		303 K		313 K		323 K	
	ln Q_e	E^2	ln Q_e	E^2	ln Q_e	E^2	ln Q_e	E^2
1.	0.5900	100930	0.6496	382287	0.6600	585739	0.6745	1240080
2.	1.4657	115075	1.5536	624796	1.5685	110956	1.5850	263329
3.	1.9996	8363.92	2.0814	15338.9	2.1642	37647.2	2.2666	448017
4.	2.6440	492.187	2.6984	610.759	2.8322	1040.78	3.1002	8898.14
5.	3.0024	66.3018	3.1098	83.1156	3.2797	122.807	3.6661	601.274
6.	3.1710	22.6208	3.3157	28.116	3.4913	37.9864	3.9545	137.782
7.	3.3550	11.6393	3.5110	14.3217	3.7021	19.1171	4.1781	59.5339

Table A-13. Effect of Adsorbent dose on the removal of IC using BFA.

Sl. No.	50 (mg/l)	
	Dose (g/l)	% Removal
1.	0	0.00
2.	2	93.96
3.	4	99.15
4.	6	99.23
5.	8	99.71
6.	10	99.22
7.	12	99.19
8.	15	99.50

Table A-14. Effect of NaCl concentration on the adsorption capacity of BFA at 303 K (Dose=5 g/l, C_o=50 mg/l).

Sl. No.	NaCl concentration	Q_t (mg/g)
1.	0	9.917
2.	0.02	9.574
3.	0.04	9.377
4.	0.06	8.860
5.	0.08	8.754
6.	0.1	8.557
7.	0	9.917

Table A-15. Effect of Contact time on removal of IC for different initial concentration at 303 K using BFA (5 g/l).

Sl. No.	Contact Time (min)	50 mg/l	100 mg/l	250 mg/l	500 mg/l
		% Removal	% Removal	% Removal	% Removal
1.	0	0.00	0.00	0.00	0.00
2.	5	79.41	55.32	61.11	29.16
3.	10	82.32	61.44	61.85	31.09
4.	20	88.50	64.88	63.41	34.47
5.	30	90.05	68.59	66.08	35.36
6.	40	91.65	69.41	66.24	35.57
7.	60	93.65	72.18	66.32	35.91
8.	90	95.37	74.49	67.37	35.81
9.	120	96.55	76.24	68.87	37.49
10.	240	98.04	79.72	71.57	38.68

Table A-16. Lagergren Plot for removal of IC for different initial concentrations at 303 K using BFA (5 g/l).

Sl. No.	Contact Time (min)	50 mg/l	100 mg/l	250 mg/l	500 mg/l
		Log (Q_e-Q_t)	Log (Q_e-Q_t)	Log (Q_e-Q_t)	Log (Q_e-Q_t)
1.	0	-	-	-	-
2.	5	0.2702	0.6883	0.7184	0.9788
3.	10	0.1962	0.5629	0.6867	0.8802
4.	20	-0.0204	0.4723	0.6108	0.6246
5.	30	-0.0973	0.3476	0.4386	0.5221
6.	40	-0.1948	0.3143	0.4255	0.4934
7.	60	-0.35800	0.1784	0.4188	0.4425
8.	90	-0.5744	0.0195	0.3218	0.4577
9.	120	-0.8287	-0.1579	0.1298	0.0779
10.	240	-	-	-	-

Table A-17. Pseudo second order kinetic Plot removal of IC for different initial concentrations at 303 K using BFA (5 g/l).

Sl. No.	Contact Time (min)	50 mg/l	100 mg/l	250 mg/l	500 mg/l
		t/Q_t (g min/mg)	t/Q_t (g min/mg)	t/Q_t (g min/mg)	t/Q_t (g min/mg)
1.	0	-	-	-	-
2.	5	0.6296	0.4518	0.1636	0.1714
3.	10	1.2146	0.8137	0.3233	0.3215
4.	20	2.2598	1.5411	0.6308	0.5801
5.	30	3.3315	2.1869	0.9079	0.8484
6.	40	4.3641	2.8814	1.2076	1.1244
7.	60	6.4064	4.1562	1.8092	1.6705
8.	90	9.4362	6.0409	2.6715	2.5126
9.	120	12.4278	7.8692	3.4844	3.2007
10.	240	24.4795	15.0524	6.7063	6.2034

Table A-18. Weber-Morris Plot removal of IC for different initial concentrations at 303 K using BFA (5 g/l).

Sl. No.	Time $(min)^{0.5}$	50 mg/l	100 mg/l	250 mg/l	500 mg/l
		Q_t (mg/g)	Q_t (mg/g)	Q_t (mg/g)	Q_t (mg/g)
1.	0	0	0	0	0
2.	2.2360	7.9409	11.0655	30.5573	29.1639
3.	3.1622	8.2328	12.2885	30.9262	31.0983
4.	4.4721	8.8500	12.9770	31.7049	34.4754
5.	5.47722	9.0049	13.7180	33.0409	35.3606
6.	6.3245	9.1655	13.8819	33.1229	35.5737
7.	7.7459	9.3655	14.4360	33.1639	35.9180
8.	9.4868	9.5377	14.8983	33.6885	35.8196
9.	10.9544	9.6557	15.2492	34.4385	37.4918
10.	15.4919	9.8041	15.9442	35.7868	38.6885

Table A-19. Freundlich isotherm for removal of IC at different temperatures with BFA (5 g/l).

Sl. No	293 K		303 K		313 K		323 K	
	ln Q_e	ln C_e	ln Q_e	ln C_e	ln Q_e	ln C_e	ln Q_e	ln C_e
1.	1.3726	-1.3075	1.3735	-1.3700	1.37413	-1.4196	2.2835	-0.059
2.	2.2807	0.0749	2.2725	0.3917	2.2859	-0.1938	2.9852	0.0401
3.	2.8103	2.8283	2.8214	2.7720	2.9020	2.1908	3.8707	2.3139
4.	3.2250	4.8220	3.2180	4.8291	3.3859	4.6276	4.2168	4.7086
5.	3.4031	5.5203	3.4123	5.5147	3.5873	5.3904	-	-
6.	3.4426	5.8396	3.5303	5.7970	3.6490	5.7294	-	-

Table A-20. Langmuir isotherm for removal of IC at different temperatures with BFA (5 g/l).

Sl. No	293 K		303 K		313 K		323 K	
	C_e/Q_e (g/l)	C_e (mg/l)	C_e/Q_e (g/l)	C_e (mg/l)	C_e/Q_e (g/l)	C_e (mg/l)	C_e/Q_e (g/l)	C_e (mg/l)
1.	0.0685	0.2705	0.0643	0.2541	0.0612	0.2418	0.0960	0.9426
2.	0.1101	1.0778	0.1524	1.4795	0.0837	0.8237	0.0526	1.0410
3.	1.0181	16.9180	0.9518	15.992	0.4910	8.9426	0.2108	10.1147
4.	4.9381	124.221	5.0082	125.102	3.4616	102.274	1.6352	110.901
5.	8.3078	249.713	8.1856	248.319	6.0682	219.303	-	-
6.	10.9895	343.6475	9.6476	329.323	8.0078	307.807	-	-

Table A-21. Temkin adsorption isotherm for removal of IC at different temperatures with BFA (5 g/l).

Sl. No	293 K		303 K		313 K		323 K	
	Q_e (mg/g)	ln C_e	Q_e (mg/g)	ln C_e	Q_e (mg/g)	ln C_e	Q_e (mg/g)	ln C_e
1.	3.9459	-1.3075	3.9491	-1.3700	3.9516	-1.4196	9.8114	-0.059
2.	9.7844	0.0749	9.7040	0.3917	9.8352	-0.1938	19.7918	0.0401
3.	16.6163	2.8283	16.8016	2.7720	18.2114	2.1908	47.9770	2.3139
4.	25.1557	4.8220	24.9795	4.8291	29.5450	4.6276	67.8190	4.7086
5.	30.0573	5.5203	30.3360	5.5147	36.1393	5.3904	-	-
6.	31.2705	5.8396	34.1352	5.7970	38.4385	5.7294	-	-

Table A-22. Dubin & Raduskevich adsorption isotherm for removal of IC at different temperatures with BFA (5 g/l).

Sl. No	293 K		303 K		313 K		323 K	
	ln Q_e	E^2	ln Q_e	E^2	ln Q_e	E^2	ln Q_e	E^2
1.	1.372	14200042	1.373	16173959	1.374	18129216	2.283	4129370
2.	2.280	2556439	2.272	1691977	2.286	4277509	2.985	3579535
3.	2.810	19570.22	2.821	23347.22	2.902	76091.51	3.870	70190.22
4.	3.225	381.486	3.218	402.2663	3.386	641.127	4.216	636.3208
5.	3.403	94.78428	3.412	102.5031	3.587	140.1657	-	-
6.	3.442	50.10333	3.530	58.33673	3.649	71.24291	-	-